Louisiana State University

LSU Digital Commons

1998

Determination of Optimal Composition of Stabilized Phosphogypsum Composites for Saltwater Application.

Tingzong Guo
Louisiana State University and Agricultural & Mechanical College

Follow this and additional works at: https://digitalcommons.lsu.edu/gradschool_disstheses

INFORMATION TO USERS

This manuscript has been reproduced from the microfilm master. UMI films the text directly from the original or copy submitted. Thus, some thesis and dissertation copies are in typewriter face, while others may be from any type of computer printer.

The quality of this reproduction is dependent upon the quality of the copy submitted. Broken or indistinct print, colored or poor quality illustrations and photographs, print bleedthrough, substandard margins, and improper alignment can adversely affect reproduction.

In the unlikely event that the author did not send UMI a complete manuscript and there are missing pages, these will be noted. Also, if unauthorized copyright material had to be removed, a note will indicate the deletion.

Oversize materials (e.g., maps, drawings, charts) are reproduced by sectioning the original, beginning at the upper left-hand corner and continuing from left to right in equal sections with small overlaps. Each original is also photographed in one exposure and is included in reduced form at the back of the book.

Photographs included in the original manuscript have been reproduced xerographically in this copy. Higher quality 6" x 9" black and white photographic prints are available for any photographs or illustrations appearing in this copy for an additional charge. Contact UMI directly to order.

DETERMINATION OF OPTIMAL COMPOSITION OF STABILIZED PHOSPHOGYPSUM COMPOSITES FOR SALTWATER APPLICATION

A Dissertation

Submitted to the Graduate Faculty of the
Louisiana State University and
Agricultural and Mechanical College
In partial fulfillment of the
Requirements for the degree of
Doctor of Philosophy

in

Department of Civil and Environmental Engineering

by:
Tingzong Guo
B.S.,   Fuzhou University, 1982
M.S.,   Xiamen University, 1986
M.S., Louisiana State University, 1995
December, 1998

UMI Number: 9922081

ACKNOWLEDGEMENTS

I wish to express my gratitude to my major professors, Dr. Ronald F. Malone and Dr. Kelly A. Rusch, for their invaluable help and guidance during my research, dissertation writing, and course studies. Many people helped me during my research and writing so I would like to extend my gratitude to Dr. Roger K. Seals, Dr. Charles A. Wilson, Dr. Shulin Chen, Dr. Ralph J. Portier, Dr. Xiaogang Xie, Dr. James P. Geaghan, Dr. E. Barry Moser and Mr. Rick Young for their support, encouragment, and comments concerning my work. I would also like to thank Miss Autumn S. Hawke, Miss Lihua Wang, Miss Attres Tagge, and Mrs. Sarah Jones for their support in my research.

Specials thanks to my father Dejin Guo, mother Yuzhu Luo, aunt Qian Zhuang, and family who contributed what they had to support my education and encourage me in all things. Extra special thanks to my wife Lixia Li and my daughter Xinmei Guo who were always there when I needed comfort and help. Finally, I adore my newborn child, Kailyn Lotus Guo. Her coming gave me the impetus to finalize my dissertation research and writing.

ii

TABLE OF CONTENTS

iv

v

LIST OF TABLES

LIST OF FIGURES

ix

xi

xiv

ABSTRACT

Phosphogypsum ($CaSO_4 \cdot 2H_2O$, PG), a solid by-product of phosphoric acid production, has been classified as a "Technologically Enhanced Natural Radioactive Material" (TENR), because it contains radionuclides (eg., radium[226]) and some trace toxic metals in concentrations, which may pose a potential hazard to human health and the environment. The current regulated disposal method for PG is on-site stockpiling, which has created a serious environmental management problem. An appealing solution to the problem is the use of stabilized PG for aquatic enhancement activities. This solution can eliminate the airborne vector of transmission for radon[222] and therefore may provide a safe alternative to the current stockpiling practices. The determination of low cement content (<10%) stabilized PG composites has been investigated. Varying combinations of PG:cement, PG:fly ash:lime and PG:fly ash:cement were fabricated for laboratory and field experiments. Field saltwater submergence studies and response surface with process variable analysis shows that only the PG:fly ash:cement composites are able to survive in the Gulf coast saltwater environment when cement content is less than 10%. Scanning electron microscopy (SEM) shows that ettringite formation is potentially responsible for degradation of PG stabilized composites. SEM and microprobe analysis showed that conditions necessary for stabilized PG composites to survive in the saltwater environment are: (1) the stabilized PG composites should have a strong sulfate resistant surface and (2) the local pH environments on the stabilized PG composites should be above 11. This higher local pH environment will result in the formation of calcium carbonates, which

xvi

protect the PG composites and reduce the diffusion of toxic metals and radium. For PG:fly ash:cement composites, the stronger calcium carbonate coating embedded with fly ash particles covers the higher sulfate resistant composite surface and both contribute to the PG:fly ash:cement composites survival in the Gulf Coast seawater environments for more than one year. Dynamic leaching test, field experiments, SEM, and microprobe analysis showed that the calcium diffusion coefficient is a good indicator for PG:cement and PG:fly ash:cement stabilized composites long term dissolution potential but does not apply to the PG:fly ash:lime stabilized composite.

CHAPTER 1

INTRODUCTION

Phosphogypsum ($CaSO_4 \cdot 2H_2O$), a solid by-product of phosphoric acid production, has been classified as a "Technologically Enhanced Natural Radioactive Material" (TENR) because it contains radionuclides and some trace metals in concentrations which may pose a potential hazard to human health and the environment (Roessler et al., 1979; May and Sweeney, 1984a; Berate, 1990; Luther et al., 1993). The main disposal method for phosphogypsum is on-site stockpiling. It has resulted in at least 33 PG stacks located in all Gulf States except Alabama and has created a serious environmental management problem (Taha and Seals, 1991). It is estimated that by year 2000, the total inventory of PG in the US will exceed 2 billion metric tons (Taha and Seals, 1991). Environmental concerns associated with PG disposal such as radioactive materials, radon gas production and surface and groundwater contamination, coupled with increasing land costs for stockpiles, has promoted research on alternative beneficial uses of this solid waste that would result in applications considered protective of public health. The primary concern PG stockpiles is the airborne vector of transmission for radon gas, which has a half-life of 3.4 days and releases γ rays upon decay. Radon gas is a daughter product of radium[226] (α decay) which has a half-life of 1635 years. The development of strategies that eliminate this airborne vector of transmission would provide a safe alternative to

1

current stockpiling practices. An appealing solution is the use of stabilized PG for aquatic enhancement activities.

Solidification technology is a widely used solid waste treatment technology that immobilizes harmful substances by adding inorganic binding materials such as lime, cement, and fly ash to aqueous or solid wastes to produce solid matrices. This decreases the waste leachability through reduction of the contact surface between the leaching medium and the waste, and transformation of forms of toxic metals (Malone et al., 1980, Barth et al., 1990). Solidification technology has been proposed to solidify the phosphogypsum solid waste for aquatic applications. The solidified PG composites submerged in an aquatic environment would provide double protection against the escape of radon gas. First, the radon gas molecules would have to diffuse out of the stabilized PG matrix. Second, those molecules that escape have to diffuse out of the water column before becoming available for human exposure.

A demonstration study conducted at Louisiana State University showed that 70%:30% PG:cement test blocks placed in experimental ponds of Grand Terre supported a diverse population of surface attached, burrowing organisms and oysters, indicating the potential use of PG for offshore artificial reefs and oyster substrate. However, 30% cement is not economical. Conversely 85%:15% PG:cement composites disintegrated within one month after submergence in saltwater at Grand Isle, Louisiana. This stimulates some questions: Can we find an economic ingredient combination to build oyster substrate and artificial reefs and what are the factors affecting composite stability?

To reduce the cost of the PG composites, other waste products were investigated as potential binding additives to the PG:cement matrix. Phosphogypsum:cement:fly ash (Class C coal fly ash) composites are currently showing promise. Composites sample with a lower bound of 62%:3%:35%, PG:cement:fly ash have remained intact in a shallow saltwater bay off the coast of Grand Isle, Louisiana for one year. Fly ash is a solid residual of coal or oil combustion in electric power plants with the volume being much higher at coal-fired plants. The mass of fly ash produced from coal combustion is about 10% of the feed coal, and only 30% of fly ash is reused (Higgins, 1995). In 1996, 948 million tons of coal was consumed (DRI/MaGraw-Hill et al 1998) and it is estimated that 94.8 million tons of fly ash were produced with only 28.4 million tons of fly ash consumed. There is 66.4 million tons of fly ash that remain unused today. The disposal of these solid wastes costs the industry about 4.3 billion dollars a year (Darnay, 1992).

The scope of this dissertation research was to determine the mechanisms affecting the integrity of PG blocks under saltwater conditions and find the optimum composition for stabilized PG composites. Scanning electron microscopy, microprobe and statistical analysis methods were used for this research.

CHPATER 2

LITERATURE REVIEW

Chemical By-Products: Phosphogypsum and Environmental Concerns

Chemical By-Products: Phosphogypsum

Phosphogypsum (PG) is the by-product of the wet manufacturing phosphoric acid process and has been classified as a "Technologically Enhanced Natural Radioactive Material" (TENR) (Taha and Seals 1991). Phosphoric acid is an important chemical and major constituent of many fertilizers (Lopez, 1971). In the wet process, mainly used in the United States, phosphate rock is reacted with sulfuric acid and water to produce phosphoric acid and the solid by-product PG (Thimmegowda, 1994):

$$Ca_{10}(PO_4)_6F_2 + 10\ H_2SO_4 + 20\ H_2O \longrightarrow 10\ CaSO_4 \cdot 2H_2O + 6\ H_3PO_4 + 2\ HF$$
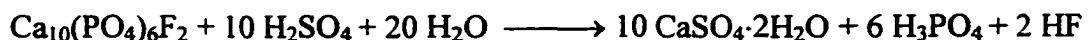
The rock and sulfuric acid are circulated through reaction tanks to maintain the optimum conditions for the reaction taking place and for the production of PG crystals. The PG is then filtered and washed with water and the slurry is pumped to a stack where evaporation and leaching of the free water takes place. The process water is usually decanted and recycled (Brown, 1990). After water recovery and evaporation occur, large PG stockpiles are formed up to 200 ft high and covering as much as 494 acres.

The wet process requires a lower capital investment and production costs with greater flexibility of processing different grades of phosphoric rock (Ferguson, 1988). Other advantages include the recovery of Uranium from the acid produced and the

4

high filtration rate. The greatest disadvantage is the production of PG with many impurities. This PG requires washing, lime neutralization, calcination and granulation to be used in the manufacturing of cement or wallboard, in which it's a main constituent. The process for the production of phosphoric acid currently used in Australia is a two-stage crystallization process (Baretka, 1990). The PG formed by this process has a low level of impurities and various research institutes have shown that PG can be successfully converted into plasterboard and other plaster products. PG can potentially be converted into a new type of low energy binder/cement and probably as a retarder in Portland cement (Taha and Seals, 1991).

The production of PG in the United States is approximately thirty-three million tons per year with Florida leading the nation. As of 1989, the state of Louisiana had almost ninety-five million tons of PG stockpiled and over twenty-five million tons exist in the Houston area (Gregory, 1983). In 1977, Japan was producing about 2,748,000 metric tons of PG per year (Miyamoto, 1980). Studies have shown that PG also exists in Canada, Europe and India.

Environmental Concerns

Recently, environmental concerns have contributed to the increasing interest in achieving environmentally acceptable means of using PG. The two major categories of concern are toxicological and radiological.

PG exists in three different forms: anhydrite, hemihydrate, and dihydrate. Dihydrate ($CaSO_4 \cdot 2H_2O$) is the most commonly found form in the world (Taha and Seals 1991). PG contains 39 elements with several trace metals included on EPA's

list of potentially toxic elements. The concentration of these elements are listed in

Table 2.1 (Taha and Seals 1991).

Table 2.1 Typical trace element concentration in phosphogypsum

Element	Concentration (ppm)	
	Louisiana	Florida
As	1-5	2-8
Ba	50	<10
Cd	0.3-0.4	3-4
Cr	2-5	15-30
Pb	2-10	2-13
Hg	0.02-0.05	<0.5
Se	1	<1
Ag	0.1-0.2	<0.3
U_3O_8	5-10	NA

The main concern of contamination is the heavy metals emanating from the stockpiles and the effects on human health and the environment. The potential for significant contamination includes the contamination of groundwater by the low pH PG leachate and the contamination of the surface water.

Many studies have been conducted on the toxicity of PG and whether leaching of these materials occur. In 1983, May and Sweeney (1983) conducted an investigation of nine PG stacks in the state of Florida to study its various physical and chemical characteristics. The results of the analysis showed that trace elements were distributed uniformly within the PG stacks and the eight metals listed as toxic by the EPA were detected at concentrations far less than the standard of EPA extraction procedure, even if 100 percent of these metals would be extracted by the EPA procedure. Besides the spectrophotometer analysis, the EPA procedure was used to find the inorganic

contaminants in the PG. The results showed that all toxic metals were found to be lower than the EPA maximum contaminant level.

Naff (1984) studied the environmental aspects of PG produced at Mobil by conducting EPA extraction procedure (EP) tests. The EP test was done on fresh, aged and stabilized stacks of PG from Mobil. Fresh and aged PG were found to meet both leaching and drinking water standards for the eight heavy metals listed as toxic elements by the EPA. Sulfates and fluoride levels exceeded drinking water levels due to the solubility of PG. The results showed that PG, stabilized with cement and fly ash, forms a monolithic slab containing insoluble compounds helping to hold the metals within the block; Thus, the impact of stabilized PG on both groundwater and drinking water will be lower than that of raw PG.

The second main category associated with phosphogypsum stockpiles is radiological concerns. The radionuclides of concern in PG, as reported by C. W. Berish (Brown, 1990), are: uranium (U-238 and U-234), thorium (Th-230), radium (Ra-226), radon (Rn-222), lead (Pb-210), and polonium (Po-210). U-238 undergoes various decay processes to eventually produce radioactive Pb-210. The various steps involved are listed in Table 2.2 (Brown, 1990).

Average radionuclide concentrations present in PG and background(BG) soils are given in Table 2.3 (Brown, 1990), the PG values are the means of samples taken from five stacks). From this information, we can observe the radionuclide concentration in PG exceeded those in background soils by nearly 10 times for U-234 to sixty times for Ra-226.

Table 2.2 The related radionuclides in raw phosphogypsum

Radionuclide	Member of series	Half-life
Uranium-238	1st	$4.9 * 10^9$ years
Uranium-234	4th	$2.4 * 10^5$ years
Thorium-230	5th	$8 * 10^4$ years
Radium-226	6th	1622 years
Radon-222	7th	3.8 days
Lead-210	12th	22 years
Polonium-210	14th	138 days

Table 2.3 Radionuclide concentrations(pCi/g) in PG and background soil

Material	Ra-226	U-234	U-238	Th-230	Po-210	Pb-210
PG	31.00	3.30	3.20	5.10	27.00	36.00
BG Soil	0.50	0.30	0.30	0.30	0.50	0.70

The primary mechanisms of radionuclide contamination from PG stacks include direct irradiation from gamma radiation and airborne emissions of radon, dust and other carcinogens. Many studies have been conducted by Roessler (1979) to investigate the potential environmental impact by the radionuclide contaminants. The United States EPA requires that PG be stored in stacks and that radon emissions be below 20 pCi/m^2-s based on the National Emission Standards for Hazardous Air Pollutants (Roessler, 1979).

Stabilization Materials

Portland Cement

Chemical Composition

Table 2.4 (Neville, 1981) contains the four major constituents of Portland cement. The silicates in cement are not, in reality, pure compounds but contain minor oxides in solution. These major oxides significantly affect the atomic arrangements, crystal form and hydraulic properties of the silicates. Minor oxides usually amount to no more than a few percent of the weight of cement. Included are MgO, TiO_2, Mn_2O_3, K_2O, and Na_2O (Neville, 1981).

Table 2.4 The main components of Portland cement

Name of compound	Oxide composition	Abbreviation
Tricalcium silicate	$3CaO \cdot SiO_2$	C_3S
Dicalcium silicate	$2CaO \cdot SiO_2$	C_2S
Tricalcium aluminate	$3CaO \cdot Al_2O_3$	C_3A
Tetracalcium aluminoferrite	$4CaO \cdot Al_2O_3 \cdot Fe_2O_3$	C_4AF

Calcium Silicate Hydrates

C_3S, normally present in the largest amount and making up 75 to 80% of Portland cement, occurs as small, equidimenstional colorless grains. Cooling below 1250°C, C_3S decomposes slowly but if cooled quickly it remains relatively stable at normal temperatures. C_2S exists in three to four forms. Alpha-C_2S exists at high temperatures and inverts to beta-C_2S at about 1450°C. Beta-C_2S inverts to gamma-C_2S at about 670°C but in commercial cooling of cement beta-C_2S is preserved

forming a rounded grain and usually twining. The hydration process is slower than that of C_3S (Swayze, 1946).

Assuming that $C_3S_2H_3$ is the final product of the hydration of both C_3S and C_2S, the reaction can be written as: (not exact stoichiometric equations)

C_3S:

$$2C_3S + 6H \rightarrow C_3S_2H_3 + 3Ca(OH)_2$$

$$100 + 24 \rightarrow 75 + 49$$

C_2S:

$$2C_2S + 4H \rightarrow C_3S_2H_3 + Ca(OH)_2$$

$$100 + 21 \rightarrow 99 + 22$$
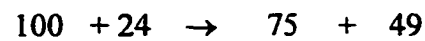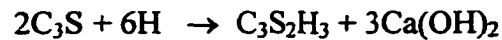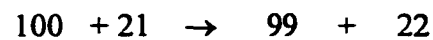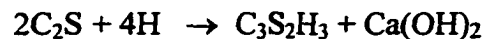
Based on the weight, both silicates require approximately the same amount of water for hydration; but, C_3S produced more than twice the amount of $Ca(OH)_2$ as C_2S. The $Ca(OH)_2$ produced in the above hydration process can neutralize the acidity of PG at certain levels.

Tricalcium Aluminate Hydrate and Function of Gypsum

The amount of C_3A present in most cements is comparatively small; but, its behavior and structural relationship with the other phases in cement make it of interest. The tricalcium aluminate hydrate forms a prismatic dark interstitial material, possibly with other substances in solid solution. It often takes the form of flat plates individually surrounded by the calcium silicate hydrates.

The reaction of C_3A with water is violent and leads to immediate stiffening of the paste, known as "flash set". This is prevented by the addition of gypsum $(CaSO_4 \cdot 2H_2O)$ which reacts with C_3A to form insoluble calcium sulphoaluminate

($3CaO \cdot Al_2O_3 \cdot 3CaSO_4 \cdot 31H_2O$) (Steinour, 1952). Eventually a tricalcium aluminate

hydrate is formed, although it is preceded by a metastable $3CaO \cdot Al_2O_3 \cdot CaSO_4 \cdot 12H_2O$

produced at the expense of the original high-sulphate calcium sulphoaluminate.

The stable form of the calcium aluminate hydrate, ultimately existing in the

hydrated cement paste, is probably the cubic crystal C_3AH_6. It is possible though that

hexegonal C_4AH_{12} crystalizes out first and later changes to the cubic form. The final

reaction can be written as $C_3A + 6H \rightarrow C_3AH_6$ (not a stoichiometric equation).

The molecular weights show that the 100 parts of C_3A react with 40 parts of

water by weight. This is much higher than that required by the silicates. C_3A is

undesirable because it contributes little or nothing to the strength of cement except at

early ages. When hardened, cement paste is attacked by sulfates and the expansion

due to the formation of calcium sulphoaluminate (ettringite) from C_3A may result in

the disruption of the hardened past. C_3A is useful, though, in its ability to act as a flux

and reduce the temperature of burning of clinker and facilitates the combination of the

lime and silica. C_4AF can also act as a flux. C_4AF is really a solid solution ranging

from C_2F to C_6A_2F (Swayze, 1946). If no liquid were formed during burning, the

reactions in the kiln would progress much more slowly and would probably be

incomplete. Gypsum reacts with C_4AF to form calcium sulphoferrite as well as

calcium sulphoaluminate and its presence may accelerate the hydration of silicates.

C_3AF yields the same products as C_3A but at a much slower rate (Neville, 1981).

Hydration of Cement

The reactions by which Portland cement becomes a binding agent take place in a

water-cement paste. The compounds listed in Table 1 form products of hydration,

which in time, produce a firm and hard mass, the hardened cement paste. There are two ways in which cement compounds may react with water. The first way is by a true reaction of hydration in which there is a direct addition of water molecules. The second type of reaction is by hydrolysis. However, hydration is the usual term for all reactions of cement with water (Neville, 1981).

The presence of gypsum is able to retard the hydration of Portland cement. The disadvantage associated with the presence of gypsum is the formation of ettringite as a result of excessive sulfate levels. There is a direct correlation between cement expansion and ettringite formation (Kalvakalva, 1995).

Fly Ash

Fly ash is a solid residual of coal of oil combustion in electric power plants with the volume being much higher at coal-fired plants. Fly ash is a mixture of metallic oxides, silicates, and other inorganic particulate matter, which is produced during the burning of coal and oil. The chemical composition of fly ash is influenced by the type of coal used, the completeness of combustion process, and the mineral contents of the coals (Atalay et al., 1990). Class C fly ash that contains abundant of calcium is added as the base material to neutralize the acidity of the raw PG. Fly ash also contains silicate allowing it to act as a binding agent in the mixture, reducing the necessary cement content. Fly ash can also inactivate C_3A in cement.

Lime

Lime is calcium hydroxide. It is a base material. It is added mainly as a base material to neutralize the acidity of raw phosphogypsum. It can also function as a binding agent.

Marine Environments

<u>Chemical Environment</u>

Most seawaters have similar compositions of dissolved salts; typically 10-35 g/L salt and containing Na^+, Mg^{2+}, Cl^-, and SO_4^{2-} as the principal components. In addition to dissolved salts, the presence of certain gases in the seawater play an important role in the chemical and electrochemical phenomena (oxidizing or reducing environments) influencing concrete durability. High concentrations of CO_2 are a result of decaying organic matter and are usually found in sheltered bays and estuaries. Marine organisms are a typical source of H_2S (Mehta, 1991).

<u>Chemical Attack of Concrete and PG:Cement Composites</u>

The surface of the blocks is the first line of defense against seawater. With a high quality impermeable skin, the chemical effects of seawater can be limited to the surface of the block. If the block becomes permeable, there is a great opportunity for several harmful reactions. PG solubility in 20 ppt seawater is 3.8 g/1000g (James, 1992) and if the amount of the binding agent (eg cement) is not high enough the PG will dissolve.

When concrete is submerged in the seawater, the sulfate ion in the seawater can react with C_3A to form ettringite crystals according to the following reaction.

$$C_3A + 2CS'H_2 + 26H \longrightarrow C_3A \cdot 3CS'H_{32}$$
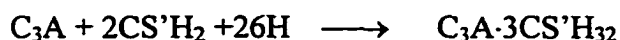
This reaction results in a volume increased of 227% (Neville, 1995). When the volume increase exceeds the tolerance-expanding limit of the hardened hydrated cement paste, ruptures develop. These ruptures increase the contacting area between

concrete and seawater, therefore enhances the formation of the ettringite. This cycle continues until degradation of the entire concrete.

Magnesium salts can also react with Portland cement paste in seawater resulting in the formation of brucite (magnesium hydroxide) and soluble products like calcium chloride and calcium sulfate. In old concrete, magnesium silicate ($4MgO \cdot SiO_2 \cdot 8H_2O$), resulting from ion exchanges between seawater and calcium silicate hydrates present in hydrated Portland cement, has been identified (Mehta, 1991). This substitution makes concrete weak and brittle.

Biological Environment

Marine growth, such as barnacles and mollusks, have been found on the surface of PG:cement composites. This growth is dependent on temperature, pH, water current, oxygen and light conditions on and surrounding the composite surface. Barnacles, sea urchins and mollusks are known to secrete acids, which can create boreholes in concrete and corrosion on the surface. It has also been reported that some mollusks are capable of producing ammonium carbonate (Lea, 1971), which is damaging to concrete, and another type of mollusk can bore into the hard limestone aggregate of concrete (Gerwick, 1986).

H_2S-generating anaerobic bacteria are found in sediments containing oil. *Theobacillus concretivorous* attacks weak and permeable concrete resulting in the corrosion of the embedded steel. Some aerobic or sulfur-oxidizing bacteria cause the conversion of H_2S to sulfuric acid, which may be highly corrosive to PG blocks. The marine environment is inhospitable for many commonly used construction materials such as concrete. Seawater contains many corrosive ions and gases along with

housing many marine organisms detrimental to construction materials. There are also temperature extremes and hydrostatic pressures capable of accelerating the deterioration of these materials.

CHAPTER 3

THE EFFECTS OF SALTWATER ON THE DISSOLUTION POTENTIAL OF
PHOSPHOGYPSUM:CEMENT COMPOSITES

Introduction

Phosphogypsum ($CaSO_4 \cdot 2H_2O$, abbreviated as PG), a solid by-product of

phosphoric acid production, has been classified as a "Technologically Enhanced

Natural Radioactive Material"(TENR) because it contains radionuclides and some

trace metals in concentrations that may pose a potential hazard to human health and

the environment (Roessler et al., 1979; May and Sweeney, 1984; Berate, 1990; Luther

et al., 1993).

The main disposal method of phosphogypsum is onsite stockpiling as

promulgated by the USEPA (Taha and Seals, 1991). This has resulted in at least 33

PG stacks located in all Gulf States except Alabama and has created a long term and

tremendous management problem(Taha and Seals, 1991). Environmental concerns

associated with PG disposal, coupled with increasing land costs for stockpiles, has

prompted research on alternative beneficial uses of this solid waste that will result in

applications considered protective of public health (Taha and Seals, 1991).

Solidification/stabilization is a widely used solid waste treatment technology,

which immobilizes harmful substances by adding inorganic binding materials such as

lime, cement, and fly ash to aqueous or solid wastes. This decreases the waste

leachability by reducing the contact surface between the leaching medium and the

waste (Malone et al., 1980, Barth et al., 1990). Portland cement solidification has

16

been proposed to prepare the phosphogypsum solid waste for aqueous applications including aquatic resource enhancement, artificial reefs, oyster substrate and shoreline erosion control.

Gypsum is an active ingredient in cement chemistry and is used to prevent "flash set". An excess of gypsum can lead to expansion and disruption of set cement, therefore, its addition is limited to a maximum of 3.5% (Neville, 1995). Phosphogypsum is readily soluble in seawater ($\approx$ 4.1 g/L at 35 ppt; James, 1977), and will dissolve to form calcium and sulfate ions. Sulfate ions can react with Ca_3Al oxides contained in cement to form ettringite crystals through the following reaction:

Ca_3Al Oxides$+2CaS$ Oxides$\cdot(H_2O)_2+26$ H_2O

$\longrightarrow Ca_3Al$ Oxides$\cdot 3CaS$ Oxides$\cdot(H_2O)_{32}$ (1)
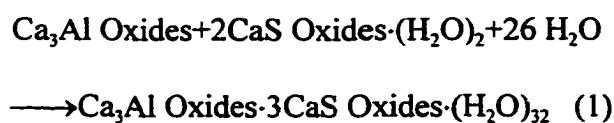
The formation of the ettringite increases the volume of the cement paste by 227% (Neville, 1995). When the volume increase exceeds the tolerance-expanding limit of the hardened, hydrated cement paste, ruptures develop, weakening the strength of the cement composites. The levels of PG (99.8% gypsum) used in this research are above 70% and can be detrimental to the composites.

A demonstration study (Chen et al., 1995) conducted at Louisiana State University showed that 70%:30% PG:cement test blocks placed in experimental seawater ponds on Grand Terre Isle, Louisiana for one year, supported a diverse population of surface attached, burrowing organisms and oysters, indicating the potential use of PG for offshore artificial reefs and oyster substrate. No loss of physical integrity was observed (Chen et al, 1995). On the other hand, the 85%:15%

PG:cement test composites placed in experimental seawater ponds in Grand Isle, Louisiana, for one month exhibited severe dissolution. Therefore, the purpose of the present investigation was to determine the mechanisms influencing the physical integrity of PG:cement composites for use in seawater applications.

Materials and Methods

PG Composite Fabrication

Raw phosphogypsum obtained from IMC-Agrico Co., Uncle Sam, Louisiana, was air-dried at room temperature for one day followed by oven drying at 45°C for 1-2 days. The dried phosphogypsum was crushed and passed through a 1.96 mm sieve. Fresh Portland Type II cement was passed through a 0.5 mm sieve. Phosphogypsum and cement were combined at the appropriate levels, mixed with water equivalent to 8% of dry weight and then compacted into 5.1 cm ϕ x 10.2 cm long cylinders at a compaction load of 2,720 kg. The target dry density was 1.6 g/cm^3. After one or two hours of air curing, composites were cured for 21 days at 100% humidity and room temperature.

One hundred 70%:30% composites were placed in one-quarter acre seawater ponds at the Louisiana Department of Wildlife and Fisheries' Lyle S. St. Amant Marine Laboratory (approximately 70 km south of New Orleans, Louisiana) for one year (Wilson et al., In Press). Composites were stacked in pyramids along the bottom of the pond and pond water was pumped out daily. Forty 85%:15% composites were placed in the bay adjacent to the Louisiana Sea Grant Oyster Hatchery in Grand Isle, Louisiana for one month (Rusch et al., 1998). The placement of these composites was

part of a larger project where blocks were strung between two bread crates approximately three feet in height. The pond and bay were located five miles from each other. Water chemistry conditions and the biological environment were similar between the two locations. Temperature ranges were 16-31°C and 14-34°C; salinity ranges were 15-28 ppt and 17-29 ppt and pH ranges were 7.8-8.5 and 7.7-8.6 for the bay and pond, respectively.

Instrumental Analyses

Petrographic, image, chemical and X-ray analyses were used to qualitatively and quantitatively characterize the composites. Samples of the 70%:30% and 85%:15% PG:cement composites were thin-sectioned to 30 μm following standard procedures (Hutchinson, 1974). Petrographic examinations for the composites were made using a polarized optical microscope in transmitted light to observe the material microstructure and microphase relationship. These images were used to identify crystal forms.

Secondary and back-scattered electron image analyses and elemental energy-dispersive X-ray spectrometry (EDS) mapping on the samples were performed using scanning electron microscopy (SEM; JEOL, 840A). The sections were coated with gold. The working distance was 5 – 10 mm and the operating voltage was 20 kV. Qualitative identification and quantitative composition analysis of the specific microzones were performed using an electron microprobe (JOEL JXA-733) equipped with a SEM capable of detecting boron, an energy-dispersive X-ray Spectrometer (EDS) capable of detecting carbon and a four wavelength-dispersive spectrometer

(WDS) capable of detecting uranium. The accelerating voltage was 15 keV, the beam current was 5nA and the takeoff angle was 40°. The data was reduced using the ZAF (Z= atomic number; A = absorption; F = fluorescence) method (Goldstein et al., 1992). Polished sections were coated with carbon for EDS and BSE (back-scattered electron) images.

Results

Surface Observations

70%:30% PG:Cement Composites. The 70%:30% PG:cement composites sampled from the Louisiana Department of Wildlife and Fisheries Marine Laboratory showed no signs of degradation. Images taken under crossed nicols from a polarized light microscope with a magnification rate of 100x clearly showed the formation of a crystalline layer on the surface of the composite (Figure 3.1). When an accessory plate (gypsum plate) was inserted, the high order white interference color remained on the coating layer. When viewing this thin-section at a magnification rate of 600x, the flash relief phenomenon was observed. This phenomenon combined with the high order white interference indicated the coating layer was composed mainly of carbonates.

The elemental content images (100x) of sulfur (S), silicon (Si) and calcium (Ca) for the 70%:30% PG:cement composites are presented in Figure 3.2. The Ca content image shows that the coating on the composite surface contains a higher content of Ca than observed in the composite body. Additionally, the Ca content in the coating is uniform, indicating that the coating may be a mineral not a mixture. The S content

image indicates that the coating does not contain S, and the S content in the composite body is not uniform. The non-uniform distribution of S and Si implies that the composite body is a mixture of high S content with low S content minerals, which coincides with the materials making up the composite. Portland Type II cement does not contain significant S, while PG ($CaSO_4 \cdot 2H_2O$) does.
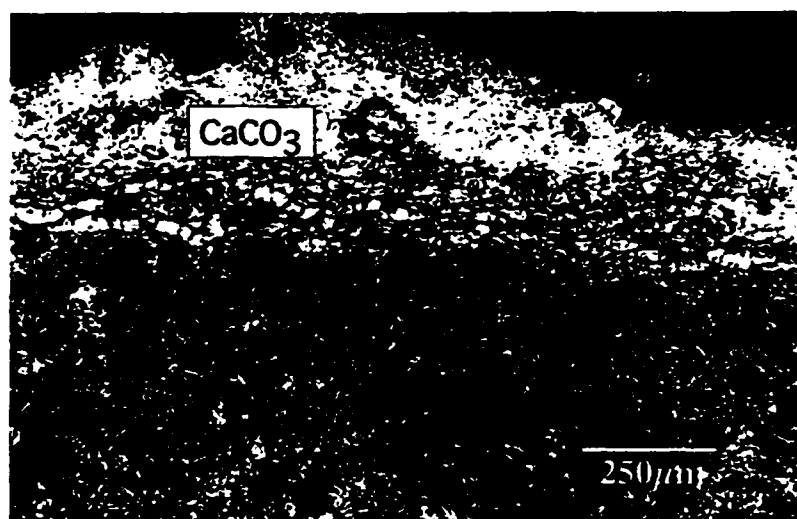
Figure 3.1 Polarized light microphotography (100×) taken under crossed nicols showed a crystalline coating layer on the surface of the 70%:30% PG:cement composites

The back scatter image of the coating (1500×, Figure 3.3) shows seven measurement points with their circular white rings, which were formed by beams of electrons during the microprobe quantitative measurement process (Table 3.1). Since the chemical composition of the coating layer is uniformly distributed, the average and standard deviation of CaO and MgO can be calculated to be 53.22±0.32% and 0.30±0.03%, respectively. The CaO content of USNM No.136321 calcite ($CaCO_3$) mineral provided by the Smithsonian Institution, Washington D.C. is 55.3%.
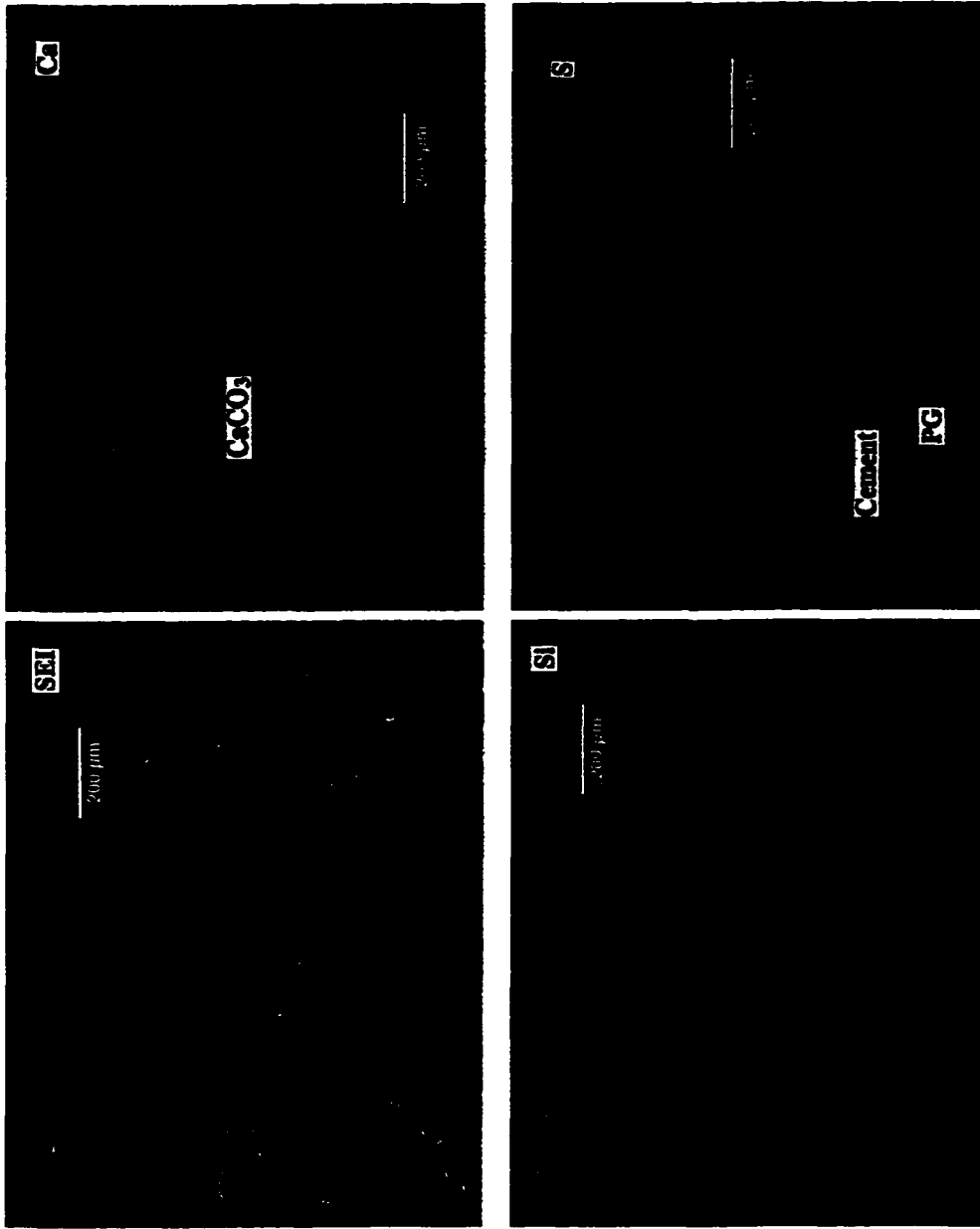
Figure 3.2 SEM X-ray microphotographs of the surface of the 70%:30% PG:cement composites confirmed the presence of calcium and the absence of sulfur and silicon

Therefore, the coating has been identified to be $CaCO_3$, with a 0.5% weight of $MgCO_3$. Since the coating sample was very small, the crystal forms of the $CaCO_3$ could not be identified; i.e. calcite or its allomorph, aragonite cannot be distinguished. Carbonates found in the marine environment consist of $CaCO_3$ and $MgCO_3$ with about 0.5% of the $CaCO_3$ being $MgCO_3$ (James, 1977; Neil and Malahoff, 1977), the same value as our results. The composite surface has a higher content of Mg than present in the body. In an estuary bottom water environment, $CaCO_3$ (calcite) is supersaturated by 590% (Guo et al., 1989). The pH value on the composite surface was determined to be above 11. The high pH and supersaturated conditions with respect to calcite would result in the precipitation of calcite. From a chemical composition point of view, the composite does not contain Mg (<0.5%) (Taha and Seals, 1991), while seawater does. All of the above data suggest that carbonate coating was formed in a high pH (>11) environment on the composite surface. Therefore, the reactants Ca^{2+}, Mg^{2+} and CO_3^{2-} are mainly from seawater and not from the PG:cement composite.

The SEM images of the 70%:30% PG:cement composites just below the surface are presented in Figure 3.4. Some 10 μm wide ruptures containing ettringite were found in this section. Identification of the ettringite was based on the work done by Roy et al. (1996).

85%:15% PG:Cement Composites. The 85%:15% PG:cement composites submerged in a coastal seawater bay in Grand Isle, Louisiana for just one month showed signs of heavy degradation. The composite diameter decreased from an average of 5.1 to 4.4 cm. Images taken under crossed nicols from a polarized light
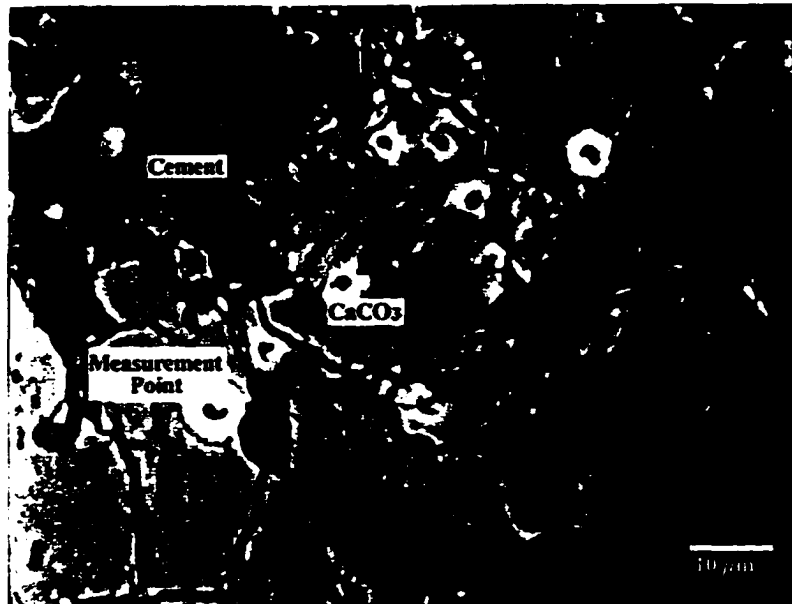
Figure 3.3 The SEM back-scattered electron microphotograph (1500x) of the 70%:30% PG:cement composite surface showed a close-up of the microprobe measurement point in the CaCO₃ coating layer
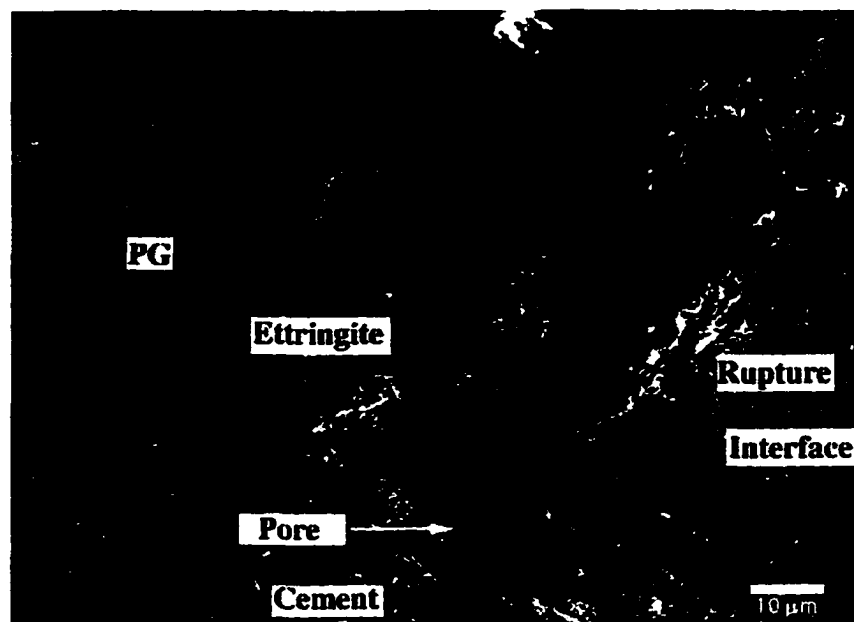
Figure 3.4 Ten-micron wide ruptures were identified in the zone just below the surface of the 70%:30% PG:cement composites

microscope with a magnification rate of 100 show 50μm wide ruptures on the surface of the composite (Figure 3.5). High order white interference color and the flash relief phenomenon were not found, indicating the absence of carbonate formation. Only some plate crystals and pastes were found.

Table 3.1 Results of X-ray microprobe analyses of the coating
layer of the 70%:30% PG:cement composites

Measurement No.	CaO (%)	MgO (%)
1	52.74	0.28
2	53.39	0.18
3	54.58	0.45
4	53.46	0.36
5	53.76	0.26
6	52.00	0.29
7	52.59	0.27
Average	53.22	0.30
DIV	0.32	0.03

The SEM image shows 100μm diameter pores and 50μm wide ruptures, both containing well developed ettringite (Figure 3.6). This layer can be easily scraped off, and the matrix is looser and physically different from what has been found in the PG composite body.

Body Observations

SEM images of the interface between the surface and body of the composites clearly shows a few 1 μm wide ruptures (Figure 3.7) and 1 μm diameter pores (Figure 3.8) with well developed ettringite (Figure 3.9) for the 70%:30% samples. In contrast,
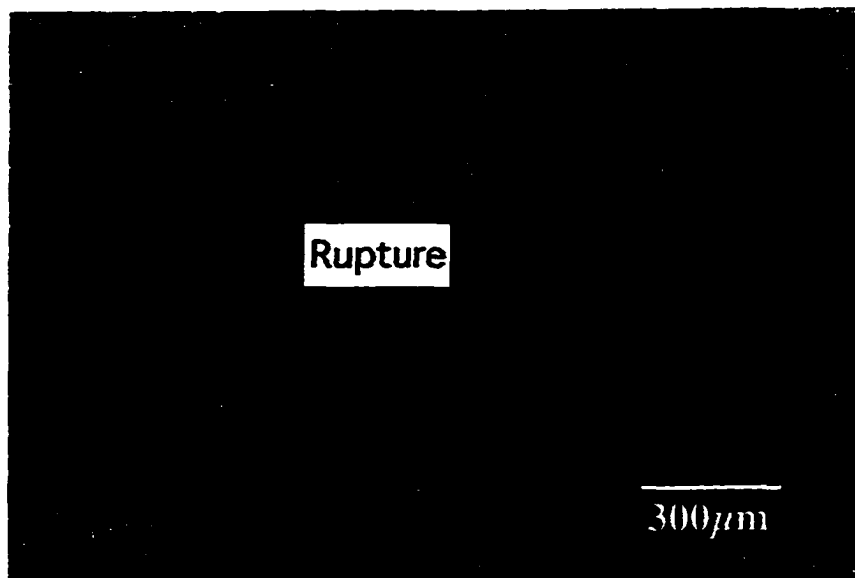
Figure 3.5 Fifty μm wide ruptures were observed in the surface zone of the 85%:15% PG:cement composites using polarized light microscopy (100x) under cross nicols
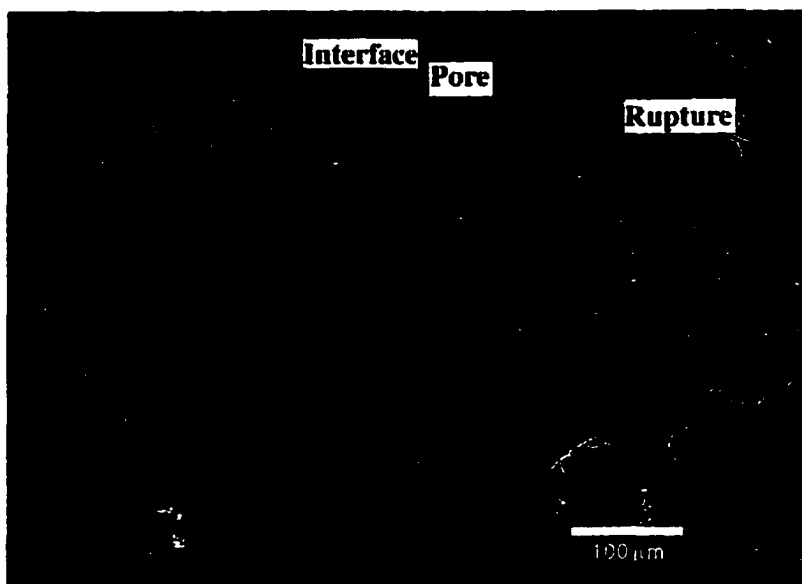
Figure 3.6 SEM microphotographs of the surface of the 85%:15% PG:cement composites corroborated the polarized light microphotographs, 50 μm wide ruptures and 100 μm diameter pores were found throughout the sample
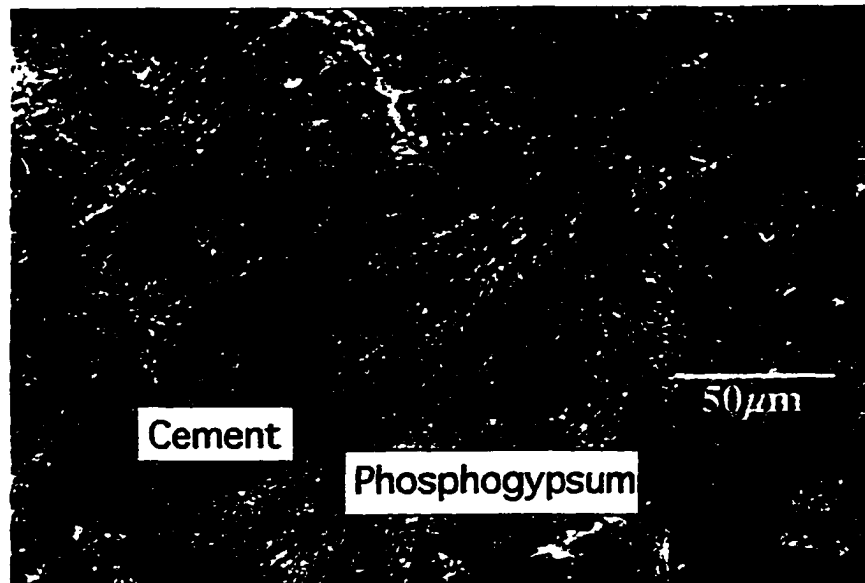
Figure 3.7 Plate crystals (phosphogypsum) and pastes (cement) were found throughout the body zone of the 70%:30% PG:cement composites using polarized light microscopy (100x) under cross nicols
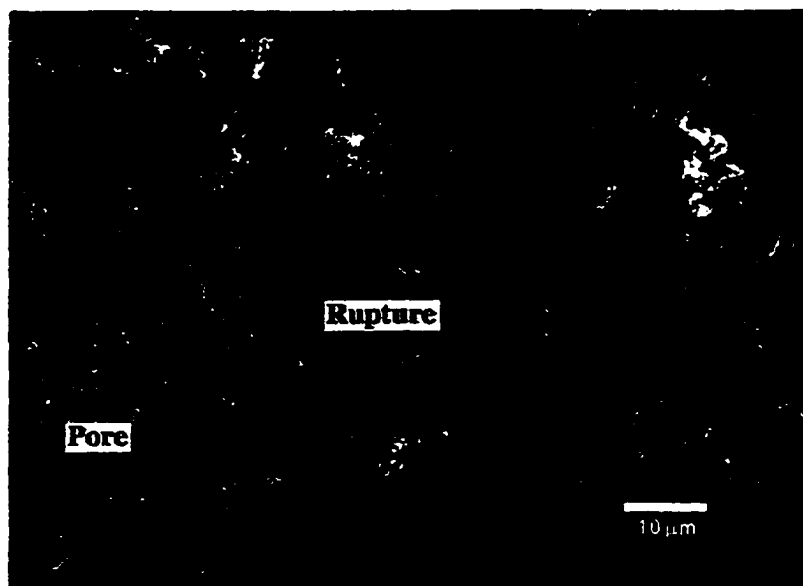
Figure 3.8 A few < 1μm wide ruptures and pores were found in the interface between the surface and the body of the 70%:30% PG:cement composites

several 10 μm wide ruptures and 5μm diameter pores (Figures 3.10 and 3.11) with well developed ettringite (Figure 3.11) were found in the 85%:15% samples.

Images (Figure 3.12) were taken under crossed nicols using a polarized light microscope with a magnification rate of 600x to observe body composition. Many plate crystals and paste were found. The plate crystals were identified as PG, while the paste is likely to be cement and cement mixed with PG. No evidence of carbonate formation was found. The 70%:30% PG:cement composite samples (Figure 3.12) exhibited a few small pores (diameter<0.5μm), while the 85%:15% sample had several small pores (diameter=1μm) and some ruptures (Figure 3.13).

Discussion

The Formation of a CaCO₃ Coating Layer and its Importance

The physical integrity of the PG:cement composites is determined by the strength of the cement paste and the permeability of blocks. Only permeability will be discussed here. The formation of the $CaCO_3$ coating layer reduces the permeability of the composites, which protects composites from seawater intrusion and prevents any possible toxic substance leaching. If this layer is breached for any reason, the newly exposed cement surface will again create the optimum condition for the formation of the $CaCO_3$ layer by creating a microzone of high pH conditions. This characteristic is very important for chronic toxicity of the PG:cement composites in the marine environment. While it was not investigated in this study, this self-repair ability may offer protection from radionuclide or other contaminant leakage. Further leaching studies are needed to confirm this hypothesis. If a solid waste is solidified and kept in
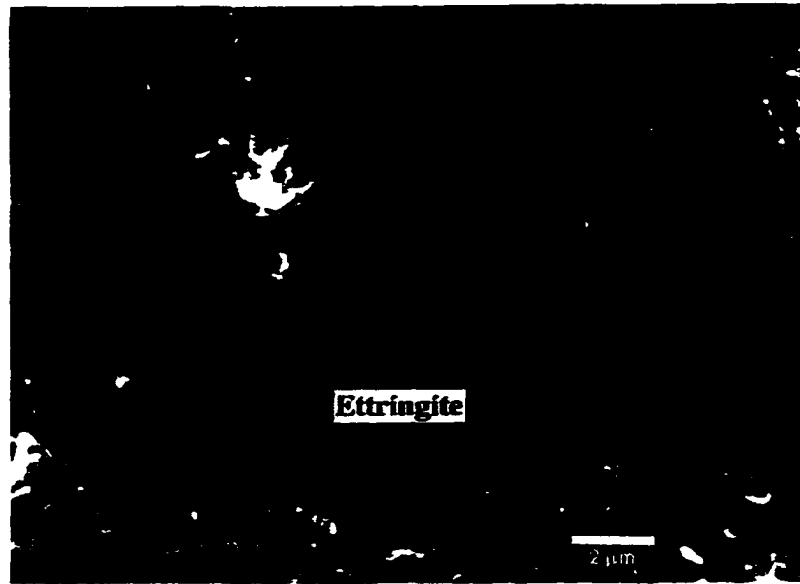
Figure 3.9 A scanning electron microscopy shows well developed ettringite on the pore walls
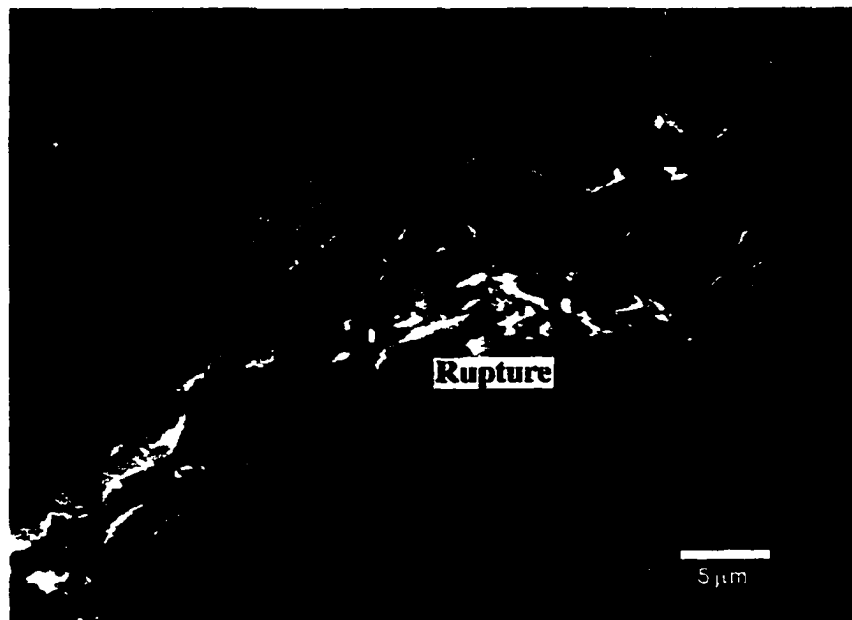
Figure 3.10 The 85%:15% PG:cement composites were found to have 5 μm wide ruptures and pores in the zone between the surface and the body of the sample
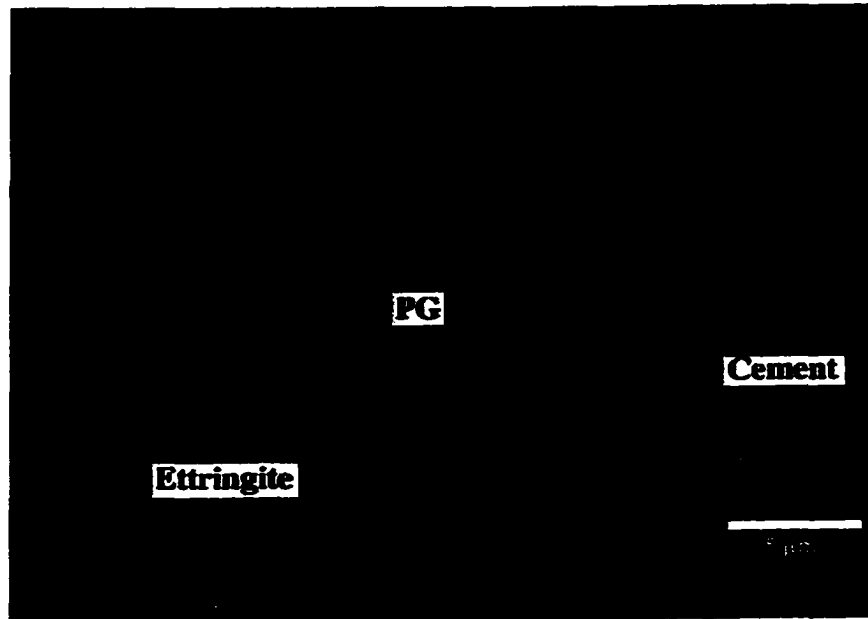
Figure 3.11 The walls of the pores shown in Figure 3.10 were found to have well developed ettringite, similar to that found in the 70%:30% PG:cement composite samples.
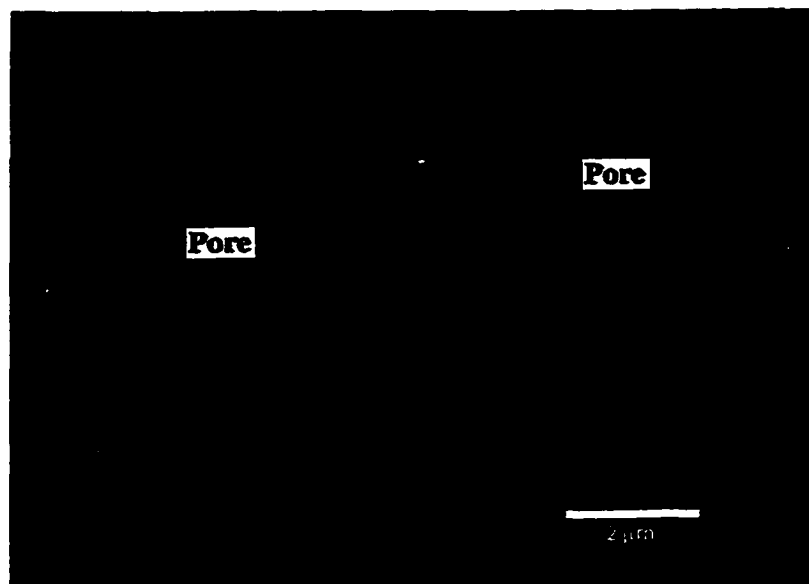
Figure 3.12 SEM microphotographs of the body zone of the 70%:30% PG:cement samples showed only a few <0.5 μm pores. The matrix, itself, was very tight and compact.
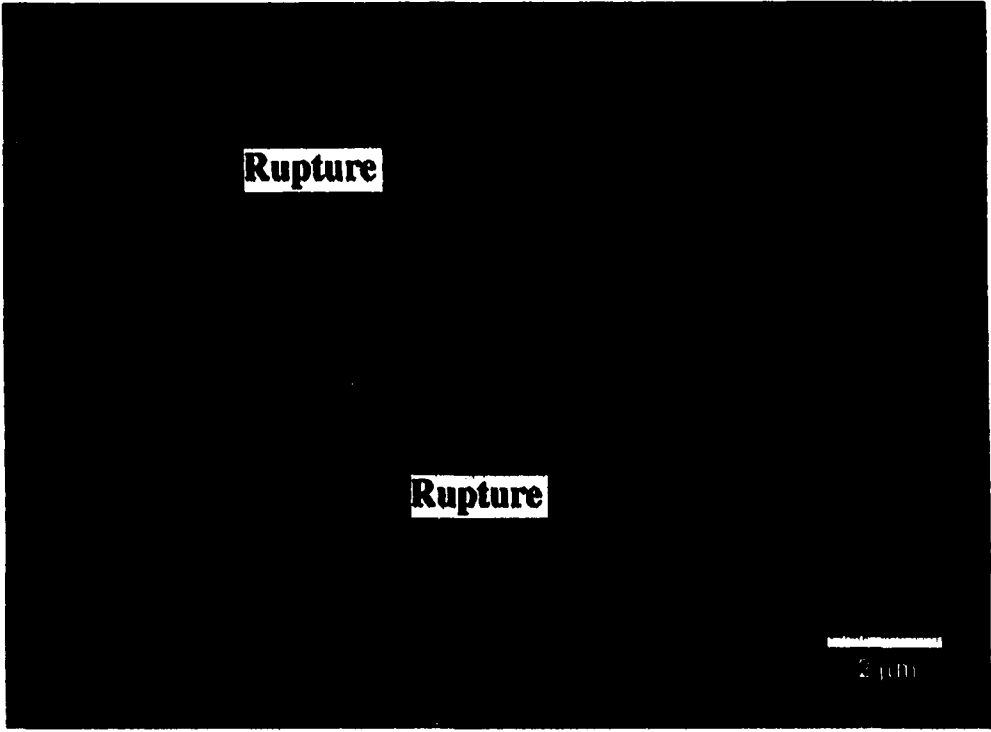
Figure 3.13 SEM microphotographs of the body zone of the 85%:15% PG:cement samples showed several 0.5 μm pores. The matrix was not as tight and compact as that found in the 70%:30% samples.

a high pH condition, a $CaCO_3$ layer will continuously form and protect wastes from leaching. The hydration of cement in the composites leads to the formation of lime, which leads to a pH increase. This increase must be high enough to neutralize the acidity of PG. Once the pH reaches approximately 11 on the composite surface, calcium carbonate begins to precipitate out and form a hard impermeable coating.

The Degradation/Dissolution Processes of the 85%:15% PG:Cement Composites

The needle crystals in the 85%:15% PG:cement composites were identified to be ettringite (Roy et al, 1996). Most of the ettringite in the 85%:15% PG:cement composites crystallized within the first few weeks during the moisture controlled curing periods. Afterwards, the ettringite content remained essentially constant (Gutti et al, 1996). When the composites were submerged in seawater, no calcium carbonate coating was formed because the 15% cement in the composite is only equivalent to 4.5% lime, which was not great enough to raise the pH value on the composite surface high enough for the formation/precipitation of $CaCO_3$. Without the protection of a $CaCO_3$ coating, the permeability of the PG composite is higher, permitting water to enter the composites and dissolve the phosphogypsum crystals in or on the block wall. According to the double layer theory (Metcalf and Eddy, 1991), the solution in the block wall pores reaches a saturated state. The high concentration of sulfate ions can react with Ca_3Al oxides (component of cement) to form ettringite crystals leading to a volume increase. When the volume increase exceeds the tolerable-expansion limit of the hardened, hydrated cement paste, ruptures develop. The ruptures increase the dissolution of the phosphogypsum by allowing more water intrusion. The dissolution

of the phosphogypsum further enhances the formation of the ettringite. This cycle continues and the composites degrade. Both the dissolution of the phosphogypsum and the formation of the ettringite crystals are judged to be jointly responsible for the degradation of the PG:cement matrix in the 85%:15% composites.

Though the composites were placed in different locations, the chemical/biological conditions of the water were similar. The only potential difference was wave action. Subsequent studies show that 70%:30% PG:cement and 85%:15% PG:cement composites placed next to each other in the bay at Grand Isle, exhibited the same behavior as the results presented here. Therefore, physical wave action can be disregarded as a potential source of difference.

In conclusion, cement content plays an important role in determining whether a $CaCO_3$ coating forms on the surface of the PG:cement composite. The Ca^{2+} and CO_3^{2-}, shown to make up the $CaCO_3$ coating of the 70%:30% PG:cement composite, comes from seawater and is illustrated by chemical composition analysis. The high cement ratio of the 70%:30% PG:cement composite provides strength and raises the pH by the production of lime from cement hydration. The quantitative relationships describing optimal composite configuration are discussed in further detail elsewhere (See Chapter 7).

CHAPTER 4

DETERMINATION OF CALCIUM DIFFUSION COEFFICIENT AS AN ESTIMATOR OF LONG-TERM DISSOLUTION POTENTIAL FOR PG:CEMENT:LIME COMPOSITES

Introduction

Phosphogypsum (PG, $CaSO_4 \cdot 2H_2O$) is a waste by-product of phosphoric acid production and is classified as a "Technologically Enhanced Natural Radioactive" (TENR) Material by EPA. The current allowable disposal method for PG is stackpiling, which has lead to the accumulation of more than 33 stacks located in Florida and Louisiana (Taha and Seals, 1991). The effects of these stacks on the environment consist primarily of groundwater contamination with trace amounts of heavy metals and air pollution from radionuclides, the most threatening being Ra^{226} and its daughter product Rn^{222}. With the US currently producing about 33 million tons a year at a cost of 800 million dollars for stackpiling, it is estimated that by the year 2000 the total US inventory of PG stacks will reach 2 billion tons (Taha and Seals, 1991).

The accumulation of PG stacks causes significant environmental problems that are placing increasingly more pressure on the fertilizer industry to find a long-term disposal solution. Various alternatives to the disposal of PG are being sought to decrease risks to human and the environment, and to reduce the cost of storage. One such alternative is the use of stabilized PG in the marine environment for aquatic resource enhancement. Because PG is highly soluble in saltwater, the stabilization of

34

PG requires cement concentrations high enough to prevent the dissolution of the PG under submerged conditions. Conversely, cement content must remain low enough to maintain the economic feasibility of such an approach. Studies have indicated the presence of a calcium carbonate coating on the surface of composites that showed no signs of deterioration following saltwater submergence (Please see Chapter 3). Calcium carbonate requires high pH conditions to form. The addition of lime to the cement:PG composites would aid in the production of calcium carbonate when submerged in saltwater thus reducing the composite permeability and the required cement concentrations needed to stabilize the PG. This paper presents mechanisms influencing composite integrity and processes this information to predict possible combinations of cement, lime, and PG that can maintain physical integrity in saltwater for prolonged periods of time.

Materials and Methods

Ingredient Selection

Based on cement chemistry, average cement and lime concentrations of 9% and 8%, respectively, with ±5% to compensate for other possible interactions between ingredients were determined necessary to reach the required pH of 11 for calcite formation. Ten ingredient combinations (Table 4.1) of PG:cement:lime were chosen by statistical methods (Kuehl, 1994). PG:lime ingredients were tested for pH effect only. The 85%:15%:0% PG:cement:lime and 70%:30%:0% PG:cement:lime composites were included for comparison. The 70%:30%:0% PG:cement:lime composites withstood saltwater submergence for one full year with no signs of

degredation while the 85%:15%:0% PG:cement:lime composites dissolved within one month.

Table 4.1 PG :cement:lime composite ingredients (%)

PG	Cement	Lime
70	30	0
83	9	8
83	3	14
83	14	3
84.6	10.7	4.7
84.6	5.7	9.7
85	15	0
86.4	7.3	6.3
87	0	13
88	9	3
88	4	8
89.6	5.7	4.7
90	0	10
93	4	3
93	0	7

Diffusion Model

Duedall et al. (1983) developed a diffusion model based on Fick's second law of diffusion $\partial C/\partial t = D(\partial^2 C/\partial x^2)$ and some related boundary conditions. This model is one-dimensional for ions in the solidified blocks and in well-stirred aqueous systems. It assumes a uniform distribution of diffused ions in the block and a flux of the ions across the block-water interface that is proportional to the concentration at the interface. This diffusion model is widely applied for diffusion constants calculations (Edwards and Duedall, 1985; Cote, 1986; and Seveque et al., 1992) because it is simple, reliable, and self-verified. The diffusion coefficient ($cm^2 \cdot day^{-1}$) was obtained

from the equation $J = S_o(D/\pi t)^{1/2}$, where J is the flux, S_o is the initial calcium concentration of the composite, and D is the effective diffusion coefficient. This equation was used for the diffusion coefficient calculation.

Composite Fabrication and Characteristics

Type II Portland cement was combined with lime and dried/crushed PG resulting in fifteen different combinations (Table 4.1). Eight-percent (dry weight base) water was added to attain the desired moisture content. Ninety grams of the mixture were weighed and compressed into a 3.81cm diameter and 3.81cm long steel mold under 9.8×10^7 N/m^2, using a static press. The composites had a surface area of 68.4 cm^2 and a dry density of 2.0g·cm^{-3}. The composites were allowed to cure at 100 % humidity and room temperature for over two weeks before testing. The average dry weight was 87 grams.

Dynamic Leach Test

The composites were subjected to a 28-day dynamic leach test (ANSI, 1986) to determine calcium diffusion from the composites. The diffusion coefficient, calculated from the calcium flux, was used to determine the governing equation representing the calcium carbonate formation. An 8:1 leachate volume to block surface area ratio was used. Composites were placed in 550 ml of 20‰ artificial saltwater (Instant Ocean™) and the leachant was completely exchanged at intervals of .08, .29, 1, 2, 3, 4, 5, 8, 11, 14, 21, and 28 days. The leachant was analyzed, in duplicate, for pH, calcium, and alkalinity. All analyses were performed in accordance with Standard Methods (APHA, 1995).

Instrumental Analyses

Qualitative and quantitative X-ray microprobe (SEM) (Joel JXA-733) analyses and scanning electron microscopy (Joel 8408) were used to analyze composite microstructure. Thirty μm sections from the 70%:30%:0%, 88%:9%:3%, and 88%:4%:8% PG:cement:lime composites were prepared in a manner to allow investigation of the composites' surface and body sections (Hutchinson, 1974). These composites were considered representative of the range of composites tested.

Statistical Analysis

The quadratic canonical polynomial (1) (See Chapter 7) was used in the data analysis.

$$y(x) = \sum_{i=1}^{k} \beta_i^* \, x_i + \sum_{i<} \sum_{j} \beta_{ij}^* \, x_i \, x_j + e_i \tag{1}$$

Where, $y(x)$ is $-\log_{10}(D)$, x_1 is cement content, x_2 is lime content, x_3 is PG content, β_i^* is the linear coefficient, β_{ij}^* is the linear interaction coefficient, e_i is the random error, a normal distribution with mean zero and variance σ^2. SAS 6.12 was used for the regression analysis, omitting the intercept.

Results

Dynamic Leach Test

Calcium released from the composites was estimated based on the following stoichiometric equations:

$$CaSO_4 \cdot 2H_2O \leftrightarrow Ca^{+2} + SO_4^{-2} \tag{2}$$

$$Ca(OH)_2 \leftrightarrow Ca^{+2} + 2OH^- \tag{3}$$

$$Ca^{+2} + CO_3^{-2} \leftrightarrow CaCO_3 \tag{4}$$

Lime breaks down into calcium and hydroxide ions. The hydroxide ions react with atmospheric carbon dioxide in a two step process to form bicarbonate and carbonate ions, respectively. From reaction stoichiometry, the carbonate and calcium ions have a 1:1 ratio and this difference in the alkalinity and measured calcium in the system yields a good estimate of the calcium leaching from the PG.

The released calcium was used to calculate the flux of Ca^{2+} and the depth of penetration for the diffusion process (x_c). Initially, Ca^{2+} fluxes ranged from 10^{-4} to 10^{-5} ($mol \cdot cm^{-2} \cdot day^{1}$) due to surface wash-off and dissolution. During the last three weeks of the dynamic leaching test, the flux decreased from 10^{-5} to 10^{-7}, ($mol \cdot cm^{-2} \cdot day^{1}$) which was attributed to diffusion. Calcium diffusion coefficients were calculated to range from 10^{-4} to 10^{-7} ($cm^{2} \cdot day^{-1}$). The 70%:30%:0% PG:cement:lime composites showed the lowest dissolution rate and highest pH of all combinations. The diffusion coefficients of the composites are presented in Table 4.2. The 83%:4%:13%, 83%:9%:8%, 84.6%:10.7%:4.7%, and the 84.6%:5.7%:9.7% PG:cement:lime composites all showed low diffusion coefficients with respect to the other combinations and developed full calcite coatings after two days. S_o was approximated to be .01 ($mol \cdot cm^{-3}$). The effective depth of penetration, x_c, was calculated from $x_c = (2Dt)^{1/2}$ and found to range from .06 mm to 30 mm. This showed that the PG:cement:lime composites can potentially survive for long period in salt water if only the diffusion process is considered.

Equation (1) was used to determine the relationship between the calcium

diffusion coefficient and composite ingredient. This relationship is:

-log(D) = -58.44*Cement - 135.62*Lime - 4.40*PG

+ 65.66*Cement*PG + 154*Lime*PG   (5)

Both cement and lime contribute negatively to the diffusion coefficients. However, the

interactions between cement and PG and between lime and PG contribute positively.

The results show that the PG:cement:lime stabilized composites can potentially

survive for long periods in saltwater if only the diffusion process is considered. Using

the regression equation (5), a range of composite compositions can be determined that

result in a diffusion coefficient equal to the 70%:30%:0% control that may have a

higher chance of survival in saltwater (Table 4.2). Since the summation of cement and

lime remain almost constant (24% - 26%) and the price of lime is currently similar to

that of cement, the addition of lime would not significantly reduce the cost of the PG

composites.

SEM Observations

SEM observations were made of four representative composites after

submergence and compared to images of composites that were not submerged. The

surface SEM images of the 70%:30%:0% PG:cement:lime composite show a dense

layer of $CaCO_3$ with a 0.5μm wide rupture between the $CaCO_3$ layer and the PG

composite (Figures 4.1a, b). A small amount of needle-like crystals identified to be

ettringite (Roy et al, 1996), were found on the pores and ruptures under the calcium

carbonate layer (Figures 4.1c, d). This layer of $CaCO_3$ is strong and can effectively

protect composites from saltwater attack. The unsubmerged 70%:30%:0%

PG:cement:lime composite (Figures 4.2a, b, c, d) did not show any surface

characteristics, such as calcium carbonate, or ettringite formation.

Table 4.2 Measured and predicted diffusion coefficients for PG:cement:lime
composites

Cement %	Lime %	PG %	Diffusion Coefficient (cm^2·day^{-1})
			Measured
70	30	0	1.52E-07
83	9	8	2.83E-05
83	3	14	1.28E-05
83	14	3	9.92E-05
84.6	10.7	4.7	4.26E-05
84.6	5.7	9.7	3.19E-05
85	15	0	5.66E-05
86.4	7.3	6.3	7.05E-05
87	0	13	1.58E-04
88	9	3	9.88E-05
88	4	8	8.77E-05
89.6	5.7	4.7	1.92E-04
90	0	10	2.81E-04
93	4	3	2.78E-04
93	0	7	2.19E-05
			Predicted
10	14	76	1.52E-07
11	13	76	1.52E-07
12	12	76	1.52E-07
13	12	75	1.52E-07
14	11	75	1.52E-07
15	11	74	1.52E-07
9	15	76	1.52E-07

*Diffusion coefficients were based on the log graph for the 28-day dynamic leach test.
The first day was omitted to account for surface wash-off.
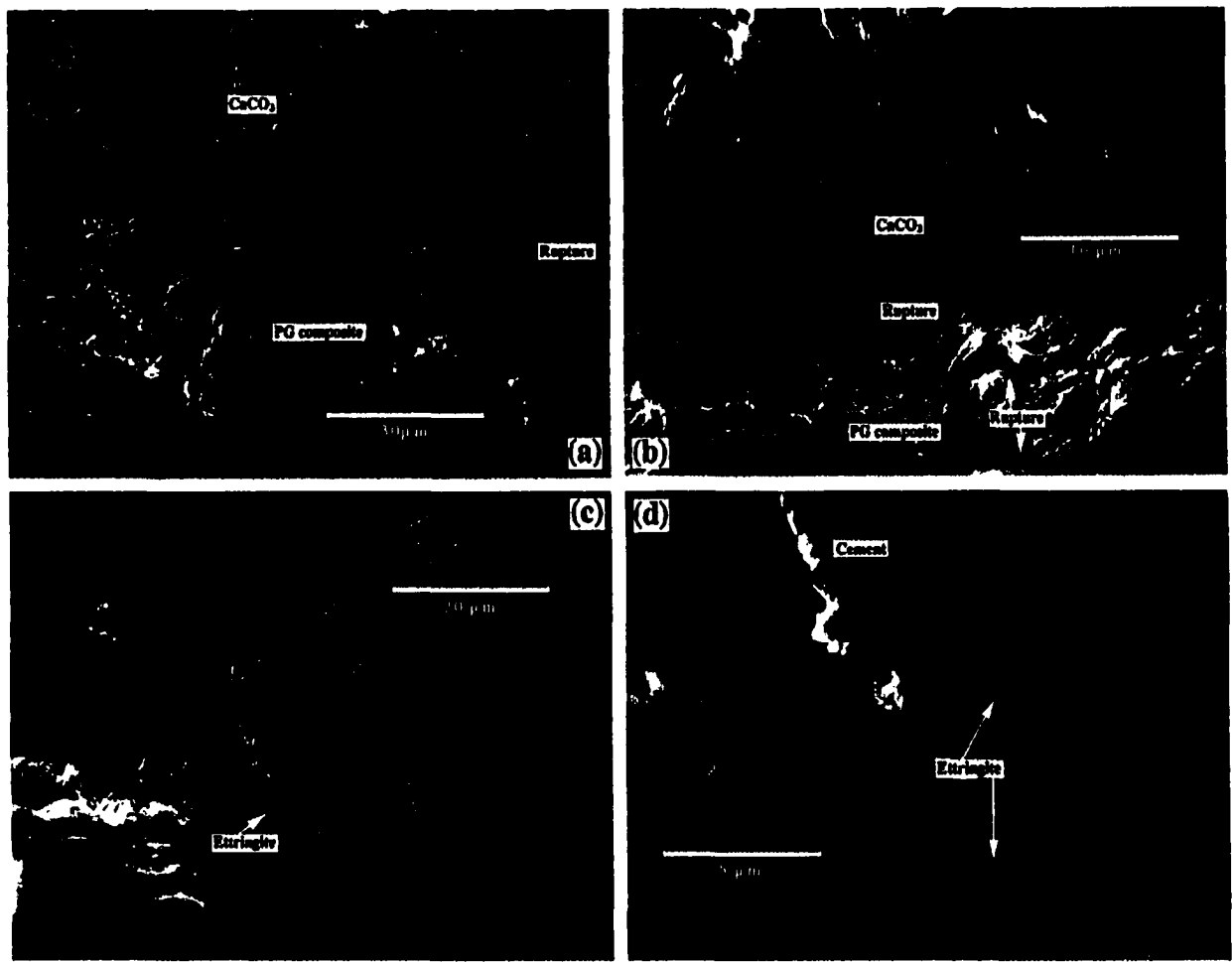
Figure 4.1 SEM images of 70%:30%:0% PG:cement:lime composite following the 28 day artificial saltwater dynamic
leaching test   (a) CaCO₃ coating on the surface zone   (b) Figure 4.1(a) under high magnification rate
                     (c) Ettringite on the pores and ruptures   (d) Figure 4.1(c) under high magnification rate
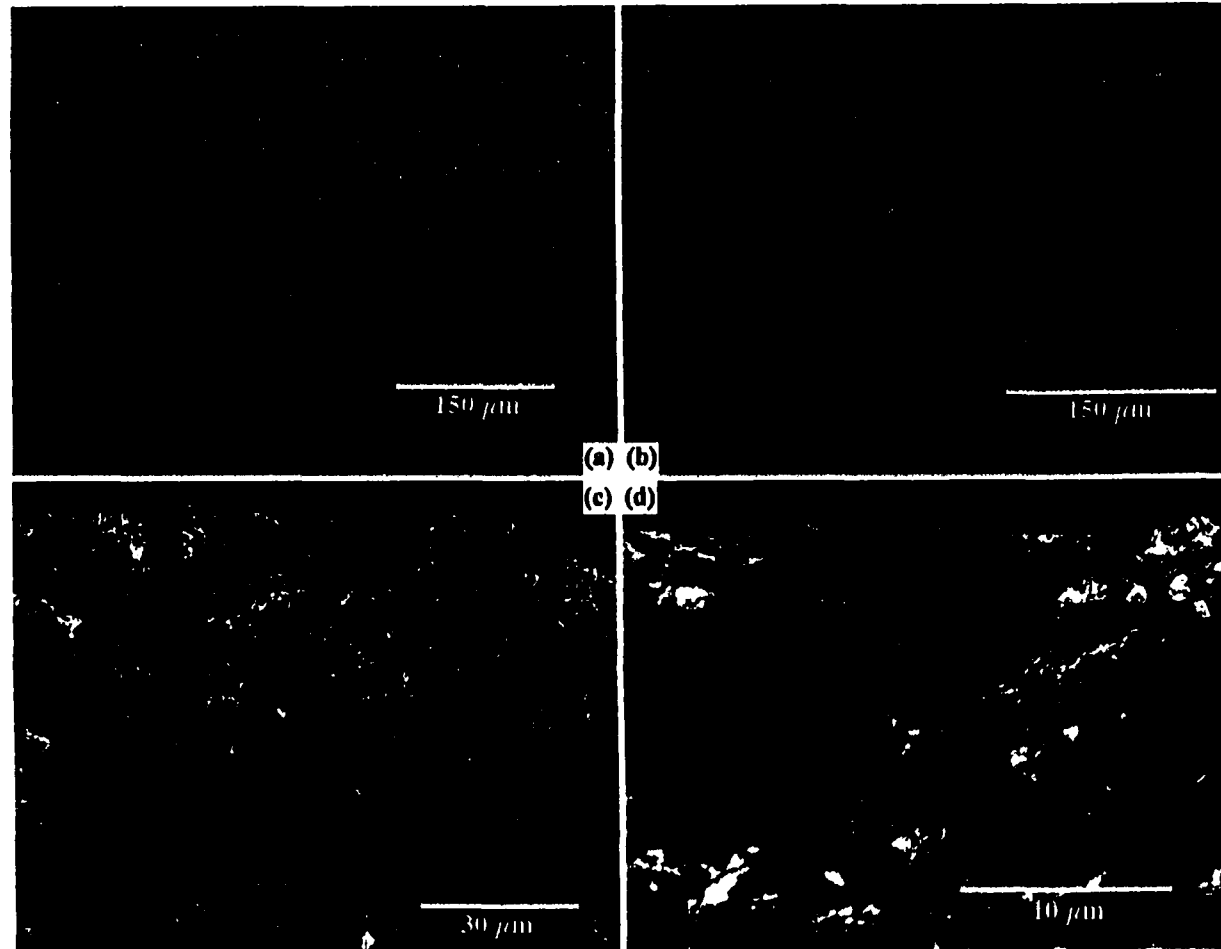
Figure 4.2   SEM images of 70%:30%:0% PG:cement:lime composite without treatment

(a) Surface zone under low magnification rate   (b) Surface zone under high magnification rate

(c) No surface characteristics in the surface zone   (d) Figure 4.2(c) under high magnification rate

The surface SEM images of the 88%:9%:3% PG:cement:lime composite show a dense layer of $CaCO_3$ and a 5 μm wide rupture between the layer and the PG composite (Figures 4.3a, b). More ettringite was found on the pores and ruptures under the calcium carbonate layer (Figures 4.3c, d). This layer can be easily scraped off, and the matrix is looser and physically different from what has been found in the PG composite body. The unsubmerged 88%:9%:3% PG:cement:lime composite (Figures 4.4a, b, c, d) did not show any surface characteristics, such calcium carbonate, or ettringite formation.

The surface SEM images of the 88%:4%:8% PG:cement:lime composite show a dense layer of $CaCO_3$ on the surface and about a 7μm wide rupture between the layer and the PG composite (Figures 4.5a, b). Fully developed ettringite was found on the pores and ruptures under the calcium carbonate layer (Figures 4.5c, d). This layer is also easily scraped off, and the matrix is looser and physically different from what has been found in the PG composite body. The unsubmerged 88%:4%:8% PG:cement:lime composite (Figure 4.6a, b, c, d) did not show any surface characteristics, such as calcium carbonate or ettringite formation.

The SEM images of the leached 93%:4%:3% PG:cement:lime composite shows a loose structure (Figure 4.7a, c) and a 20-60 μm wide ruptures (Figure 4.7a, b, c, d). The image shows no $CaCO_3$ dense layer of formed on the composite surface. The light touch could break the composite.
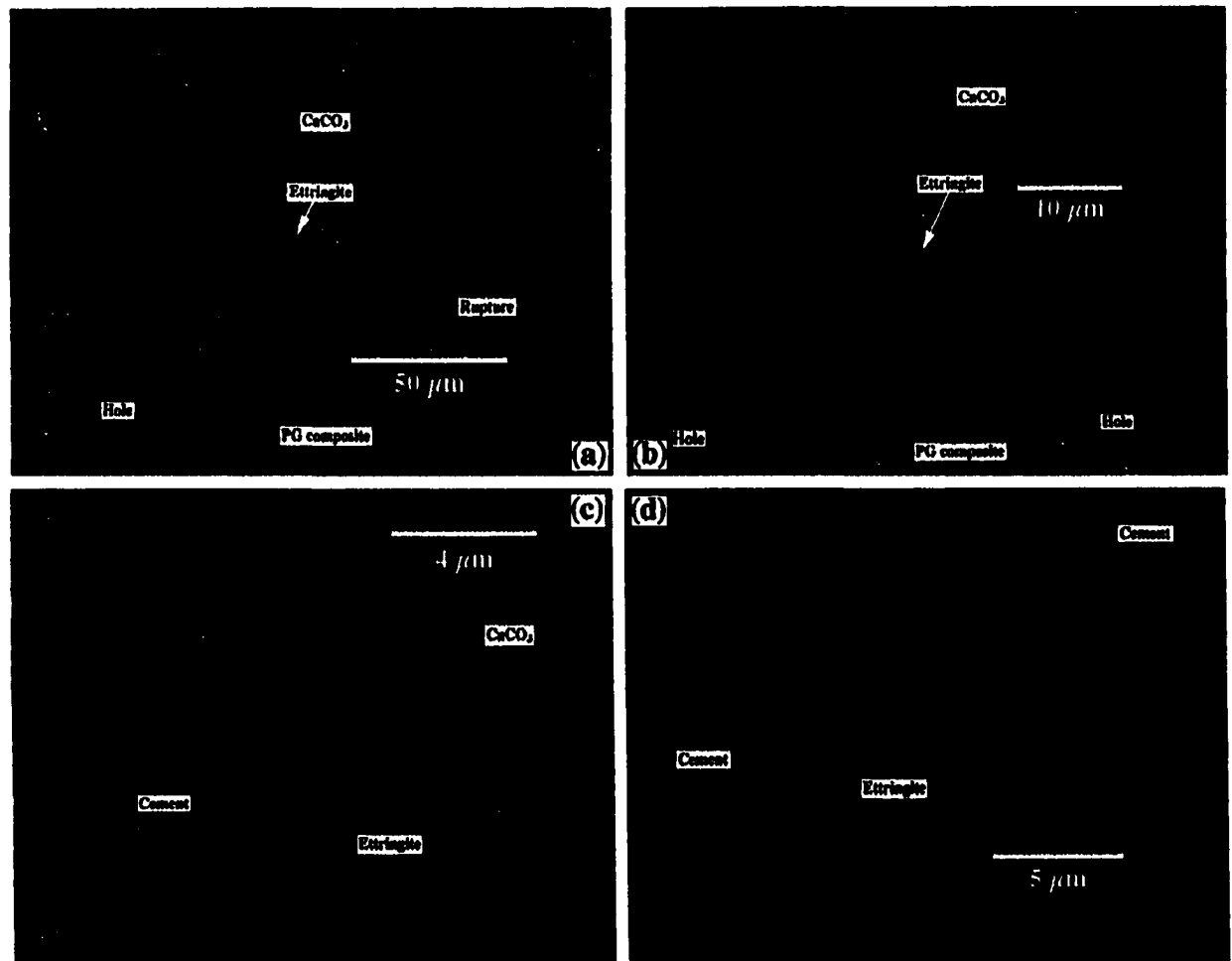
Figure 4.3 SEM images of 88%:9%:3% PG:cement:lime composite following the 28 day artificial saltwater dynamic leaching test   (a) $CaCO_3$ coating and ruptures on the surface zone   (b) Figure 4.3(a) under high magnification rate   (c) Ettringite on the pores and ruptures   (d) Figure 4.3(c) under high magnification rate
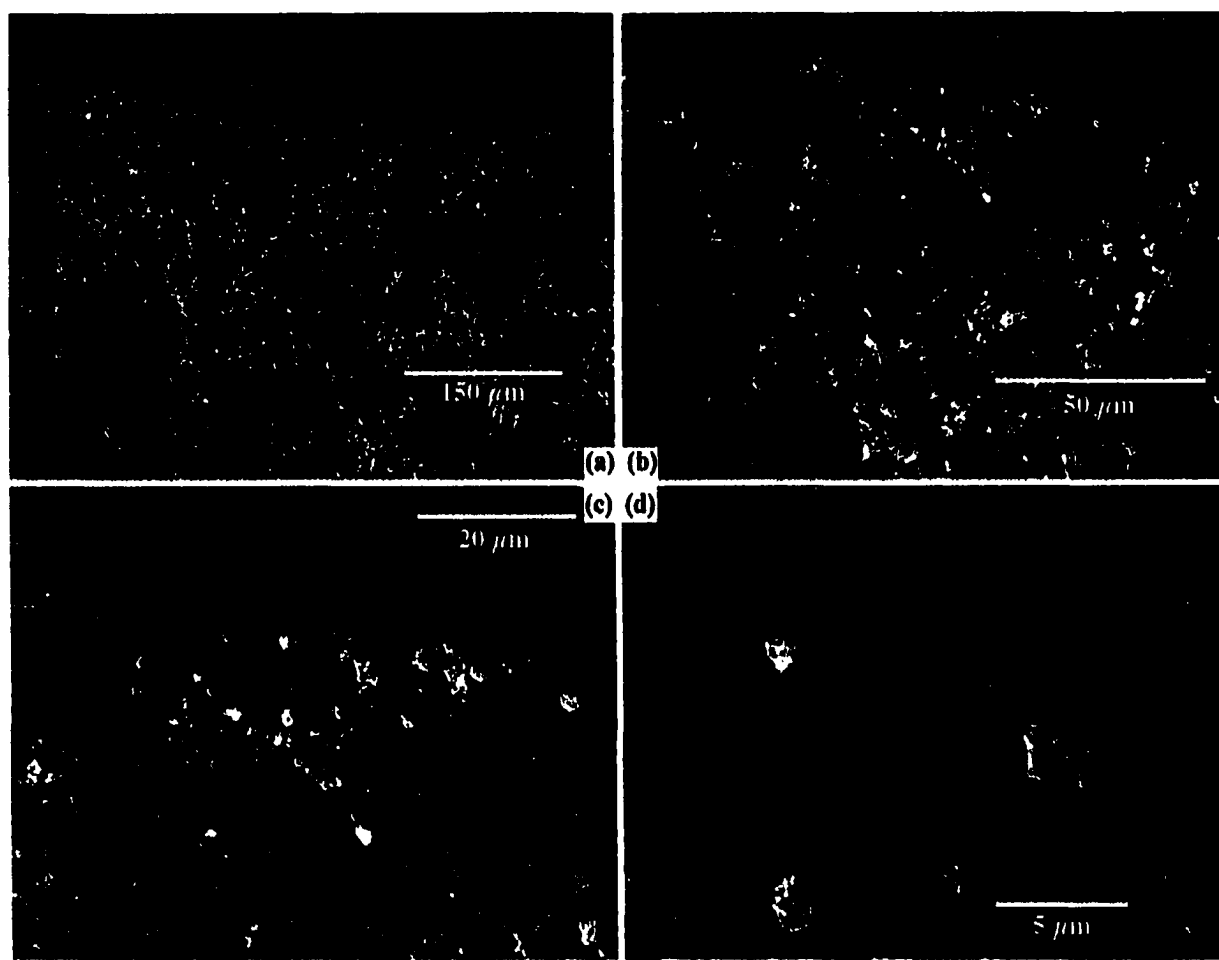
Figure 4.4 SEM images of 88%:9%:3% PG:cement:lime composite without treatment

(a) Surface zone under low magnification rate   (b) Surface zone under high magnification rate

(c) No surface characteristics in the surface zone   (d) Figure 4.4(c) under high magnification rate
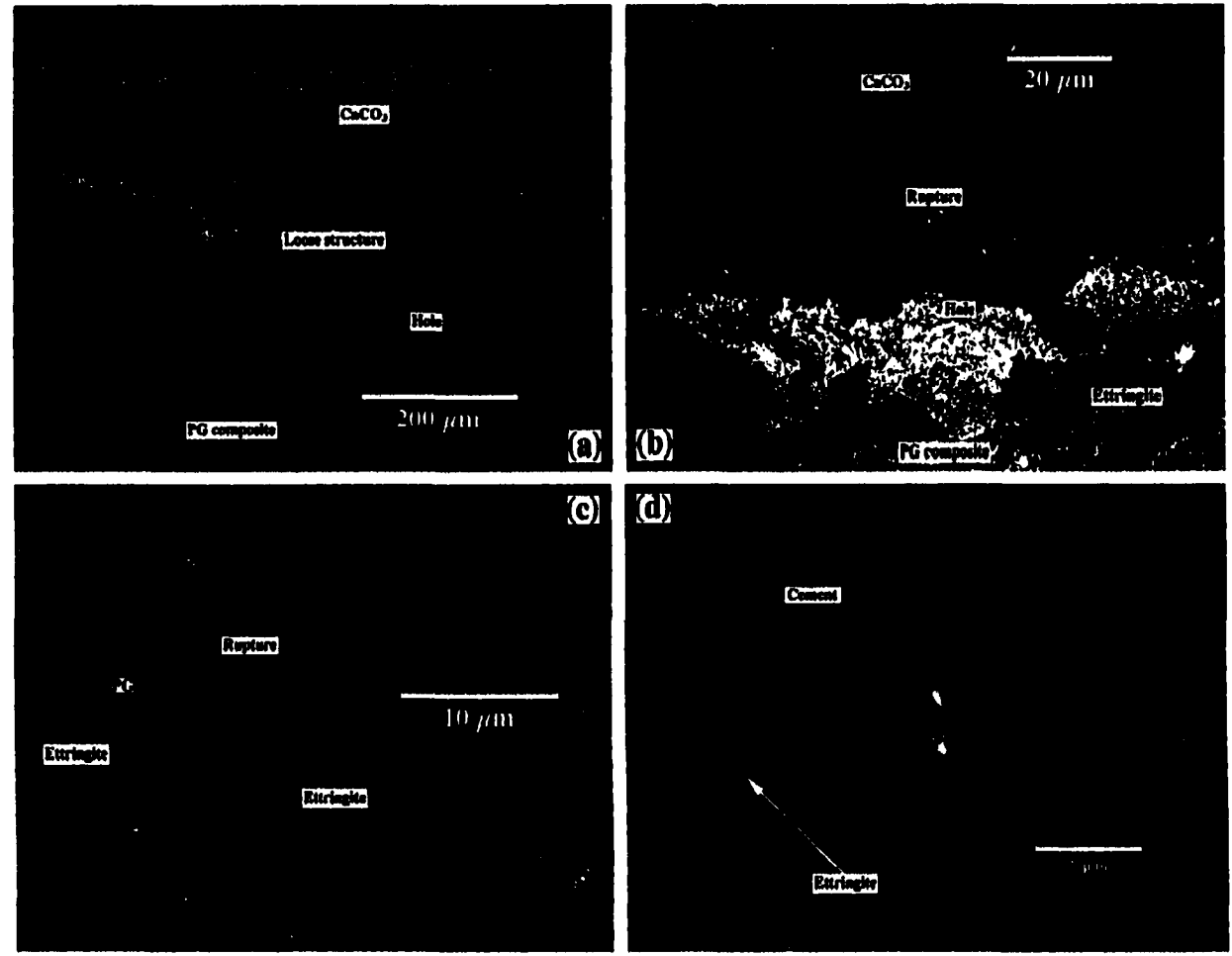
Figure 4.5 SEM images of 88%:4%:8% PG:cement:lime composite following the 28 day artificial saltwater dynamic leaching test   (a) $CaCO_3$ coating on the looser surface zone   (b) Figure 4.5(a) under high magnification rate
    (c) Ettringite on the ruptures and pores under the $CaCO_3$ coating   (d) Ettringite in a rupture under high magnification rate

47
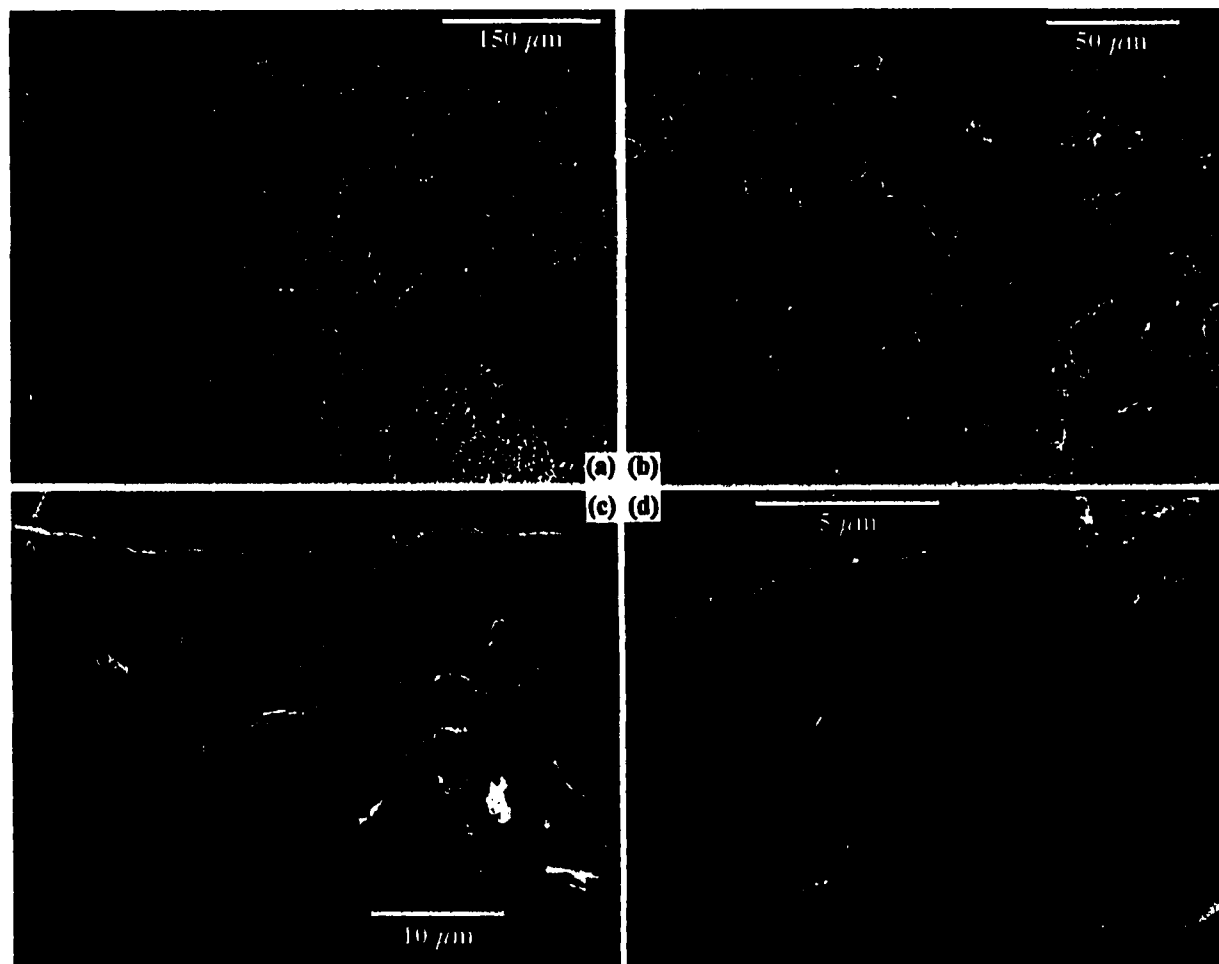
Figure 4.6 SEM images of 88%:4%:8% PG:cement:lime composite without treatment

(a) Surface zone under low magnification rate

(b) Surface zone under high magnification rate

(c) No surface characteristics in the surface zone

(d) Figure 4.6(c) under high magnification rate
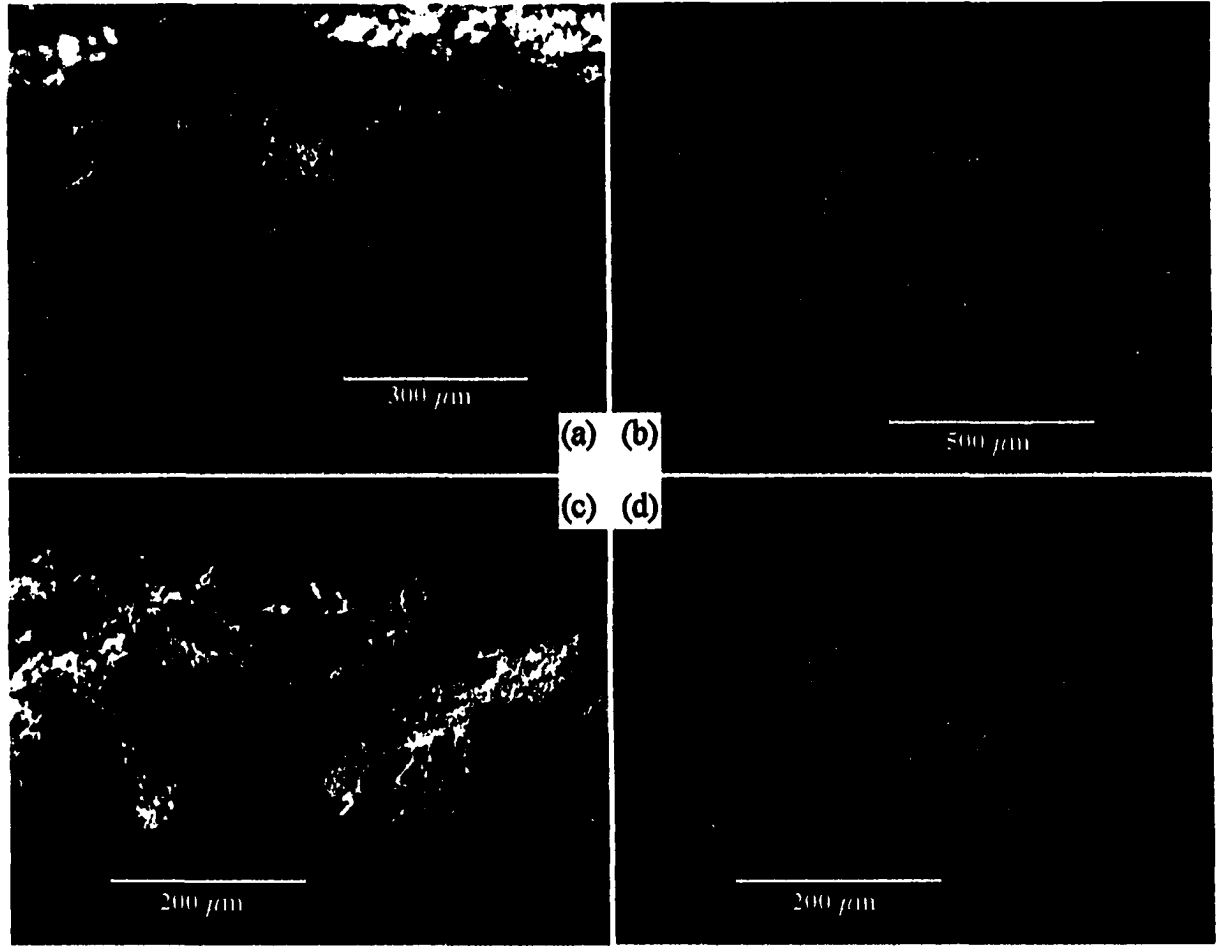
Figure 4.7 SEM image of 88%:4%:3% PG:cement:lime composite following the 28 day artificial seawater dynamic
leaching test (a) Loose structure in surface zone (b) Ruptures in surface zone
                (c) Pores in surface zone   (d) Ruptures in body zone

Microprobe Observations

The back-scatter image and X-ray element content images of sulfur (S), silicon (Si), and magnesium (Mg) for the 70%:30%:0% PG:cement:lime composites are presented in Figure 4.8. The back-scatter image (Figure 4.8a) shows that ruptures developed in the composite while S content image (Figure 4.8b) indicates a region of low S content along the tiny ruptures. There was also a region of high Si content (Figure 4.8c) along the tiny ruptures resulting from saltwater intrusion. Interaction with saltwater causes PG ($CaSO_4 \cdot 2H_2O$) to dissolve, decreasing the S content and increasing the Si content correspondingly. The 88%:9%:3% PG:cement:lime composite (Figures 4.9a, b, c) and 88%:4%:8% PG:cement:lime composite (Figures 4.10a, b, c) have similar distribution patterns for S and Si. Saltwater contains Mg, while PG contains less than 0.1% Mg. Mg ions in the saltwater exhibit an ion exchange reaction with the solid cement matrix, which contains some insoluble calcium, increasing the Mg content along the ruptures (Figure 4.8d). Therefore Mg content is considered to be an indicator of saltwater intrusion; the longer the ruptures are in contact with saltwater, the higher the content of Mg on the rupture walls. Our results show that the 88%:4%:8% PG:cement:lime composite has the highest Mg content (Figure 4.10d), 88%:9%:3% PG:cement:lime composite has medium Mg content (Figure 4.9d) and 70%:30%:0% PG:cement:lime composite has the lowest Mg content (Figure 4.8d). These results indicate that the 70%:30%:0% PG:cement:lime composite has the highest ability to resist saltwater attack, 88%:9%:3%
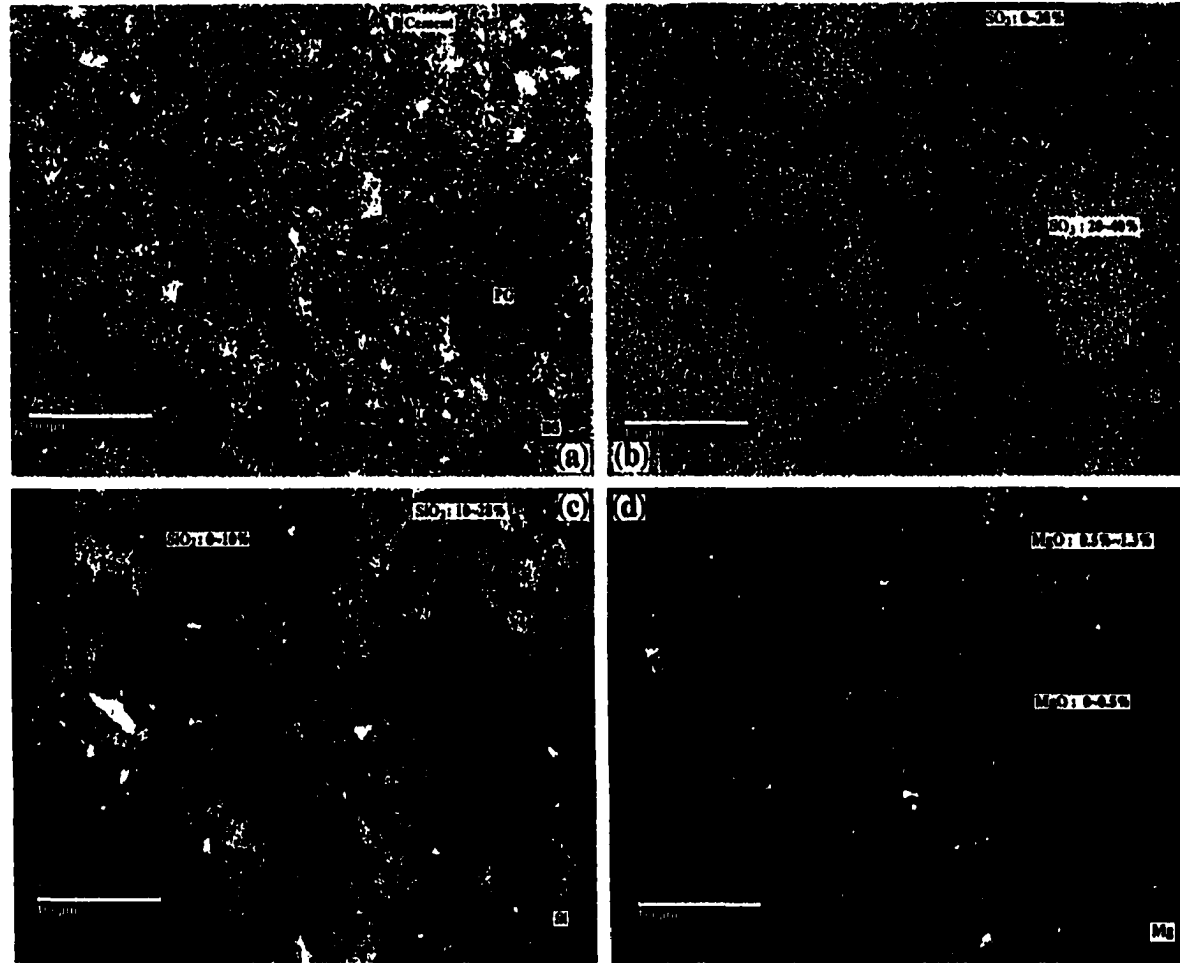
Figure 4.8 X-ray element images of 70%:30%:0% PG:cement:lime composite following the 28 day artificial saltwater dynamic leaching test
(a) BS image   (b) S image
(c) Si image   (d) Mg image
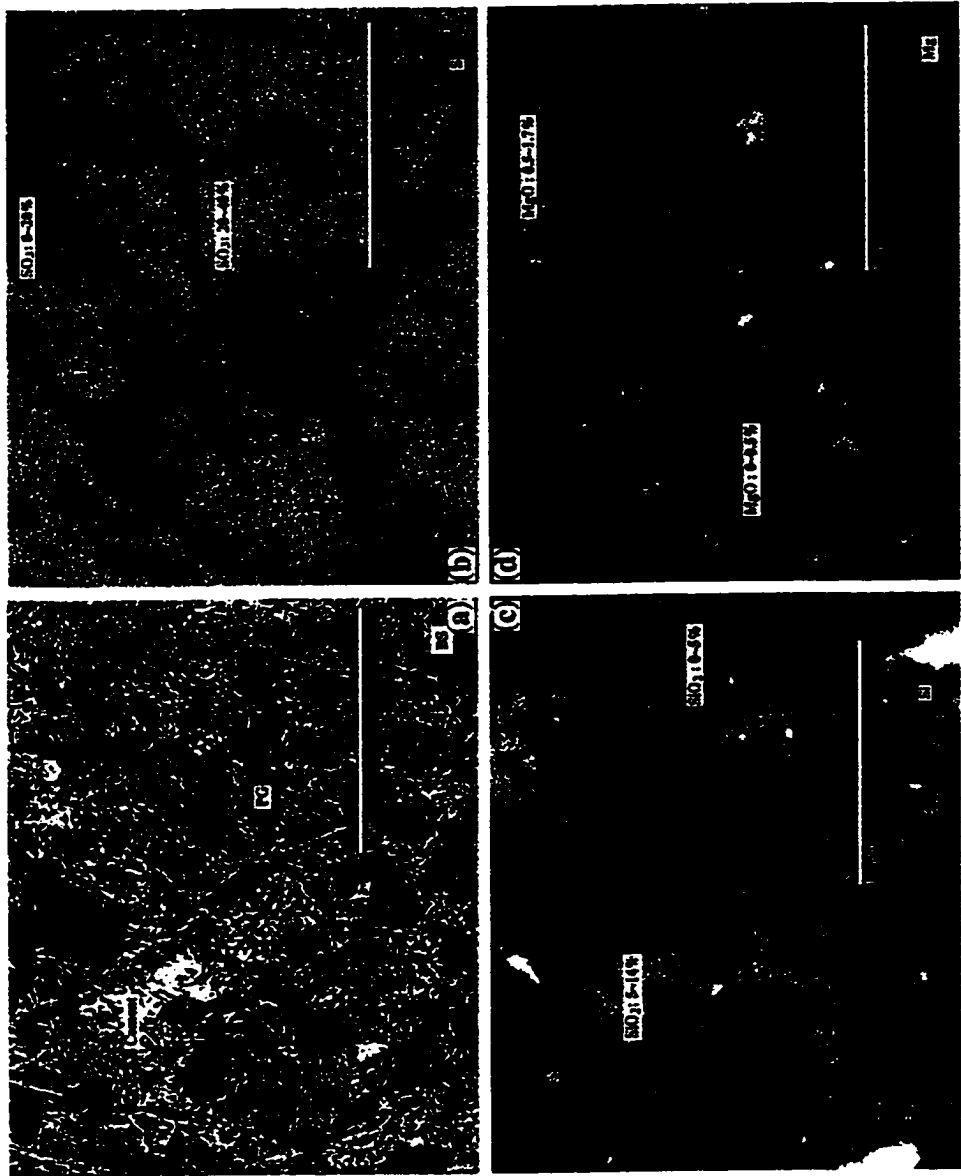
Figure 4.9 X-ray element images of 88%:9%:3% PG:cement:lime composite following the 28 day artificial saltwater dynamic leaching test

(a) BS image
(b) S image
(c) Si image
(d) Mg image
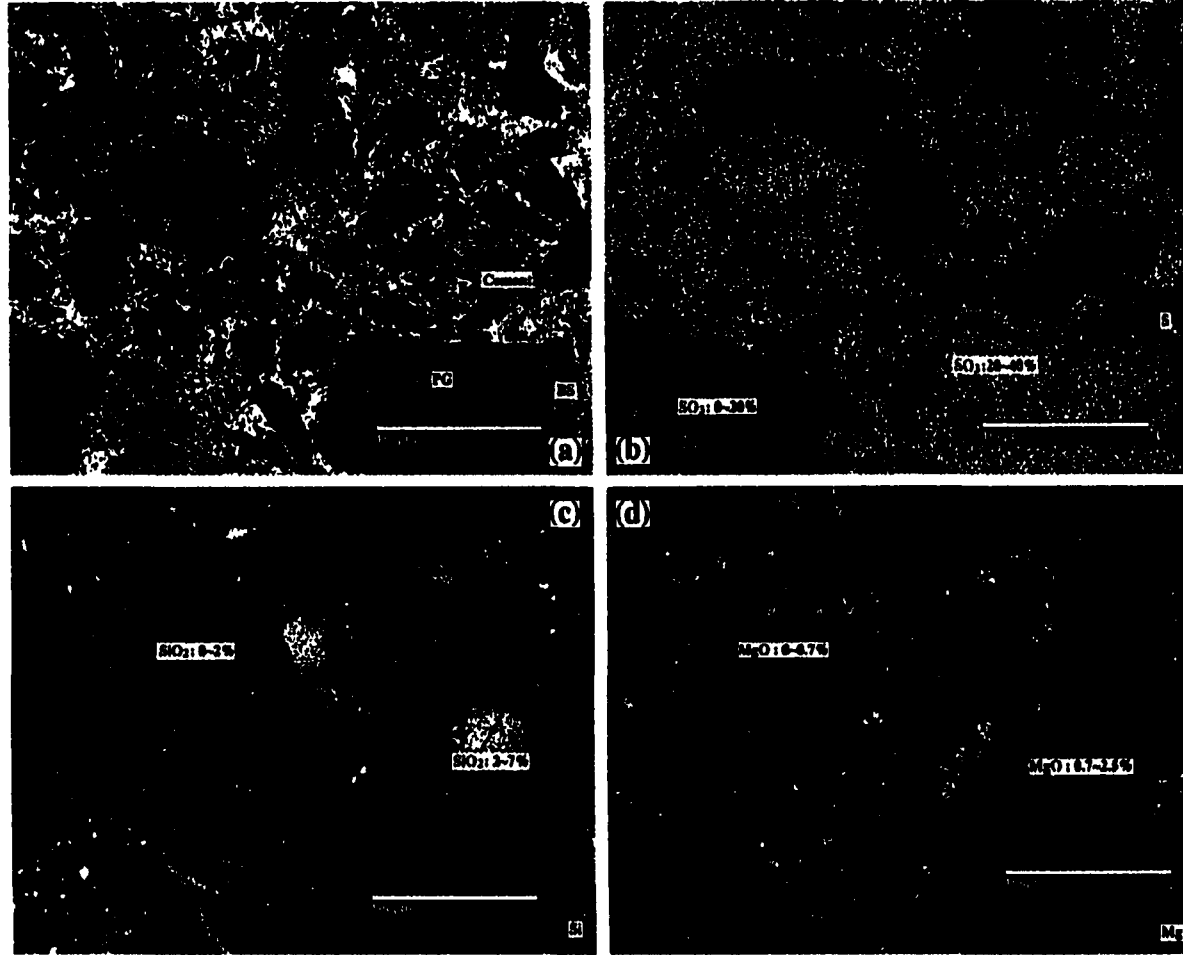
Figure 4.10 X-ray element images of 88%:4%:8% PG:cement:lime composite following the 28 day artificial saltwater dynamic leaching test   (a) BS image   (b) S image
                                                                            (c) Si image   (d) Mg image

PG:cement:lime composite has a medium ability to resist saltwater attack, while 88%:4%:8% PG:cement:lime composite has the lowest ability to resist saltwater attack. These results coincide with SEM observations.

Discussion

Scanning Electron Microscope observations of the composites used in the dynamic leaching test showed that ruptures developed in all combinations. SEM and microprobe results showed that the formation of the ettringite was responsible for rupture development. The formation of a $CaCO_3$ coating and a stable composite matrix were responsible for maintenance of physical integrity. When the PG composites were submerged in saltwater, the higher pH value on the composite surface would allow Ca^{2+} and CO_3^{2-} in the saltwater to form a dense layer of $CaCO_3$ on its surface. There was some saltwater included in the composite wall surface pores under the $CaCO_3$ layer. The included saltwater dissolves the phosphogypsum crystals in the composite resulting in an increase in sulfate ion concentration. The elevated content of sulfate ions in the included saltwater reacts with Ca_3Al oxides (a component of cement) in the PG composite surface region to form ettringite crystals leading to a volume increase. When the volume increase exceeded the tolerable-expansion of the hardened hydrated cement paste, ruptures developed. Both PG dissolution and ettringite formation processes weaken and loosen the matrix structure on the PG composite surface region. Based on the SEM observations, the extent of these desstructive processes are highest for the 93%:4%:3% PG:cement:lime composite, higher for the 88%:4%:8% PG:cement:lime composites, medium for the 88%:9%:3% PG:cement:lime

composites and lowest for the 70%:30%:0% PG:cement:lime composites. The lower the content of PG, the less destructive the processes are to the PG composite since PG is saltwater soluble. The higher the content of cement, the less destructive the processes are on the PG composite since cement provides the insoluble silicate matrixes and strength for the composite. With a loose and weakened infrastructure, the $CaCO_3$ layer can be easily washed away by saltwater currents or broken by some disturbances, such as burrowing organisms. With a broken $CaCO_3$ layer, saltwater can infiltrate the composite and a $CaCO_3$ layer can be reformed, but the infrastructure will still be weak and loose. This cycle would repeat until the 88%:9%:3% PG:cement:lime and 88%:4%:8% PG:cement:lime composites dissolved entirely. For the 93%:4%:3% PG:cement:lime composite, the destructive processes were so strong that no $CaCO_3$ layer was formed. This destructive process has only a limited effect on the 70%:30%:0% PG:cement:lime composite because of its higher content of cement and lower content of PG. The $CaCO_3$ layer adheres on the composite surface firmly to protect from saltwater attack.

The relationship between the diffusion coefficients and the microstructures is shown in Table 4.3. Table 4.3 shows that the ruptures can dramatically increase the diffusion coefficients. The $CaCO_3$ layer may decrease the diffusion coefficients. Calculation for the diffusion coefficients were based on the composite surface area, not actural area, which should include the rupture surface area that contacts the saltwater. The development of rupture will increase the diffusion coefficients even under the conservative assumption that the actural diffusion constants are the same for

Table 4.3 Relationship between diffusion coefficients (D) and microstructure for PG:cement:lime composites

PG%	Cement%	Lime%	D $(cm^2 \cdot day^{-1})$	Rupture width (μm)	$CaCO_3$ layer
70	30	0	1.52E-07	No	Yes
88	9	3	9.88E-05	4-7	Yes
88	4	8	8.77E-05	6-10	Yes
93	4	3	2.78E-04	20-60	No

all PG composites. Therefore, calcium diffusion coefficients is an estimator of long-term dissolution potentials. The PG:lime ingredients could not reduce the diffusion coefficient (Table 4.2) and will not be recommended for further experiments. Based on the model prediction, the combinations listed in Table 4.3 such as 76%:10%:14% PG:cement:lime and 75%:14%:11% PG:cement:lime show the greatest potential for satisfactory field performance based on their lower predicted diffusion coefficients.

CHAPTER 5

DISSOLUTION POTENTIAL AND MECHANISMS INFLUENCING PHYSICAL INTEGRITY OF PG:FLY ASH:LIME COMPOSITES

Introduction

Phosphogypsum (PG, $CaSO_4 \cdot 2H_2O$) is a solid waste produced during the production of phosphoric acid. PG contains some radionuclides and trace metals in concentrations, which may pose a potential hazard to human health and the environment. The current allowable disposal method of stockpiling has resulted in at least 33 PG stacks with an average area of 224 acres per stack. PG stacks have created significant environmental concerns from airborne radiation to surface and groundwater contamination (Taha and Seals, 1991). In the last 20 years, much effort has been engaged to the research on various alternatives to the disposal of PG (Taha and Seals, 1991).

Previous research done at Louisiana State University showed that different combinations of cement and lime added to stabilize PG did not meet economic requirements therefore, more cost-effective materials are being investigated to replace or significantly reduce cement as a binding agent. Class C fly ash with cementous properties was chosen to replace cement as the binding agent. Fly ash is a solid residual of coal or oil combustion in electric power plants and is composed of metallic oxides, silicates, and other inorganic particulate matter. The chemical composition of fly ash is influenced by the type of coal used, the completeness of the combustion process, and the mineral content of the coals (Atalay et al., 1990). The volume of fly

57

ash produced from coal combustion is about 10% of the feed coal, and only 30% of fly ash is currently reused (Higgins, 1995). In 1996, 948 million tons of coal was consumed (DRI/MaGraw-Hill etal. 1998) and it is estimated that 94.8 million tons of fly ash was produced with only 28.4 million tons of fly ash consumed. There is 66.4 million tons of fly ash that remain unused today. Different PG:fly ash:lime ingredients are being tested to find a possible ingredient composition that can maintain structural integrity when submerged in saltwater.

Materials and Methods

Binding Agent Selection

The chemical compositions of the fly ash reflect the geological setting of the coals: some ash are aluminum-rich or aluminum/iron-rich silicates, Class F, while others may contain a lot of Ca, Class C (Glasser et al., 1987). Figure 5.1 shows some major characteristic composition ranges, projected on a $CaO-Al_2O_3-SiO_2$ ternary grid. The compositions are averages, and the method of projection ignores the presence of other minor oxides, such as MgO, Fe_2O_3 (Glasser et al., 1987). It is obvious that Class C fly ash pastes possess good cementing characteristics as evidenced by the highest silicon content recovered as oligomeric silicates from hydration products. Class F fly ash pastes, on the other hand, possesses minimum cementing characteristics unless mixed with cement or Class C fly ash (Malek et al. 1988). The function of fly ash in solidified PG composites is similar to that of cement. Fly ash serves as a source of dehydrated silicates and is used as a basic material. Dehydrated silicates provide strength for the PG composites and the fly ash is able to neutralize the acidity of raw

PG, creating the necessary basic environment to prevent possible leaching of toxic metals from the PG composites. With this new approach, two types of solid waste can be converted into useful resources such as artificial reefs and oyster substrates.

Figure 5.1 Major composition of cement and other binding agents

Three PG composites with typical ingredient combinations, 62%:35%:3% PG:fly ash:lime, 55%:42%:3% PG:fly ash:lime and 58.5%:35%:6.5% PG:fly ash:lime, were sampled for SEM observation. These PG composites were divided into two groups. One group was submerged in the artificial saltwater for one month and the other group was stored in plastic bags and did not receive any treatment.

Scanning electron microscopy indicated the presence of a calcium carbonate coating on the surface of the PG composites that maintained their physical structural integrity. Conversely, PG composites that exhibited severe degradation were lacking the calcium carbonate coating. The catalyst affecting the presence or absence of the calcium carbonate coating on the composite surface was determined to be a localized zone of high pH (see Chapter 3). Experimental analysis of fly ash determined that a paste mixture of 38.5% fly ash and 61.5% PG has a pH of 10.8, so the searching center for fly ash was determined to be 38.5%. According to thermodynamic calculations, the pH must reach 11 in order for calcium carbonate to precipitate out on the surface of the PG blocks. Augmented simplex centroid design with pseudocomponents method was applied for ingredient content selection (see Chapter 7). The composite combinations for PG:fly ash:lime are listed in Table 5.1.

PG Composite Fabrication

Lime was combined with fly ash and PG according to the ingredient composition. Dry raw materials were mixed to form the dry mixture. The dry mixture was mixed with water equivalent to 8% of dry weight and completely homogenized. Ninety-six grams of the resulting mixture was weighed and poured into a 1.5 inch steel mold, then compacted to a 1.5 inch long cylinder under 9.8×10^7 N/m^2, using a static press. Theoretically, the dry density should reach 2.0 g/cm^3. Blocks were allowed to cure at room temperature and 100% humidity for over two weeks before testing and the average dry weight was 87 grams. Ten months after the composites were made the diameters were measured.

Table 5.1 PG:fly ash:lime composite ingredients (%)

PG	Fly ash	Lime
62	35	3
58.5	38.5	3
55	42	3
59.6	36.2	4.2
56.2	39.6	4.2
57.4	37.3	5.3
58.5	35	6.5
55	38.5	6.5
56.2	36.2	7.6
55	35	10

Dynamic Leach Test

A variation of the dynamic leach test (ANS, 1986) was performed to determine calcium release rates from the PG composites. The leachate volume to block surface area ratio was 8:1. Composites were tested in duplicate and were placed in 550 ml of 20‰ artificial saltwater (Instant Ocean™). The leachate was completely exchanged at intervals of .08, .29, 1, 2, 3, 4, 5, 8, 11, 14, 21, and 28 days and analyzed for pH and alkalinity (APHA, 1995). Calcium was measured by Inductively Coupled Argon Plasma (ICAP) in Department of Agronomy, Louisiana State University.

SEM & Microprobe Analyses

Qualitative and quantitative X-ray microprobe (Joel JXA-733) analyses and scanning electron microscopy (Joel 8408) were used to analyze the composite microstructure of the composites involved in the dynamic leaching test. Thirty μm sections from the 62%:35%:3%, 55%:42%:3%, and 58.5%:35%:6.5% PG:fly ash:lime composites, were prepared in a manner to allow investigation of the composite surface

and body (Hutchinson, 1974). The three composites are representative of the degree of strength with the exceptions of the most fragile since they were too soft to prepared for microprobe analysis.

Results

<u>SEM Observations</u>

SEM images of varying magnification   (Figures 5.2a, b, and c) of the 62%:35%:3% PG:fly ash:lime composite surface zone in leached group showed a 20 μm loose layer of $CaCO_3$ embedded with spherical fly ash particles covered on the 10 μm wide rupture. These images also showed that ruptures developed across the $CaCO_3$ layer and that no PG crystals were found in surface zone. The SEM image (Figure 5.2d) of the 62%:35%:3% PG:fly ash:lime composite body zone in the submergence group showed that the PG and fly ash were mixed together to form the PG composites and that all fly ash particle surfaces were covered with a new layer of crystals.

For the control group of the 62%:35%:3% PG:fly ash:lime composite, the SEM images (Figure 5.3a, b, c) of the composite surface zone showed both PG and fly ash particles exposed on the composite surface. The images also showed that in some areas a 5-15 μm layer of paste covered the PG surface and that 1 μm wide ruptures developed throughout the composite. The SEM image (Figure 5.3d) of the control composite body zone showed that the PG and fly ash were mixed together to form the PG composites.

SEM images of varying magnification (Figures 5.4a, b, c) of the 55%:42%:3% PG:fly ash:lime composite surface zone in leached group showed a 10 μm loose layer

Figure 5.2 SEM images of the 62%:35%:3% PG:fly ash:lime composite after 28 day artificial saltwater dynamic leaching

test   (a) 10 μm ruptures in the surface zone

       (b) 20 μm looser $CaCO_3$ embedded with fly ash on a 10 μm rupture in the surface zone

       (c) Figure 5.2(b) under high magnification rate   (d) PG mixed with fly ash in body zone
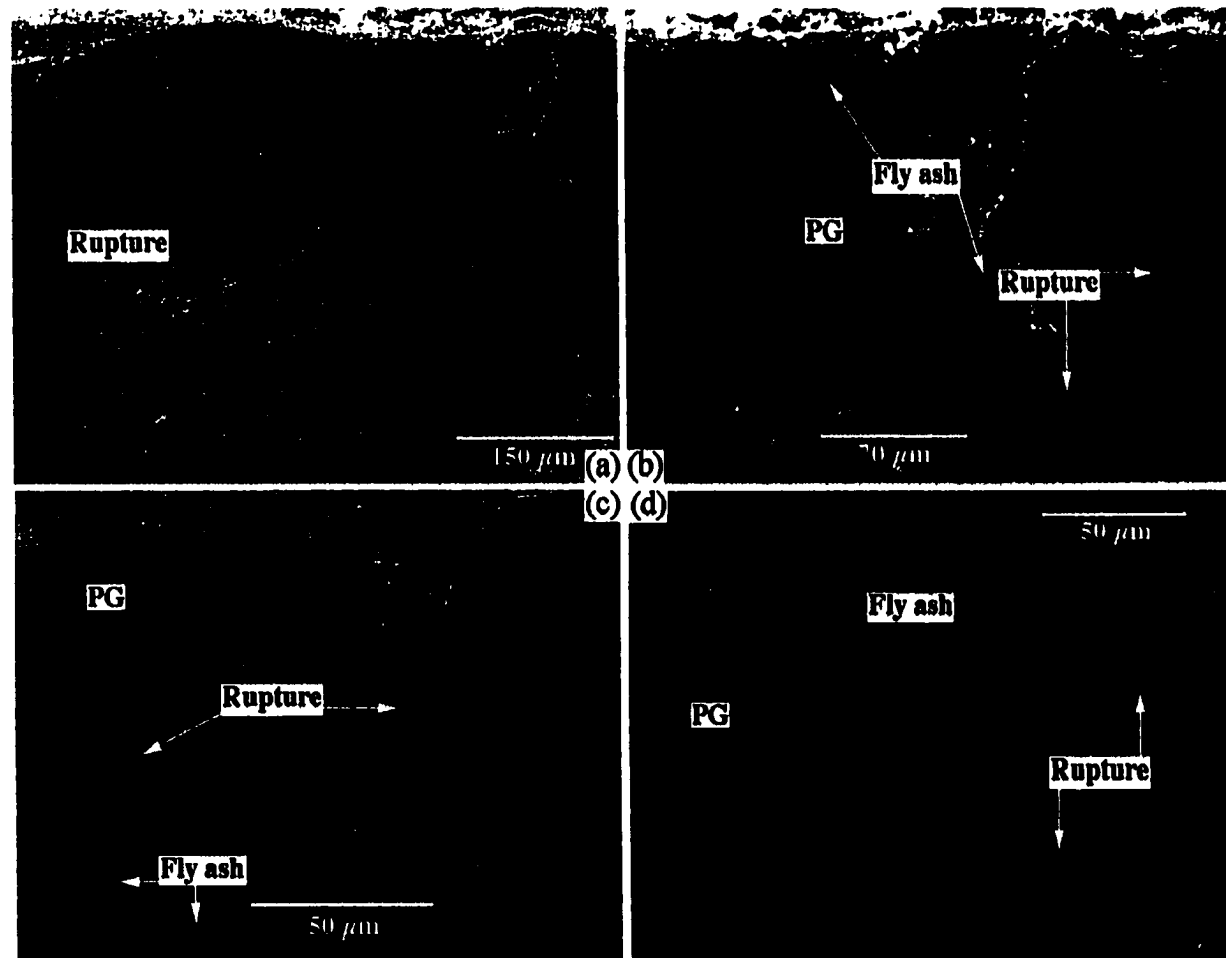
Figure 5.3 SEM images of the 62%:35%:3% PG:fly ash: lime composite after ten month air curing

(a) Surface zone under low magnification rate   (b) Figure 5.3(a) under high magnification rate

(c) PG exposed on the surface   (d) PG, fly ash and ruptures in body zone
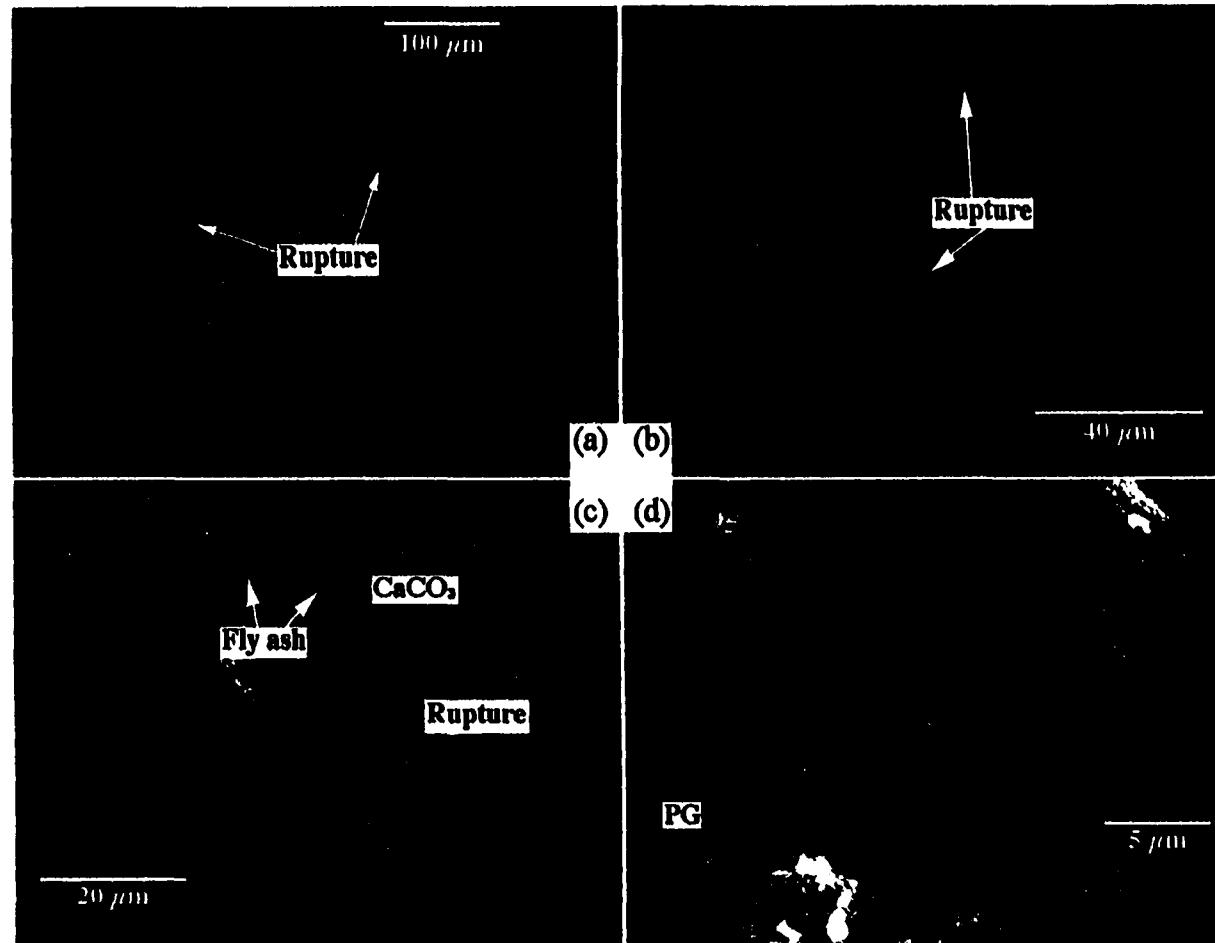
Figure 5.4 SEM images of the 55%:42%:3% PG:fly ash:lime composite after 28 day artificial saltwater dynamic leaching test   (a) 40 μm ruptures in the surface zone   (b)10 μm ruptures in the surface zone
(c)10 μm loose layer of CaCO₃ embedded with spherical fly ash particles on the 40 μm rupture
(d) Newly formed crystals on fly ash surface

of $CaCO_3$ embedded with spherical fly ash particles on the 40 μm wide rupture. The images also show that no PG crystals were found in surface zone. The SEM image (Figure 5.4d) of the 55%:42%:3% PG:fly ash:lime composite body zone in the submergence group shows that the PG and fly ash were mixed together to form the PG composites and that all fly ash particle surfaces were covered with a layer of newly formed crystals.

For the control group of the 55%:42%:3% PG:fly ash:lime composite, the SEM images (Figure 5.5a, b) of the composite surface zone showed a 5-15 μm layer of paste covering the PG and fly ash particle surface. The SEM image (Figures 5.5c, d) of the control composite body zone showed that the PG and fly ash were mixed together to form the PG composites. These images all showed that 1 μm wide ruptures developed throughout the composite surface.

SEM images of varying magnification (Figures 5.6a, b) of the 58.5%:35%:6.5% PG:fly ash:lime composite surface zone in the leached group showed 50μm wide ruptures developed on the composite surface, which is loose and easily scraped off. The SEM image (Figures 5.6c, d) of the 58.5%:35%:6.5% PG:fly ash:lime composite body zone in the submergence group showed the PG and fly ash covered with crystals and mixed together to form the PG composites and that all fly ash particle surfaces were covered with a layer of gypsum crystals. X-ray qualitative analysis determined that the crystals were composed of calcium and sulfur.

For the control group of the 58.5%:35%:6.5% PG:fly ash:lime composite, the SEM images (Figures 5.7a, b, c) of the composite surface zone showed both PG and
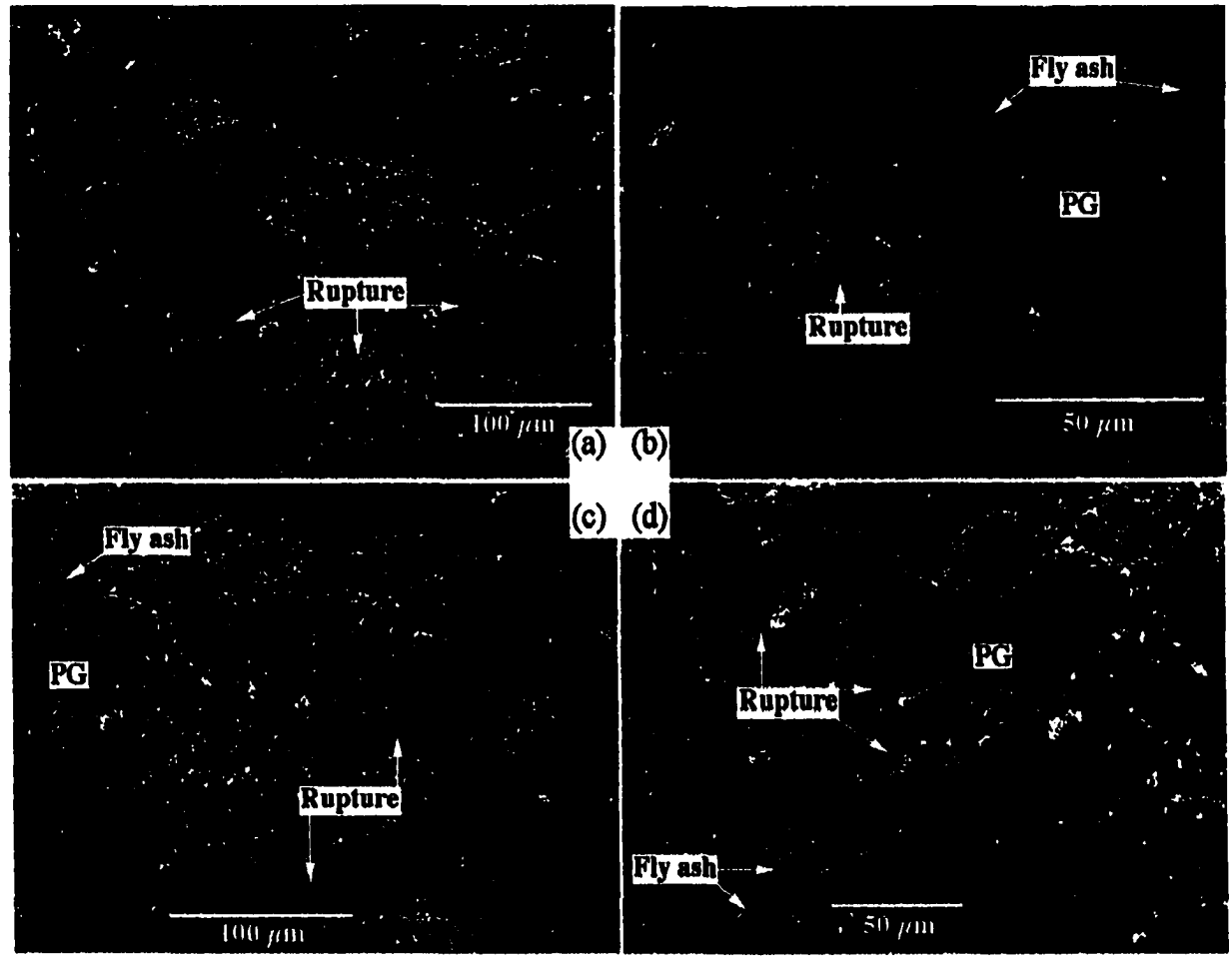
Figure 5.5 SEM images of the 55%:42%:3% PG:fly ash: lime composite after ten month air curing
   (a) Surface zone under low magnification rate   (b) A layer of paste covered on the PG and fly ash surface
   (c) Ruptures, PG and fly ash in the body zone   (d) Figure 5.5(c) under high magnification rate
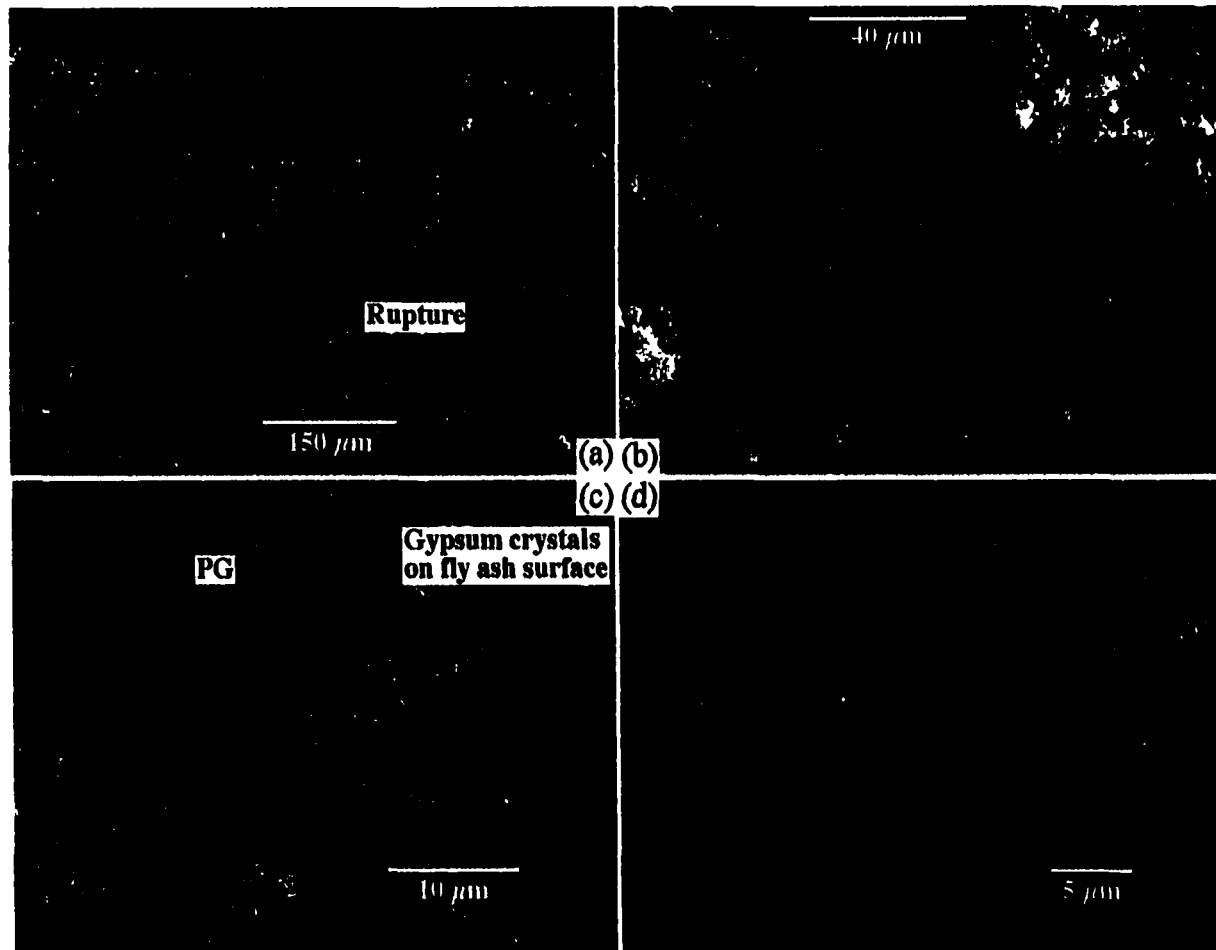
Figure 5.6 SEM images of the 58.5%:35%:6.5% PG:fly ash:lime composite after 28 day artificial saltwater dynamic leaching test (a) 50 μm ruptures in loose surface zone (b) Ruptures in loose surface zone (c) Gypsum covered on all fly ash particles (d) Gypsum covered on a fly ash particle
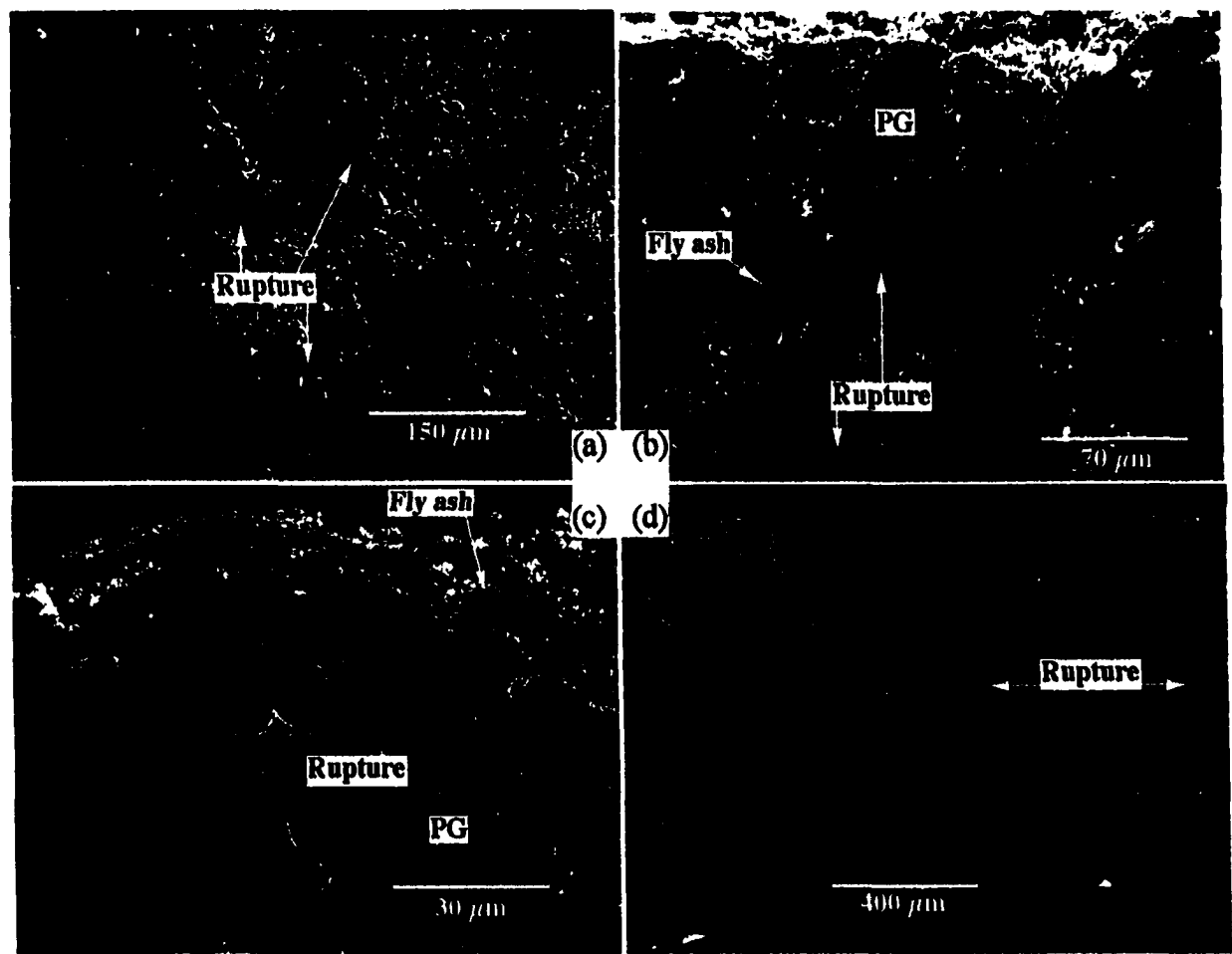
Figure 5.7 SEM images of the 58.5%:35%:6.5% PG:fly ash: lime composite after ten month air curing

    (a) Rupture, fly ash and PG in the surface zone   (b) Figure 5.7(a) under high magnification rate

    (c) Fly ash and PG exposed on the surface   (d) 50 μm ruptures in loose surface zone

fly ash exposed on the composite surface. The images also showed that in some areas a 5-15 μm layer of paste covered the PG surface. The low magnification rate of the SEM image (Figure 5.7d) shows that 20 μm wide ruptures developed throughout the composite and all images showed ruptured. These images all showed that the PG and fly ash were mixed together to form the PG composites.

For the control group of the 55%:35%:10% PG:fly ash:lime composite, the SEM images (Figures 5.8a, b) of the composite surface zone showed a 5-15 μm layer of paste covering the PG and fly ash surface. The SEM image (Figure 5.8c) of the control composite body zone shows that the PG and fly ash were mixed together to form the PG composites. The SEM image (Figure 5.8d) showed that the 15 μm wide ruptures developed throughout the composite and all images showed ruptures on the composite body. The SEM images (Figure 5.8e, f) showed fully developed ettringite in the composite body zone.

Microprobe Observations

The back-scattered electron (BS) images of the 62%:35%:3% PG:fly ash:lime (Figure 5.9a), 55%:42%:3% PG:fly ash:lime (Figure 5.9b) and the 58.5%:35%:6.5% PG:fly ash:lime (Figure 5.9c) composites showed that there are 50 μm wide ruptures along the composite/saltwater interfaces.

Diffusion Coefficient

The diffusion coefficients of the composites were calculated based on one dimension diffusion model (See Chapter 4). The calculated diffusion coefficients are listed in Table 5.2.
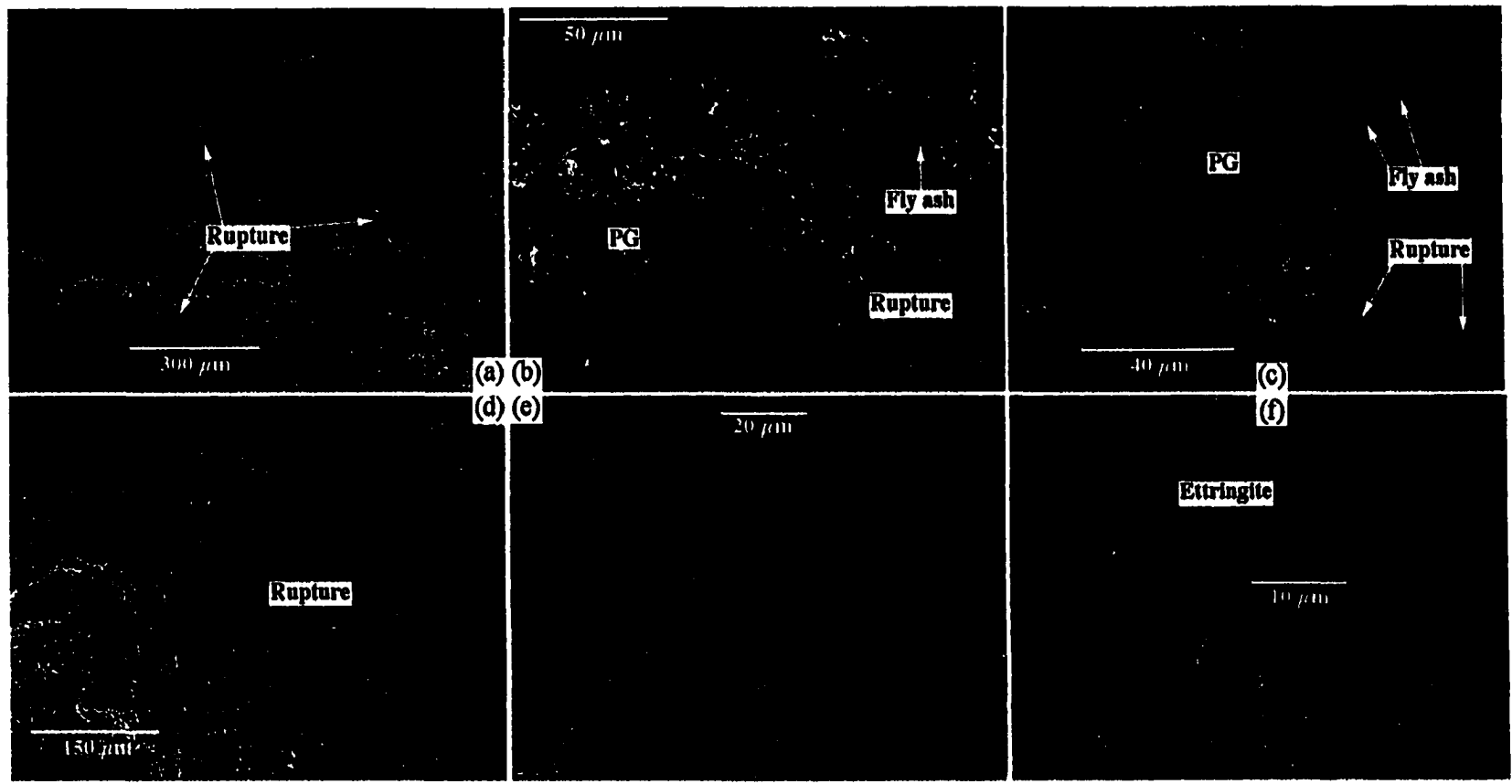
Figure 5.8 SEM images of the 55%:35%:10% PG:fly ash:lime composite after 28 day artificial saltwater dynamic leaching test

(a) Ruptures, PG and fly ash in the surface zone (b) Figure 5.8(a) under high magnification rate
(c) PG, fly ash and ruptures in body zone   (d)15 μm ruptures throughout the composites
(e) Ettringite in the body zone   (f) Figure 5.8(e) under high magnification rate
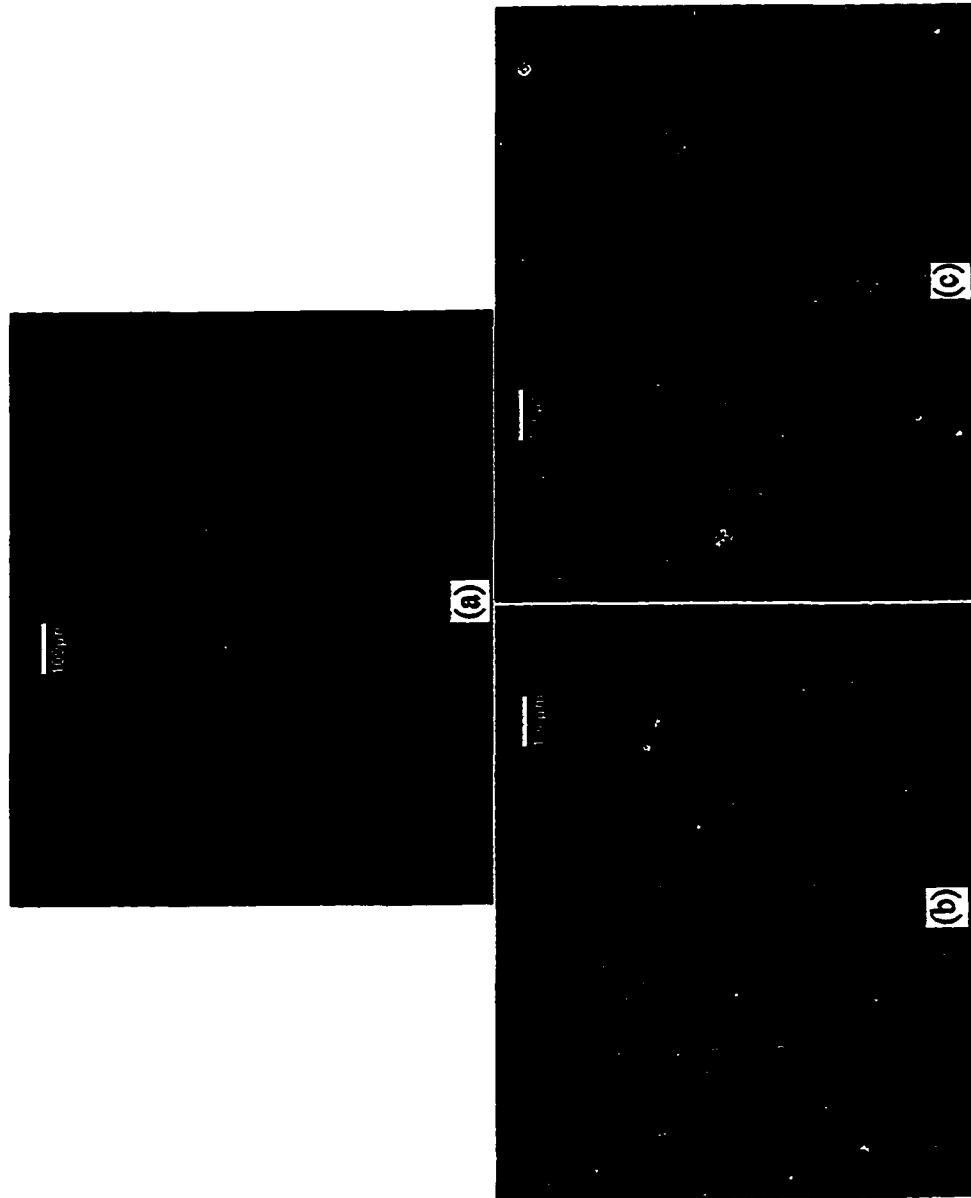
Figure 5.9 Backscattered images of the PG composites surface zone after 28 day artificial saltwater dynamic leaching test
(a) 62%:35%:3% PG:fly ash:lime
(b) 55%:42%:3% PG:fly ash:lime
(c) 58.5%:35%:6.5% PG:fly ash:lime

Table 5.2 Diffusion coefficients (D) and pH of leachate solution (day 2)
for PG:fly ash:lime composites

PG	Fly ash	Lime	D $(cm^2 \cdot day^{-1})$	pH (leachate)	Group
62	35	3	7.59E-5	8.53	1
58.5	38.5	3	6.69E-5	8.67	1
55	42	3	5.09E-5	8.36	1
59.6	36.2	4.2	6.79E-5	8.34	1
56.2	39.6	4.2	6.90E-5	8.36	1
57.4	37.3	5.3	4.64E-5	8.42	1
58.5	35	6.5	4.18E-5	8.77	2
55	38.5	6.5	1.53E-5	8.62	2
56.2	36.2	7.6	6.02E-6	8.98	2
55	35	10	4.19E-6	9.58	2

Diameter Measurements

Diameters (D) of the ten different combinations are listed in Table 5.3. The

percent diametrical expansion α is defined to be $(D_{10 \, month} - D_{1 \, day})/ D_{1 \, day}$. Table 5.3

shows that as the lime content increases, the diameters of the PG composites increase

too. It was found that after ten month air curing (control condition), the ruptures

(>1mm) developed on the surfaces of all PG composites with lime content greater

than 5.3%.

Discussion

When the PG:fly ash:lime composites were made, the pozzolanic reaction

between fly ash and lime resulted in the formation of a hard paste (Minnick, 1967;

Ferrell et al.,1988). As time went on, in the presence of PG, the pozzolanic reaction

continued and the development and modification of ettringite and other calcium

Table 5.3 Diameter (D) of the PG:fly ash:lime composites after 10 month air curing, the original diameter was 38.1 mm

Lime(%)	Fly ash(%)	PG(%)	D(mm)	α (%)
3	35	62	39.0	2.3
3	38.5	58.5	39.3	3.2
3	42	55	39.9	4.7
4.2	36.2	59.6	41.4	8.7
4.2	39.6	56.2	40.7	6.8
5.3	37.3	57.4	40.4	6.0
6.5	35	58.5	42.5	11.6
6.5	38.5	55	43.1	13.1
7.6	36.2	56.2	41.5	8.9
10	35	55	44.6	17.1

silicate hydrate products (Minnick, 1967; Ferrell et al.,1988) lead to the expansion of the harden paste. Ettringite was frequently found in the control composites. Because of the higher density (2.0 g/cm^3) of the composite, there is only a little room for expansion. The maximum percent diametrical expansion, α_{max}, was determined from the percent diametrical expansion of PG:fly ash:cement composites tested because of their ability to maintain structural integrity. This maximum percent diametrical expansion α_{max} was 1.8%. All percent diametrical expansions for the PG:fly ash:lime composites were greater than 1.8%. This resulted in ruptures developing in all control composites. Increases in lime content resulted in greater percent diametrical expansions (Table 5.3) and the wider the ruptures. When the ruptured PG:fly ash:lime composites were submerged in saltwater, the saltwater was able to intrude throughout the PG entire composites and dissolve the phosphogypsum. The dissolution of the PG

would increase concentration of sulfate that can react with calcium aluminum oxides in fly ash to form ettringite to accelerate rupture developing. In these ruptures, the solution could easily reach its saturated state allowing the re-crystallization of gypsum on the fly ash surface. The re-crystallized gypsum was observed in SEM images. Eventually, the PG:fly ash:lime composites would dissolve in the saltwater.

The group two with lime content greater than 6% in Table 5.2 has an average pH value 8.99 in the leachate solution, on the other hand the group one with lime content less than 6% has an average pH value 8.45 in the leachate solution. The higher pH value would lead us to conclude that higher pH value in the local surface area. This higher pH value on the PG composite surface resulted in the deposition of $CaCO_3$ at higher rate, therefore reduced the calculated calcium diffusion coefficients (Table 5.2).

The lime content of the PG:fly ash:lime composites is an important parameter. Table 5.3 indicates an increase in lime content yields a high percent diametrical expansion. The minimum lime content in this experiment is 3%, which is all active. In the PG:fly ash:cement experiment, the maximum content of cement was 10%, which is equivalent to 3.3% hydrated lime, but some of this hydrated lime is concealed by cement paste and is not active. Therefore for the PG:fly ash:lime composites, experiments with lime content less than 3% is suggested to be tested to see whether it could maintain physical integrity because of its predicted smaller percent diametrical expansion.

CHAPTER 6

DISSOLUTION POTENTIAL AND MECHANISMS INFLUENCING PHYSICAL INTEGRITY OF PG:FLY ASH:CEMENT COMPOSITES

Introduction

Phosphogypsum (PG, $CaSO_4 \cdot 2H_2O$) is a solid waste by-product produced during the production of phosphoric acid. PG contains some radionuclides such as radium[226] and trace metals such as arsenic and lead that may pose a potential hazard to human health and the environment. The current allowable disposal method of stackpiling has resulted in at least 33 PG stacks with an average area of 224 acres per stack. PG stacks have created significant environmental concerns from airborne radiation to surface and groundwater contamination (Taha and Seals, 1991). It is estimated that by year of 2000, the total inventory of PG in the US will exceed two billion metric tons (Taha and Seals, 1991). Various alternatives to the disposal of PG are being sought in order to decrease the risk to humans and the environment but none have been successful (Taha and Seals, 1991).

Previous research done at Louisiana State University has shown that different combinations of cement and lime added to stabilize PG did not meet economic requirements therefore, more cost-effective materials are being investigated to replace or significantly reduce cement as a binding agent. After reviewing many possible candidates, fly ash with cementous properties was able to replace cement as the binding agent. Fly ash is a solid residual of coal of oil combustion in electric power

76

plants with the volume being much higher at coal-fired plants. Fly ash is a mixture of metallic oxides, silicates, and other inorganic particulate matter, which is produced during the burning of coal. The chemical composition of fly ash is influenced by the type of coal used, the completeness of the combustion process, and the mineral contents of the coals (Atalay et al., 1990). The volume of fly ash produced from coal combustion is about 10% of the feed coal, and only 30% of the fly ash is reused (Higgins, 1995). In 1996, 948 million tons of coal was consumed (DRI/MaGraw-Hill et al., 1998) and it is estimated that 94.8 million tons of fly ash were produced with only 28.4 million tons of fly ash consumed. There is 66.4 million tons of fly ash that remain unused today. Different PG:fly ash:cement and PG:fly:lime ash ingredient combinations are proposed as possible ingredients for solidified PG composites.

Materials and Methods

<u>**Ingredient Selection**</u>

Figure 5.1 shows major composition of cements and other binding agents, projected on a $CaO-Al_2O_3-SiO_2$ ternary grid. The compositions are averages, and the method of projection ignores the presence of other minor oxides, such as MgO, Fe_2O_3 (Glasser et al., 1990). Figure 5.1 also shows that Clsaa C fly ash has properties close to cement and for this reason it was chosen as an ingredient in for the PG composites to reduce the cement content necessary. The mineralogy of Clsaa C fly ash is composed of quartz, anhydrite, CaO, Ca_3Al oxides, hematite, magetite, melilite, merwinite, periclase, and aluminosilicate glass (Maleak et al., 1988). The majority of the fly ash particles have a diameter between less than 1 μm and 100 μm and are spherical

(Neville, 1995). The function of fly ash in solidified PG composites is similar to that of cement. Fly ash serves as a source of dehydrated silicates and is used as a basic material. The fly ash neutralizes the acidity of raw PG and creates the necessary basic environment to prevent possible leaching of toxic metals from the PG composites. With this new approach, two types of solid waste may be converted into useful resources such as artificial reefs and oyster substrates.
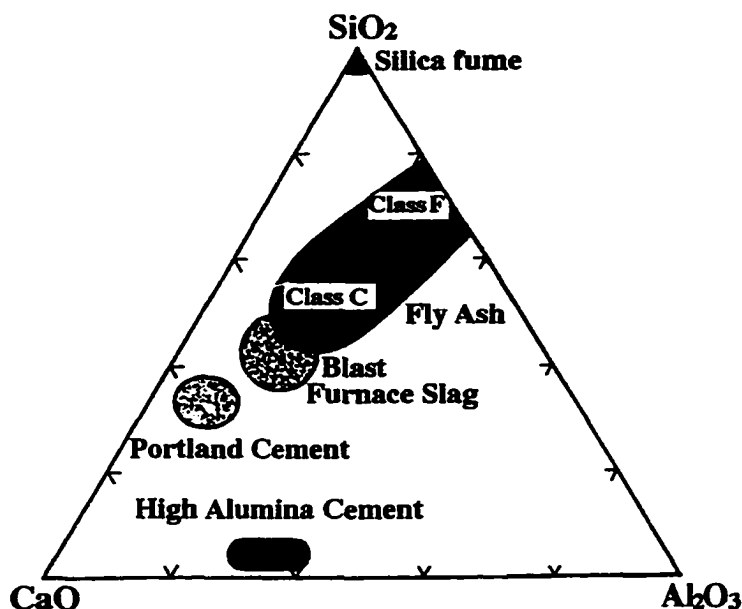
Scanning electron microscopy indicated the presence of a calcium carbonate coating on the surface of the PG composites that remained physical structure integrity. On the other hand, PG composites that exhibited severe degradation were lacking the calcium carbonate coating. A localized zone of high pH (See Chapter 4) control the formation of the calcium carbonate coating. Experimental analysis of fly ash determined that a paste mixture of 38.5% fly ash and 61.5% PG has a pH of 10.8, so the searching center for fly ash was determined to be 38.5%. According to thermodynamic calculations, the pH must reach 11 in order for calcium carbonate to precipitate out on the surface of the PG blocks. The cement content in the PG:fly ash composite is suggested to be 3-10% since fly ash contains some active dehydrated silicates. This is a much lower cement content than the previous 30% cement content needed to stabilize the PG composites. Augmented simplex centroid design with Psuedocomponents (See Chapter 7) method was applied for ingredient content selection. The composite combinations for PG:fly ash:cement are listed in Table 6.1.

Table 6.1 PG:fly ash:cement composite ingredients (%)

Cement	Fly ash	PG
3	35	62
3	38.5	58.5
3	42	55
4.2	36.2	59.6
4.2	39.6	56.2
5.3	37.3	57.4
6.5	35	58.5
6.5	38.5	55
7.6	36.2	56.2
10	35	55

PG Composite Fabrication

Type II Portland cement was combined with fly ash and PG for ten different combinations. According to the ingredient composition, dry raw materials are mixed to form the dry mixture. The dry mixture is mixed with water equivalent to 8% of dry weight and completely homogenized. Ninety-six grams of the resulting mixture were weighed and poured into a 1.5 inch steel mold, then compacted to a 1.5 inch long cylinder under 14,150 psi using a static press. Theoretically, the dry density should reach 1.9 g/cm³. Blocks were allowed to cure at room temperature and 100% humidity for at least two weeks before testing and the average dry weight was 87 grams.

Dynamic Leach Test

A variation of the dynamic leach test (ANS, 1986) was performed to determine calcium release rates from the PG composites. The leachate volume to block surface area ratio was 8:1. Composites were run in duplicate and were placed in 550 ml of

20‰ artificial saltwater (Instant Ocean™). The leachate was completely exchanged at intervals of .08, .29, 1, 2, 3, 4, 5, 8, 11, 14, 21, and 28 days and analyzed for pH and alkalinity (APHA, 1995). Calcium was measured by Inductively Coupled Argon Plasma (ICAP) in Department of Agronomy, Louisiana State University.

Instrumental Analyses

Qualitative and quantitative X-ray microprobe (Joel JXA-733) and scanning electron microscopy (Joel 8408) were used to analyze the composite microstructure. Thirty μm sections from the 62%:35%:3% PG:fly ash:cement, 58.5%:38.5%:3% PG:fly ash:cement, 55%:42%:3% PG:fly ash:cement and the 55%:35%:10% PG:fly ash:cement composites were prepared in a manner to allow investigation of the composite surface and body characteristics (Hutchinson, 1974). The three composites are representative of the degree of strength with the exceptions of the most fragile since they were too soft to prepared for microprobe analysis

Results

SEM Observations

Some PG composites with typical ingredient combinations of 62%:35%:3% PG:fly ash:cement, 58.5%:38.5%:3% PG:fly ash:cement, 55%:42%:3% PG:fly ash:cement and 55%:35%:10% PG:fly ash:cement were sampled for SEM observation. These PG composites were divided into two groups. Group one was submerged in the artificial saltwater for one month during the dynamic leaching test. Group two was the control group and did not receive any treatment.

SEM images of varying magnification (Figures 6.1a, b, c) of the 62%:35%:3% PG:fly ash:cement composite surface zones in submergence groups showed a 40-60 μm dense layer of crystals embedded on the spherical fly ash particles. No PG crystals were found in the surface zone. The SEM image (Figure 6.1d) of the 62%:35%:3% PG:fly ash:cement composite body zone in the submergence group showed that the PG and fly ash were mixed together to form the PG composites.

SEM images (Figure 6.2a) of the 62%:35%:3% PG:fly ash:cement composite surface zone in submergence group showed a large paste of 5-15 μm is covering the PG surface. The image also showed that fly ash is exposed on the composite surface. The SEM image (Figure 6.2b) of the control composite body zone showed that the PG and fly ash were mixed together to form the PG composites which is the same as the body zone of the submergence group.

SEM images of varying magnification (Figures 6.3a, b, c) of the 58.5%:38.5%:3% PG:fly ash:cement composite surface zone in submergence group and the SEM image (Figure 6.3d) of the 58.5%:38.5%:3% PG:fly ash:cement composite body zone showed a similar phenomena to the submerged 62%:35%:3% PG:fly ash:cement composite.

SEM images (Figure 6.4a) of the 58.5%:38.5%:3% PG:fly ash:cement composite, surface zone in control group showed both PG and fly ash were exposed on the composite surface. The SEM image (Figure 6.4b) of the control composite body zone showed that the PG and fly ash were mixed together to
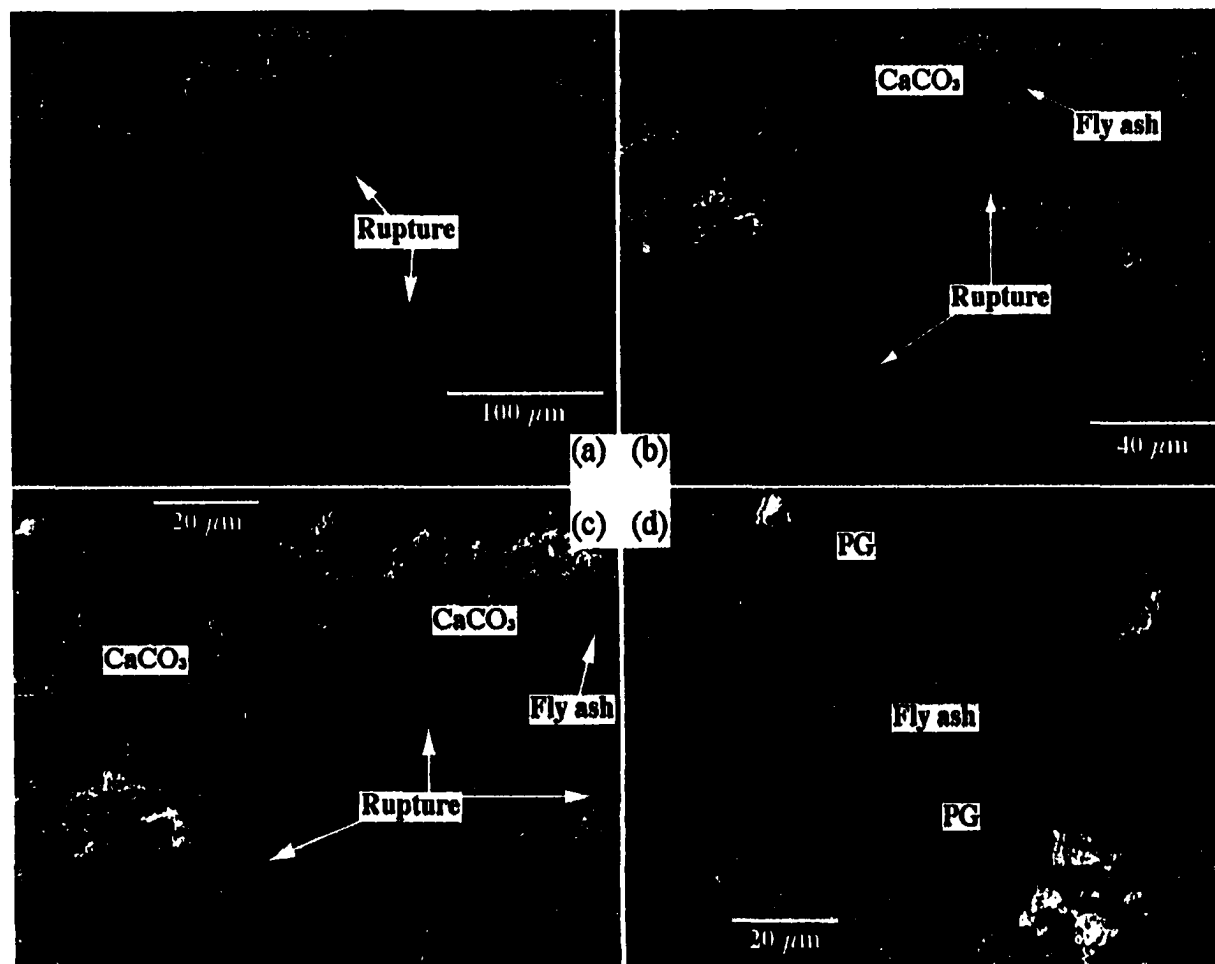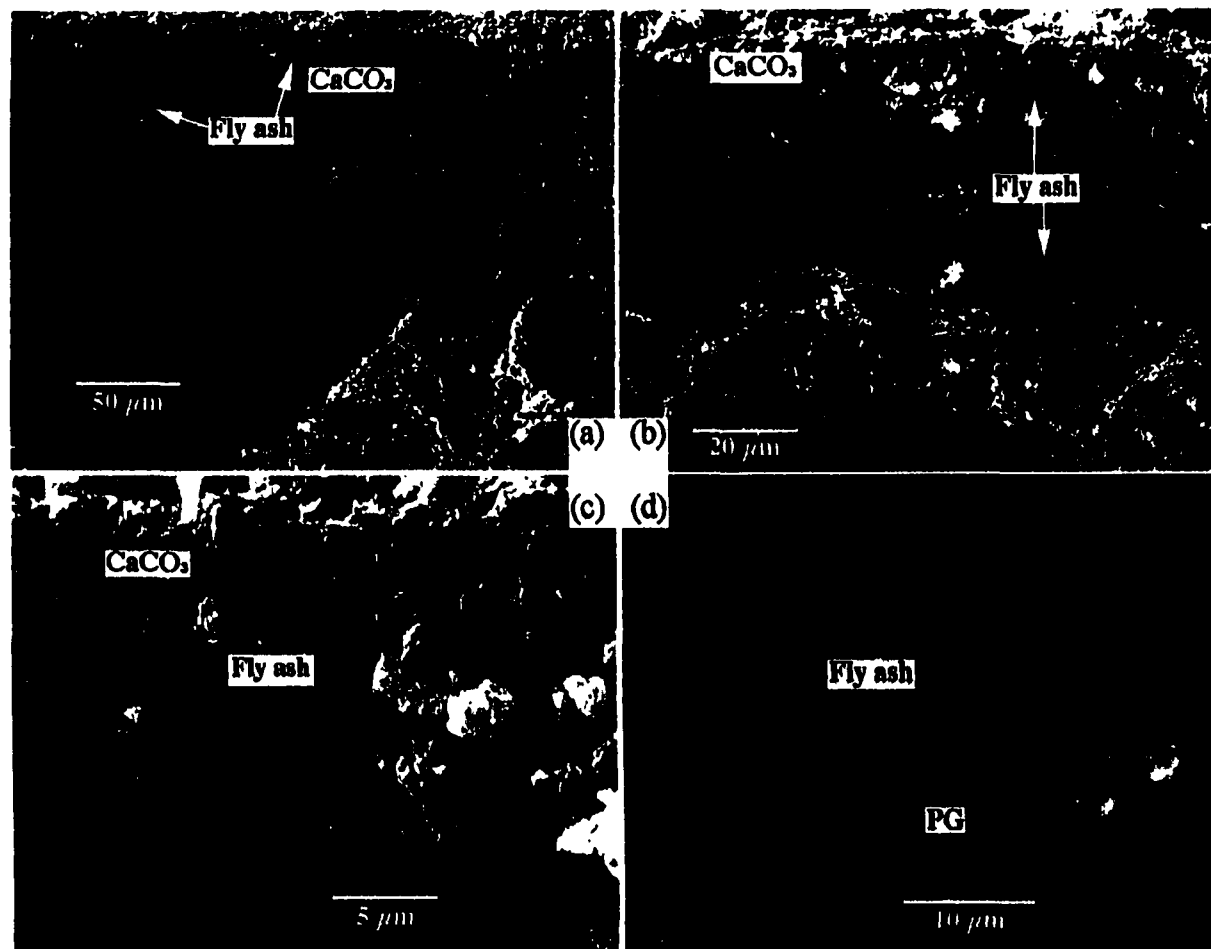
Figure 6.1 SEM images of the 62%:35%:3% PG:fly ash:cement composite after 28 day artificial saltwater dynamic leaching test

(a) CaCO₃ embedded with fly ash on the surface (b) Figure 6.1(a) under high magnification rate
(c) Figure 6.1(a) under higher magnification rate (d) PG mixed with fly ash in body zone

(a)

(b)
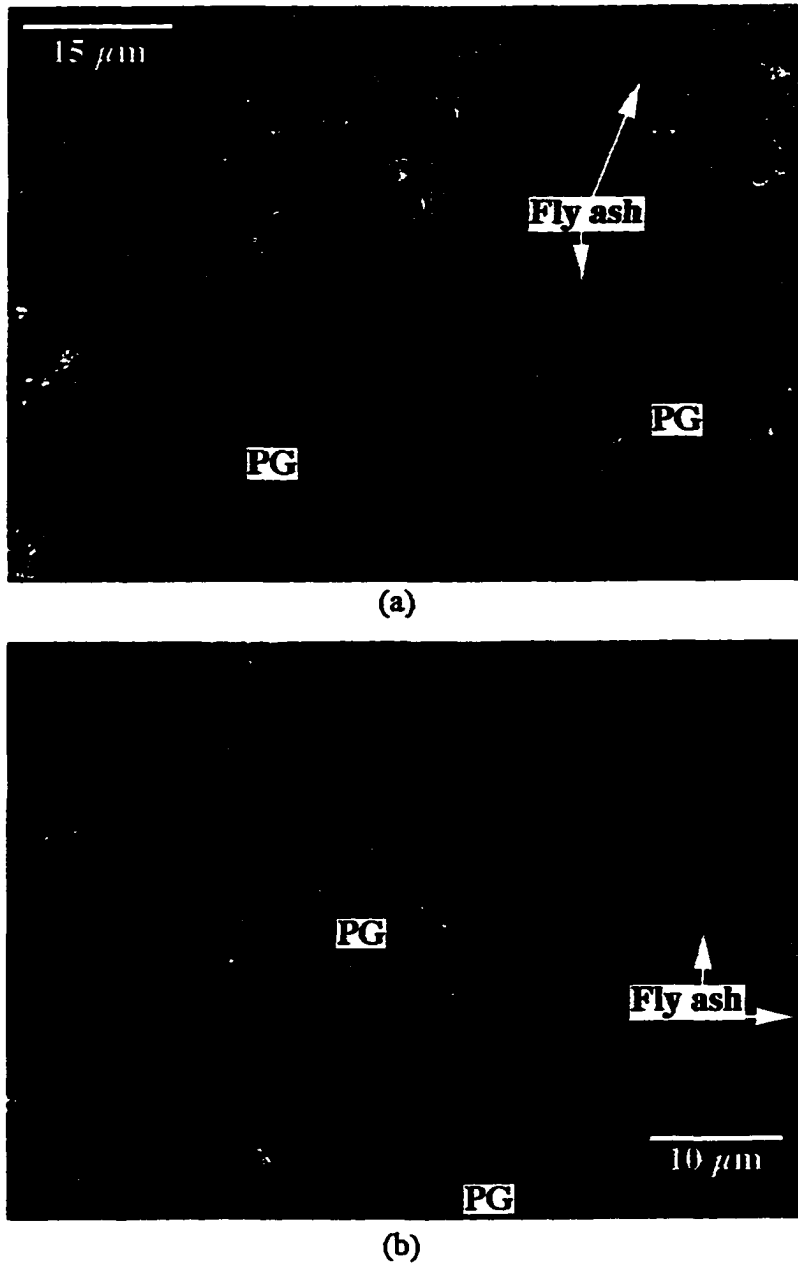
Figure 6.2 SEM images of the 62%:35%:3% PG:fly ash:cement
composite after ten month air curing
(a) PG and fly ash in surface zone
(b) PG mixed with fly ash in body zone
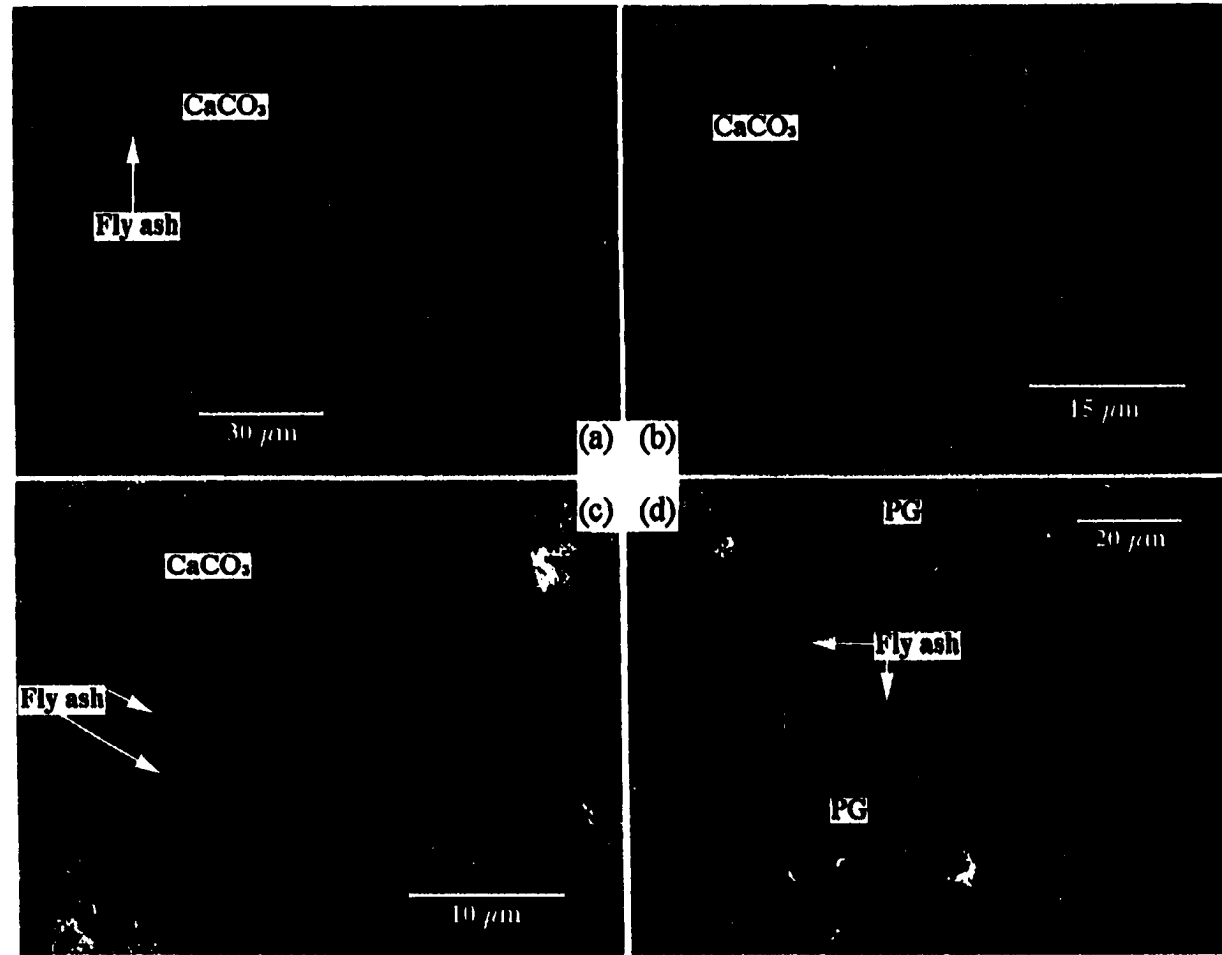
Figure 6.3 SEM images of the 58.5%:38.5%:3% PG:fly ash:cement composite after 28 day artificial saltwater dynamic leaching test

(a) $CaCO_3$ embedded with fly ash on the surface
(b) Figure 6.3(a) under high magnification rate
(c) Figure 6.3(a) under higher magnification rate
(d) PG mixed with fly ash in body zone
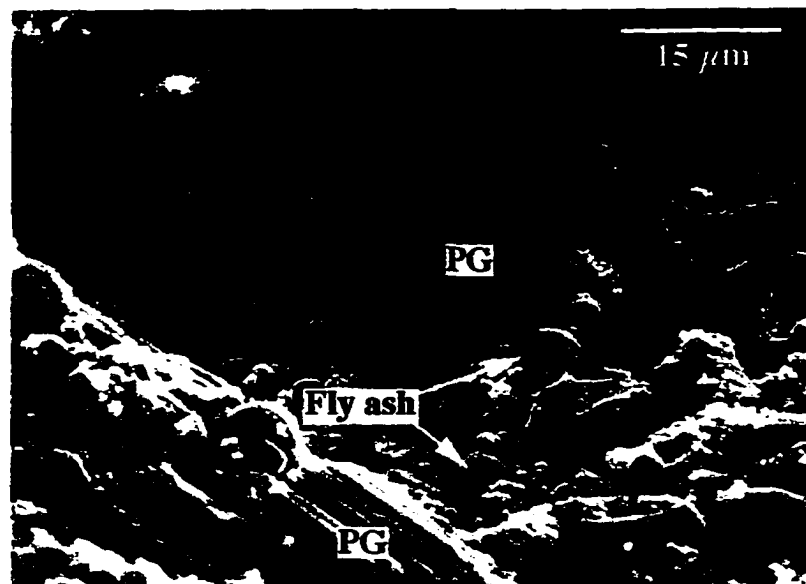
(a)
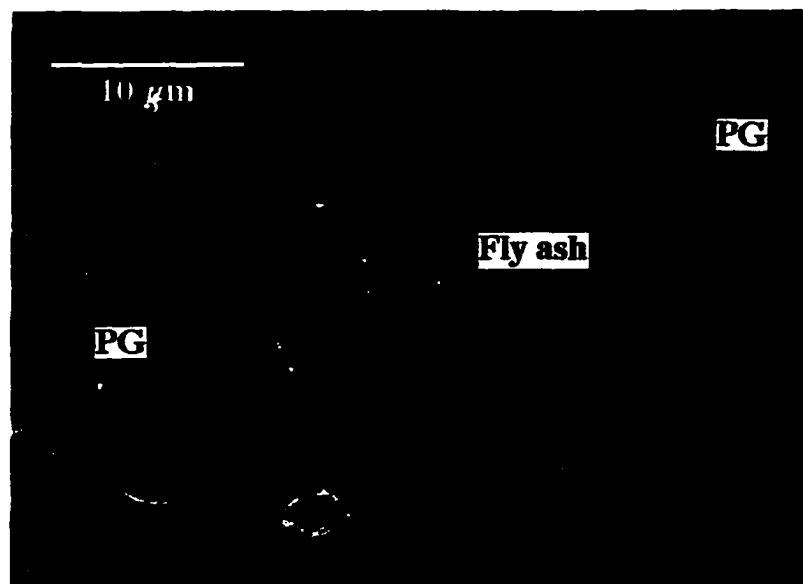
(b)

Figure 6.4 SEM images of the 58.5%:38.5%:3% PG:fly ash:cement
composite after ten month air curing
(a) PG and fly ash exposed on the surface
(b) PG mixed with fly ash in body zone

form the PG composites which is the same as the body zone of the submergence group.

In the submergence group, the SEM images of varying magnification (Figures 6.5a, b and c) of the 55%:42%:3% PG:fly ash:cement composite surface zone and the SEM image (Figure 6.5d) of the 55%:42%:3% PG:fly ash:cement composite body zone showed a similar phenomena to the submerged 62%:35%:3% PG:fly ash:cement composite.

In the control group, the SEM images (Figure 6.6a) of the 55%:42%:3% PG:fly ash:cement composite surface zone and the SEM image (Figure 6.6b) of the 55%:42%:3% PG:fly ash:cement composite body zone showed a similar phenomena to the control 62%:35%:3% PG:fly ash:cement composite.

The SEM images of varying magnification (Figures 6.7a, b, and c) of the 55%:35%:10% PG:fly ash:cement composite surface zone in submergence group showed a dense 50 μm layer of $CaCO_3$ embedded on the spherical fly ash particles. The images also showed that no PG crystals were found in surface zone. The high magnification image of the crystal coating (Figure 6.7c) showed the new-formed $CaCO_3$ crystals, aragonite, on the PG composite surface. The SEM image (Figure 6.7d) of the 55%:35%:10% PG:fly ash:cement composite body zone in submergence group showed that the PG and fly ash were mixed together to form the PG composites.

In the control group of the 55%:35%:10% PG:fly ash:cement composite, the SEM images (Figure 6.8a) of the composite surface zone showed that both PG and fly ash were exposed on the composite surface pore. The SEM image (Figure 6.8b) of the
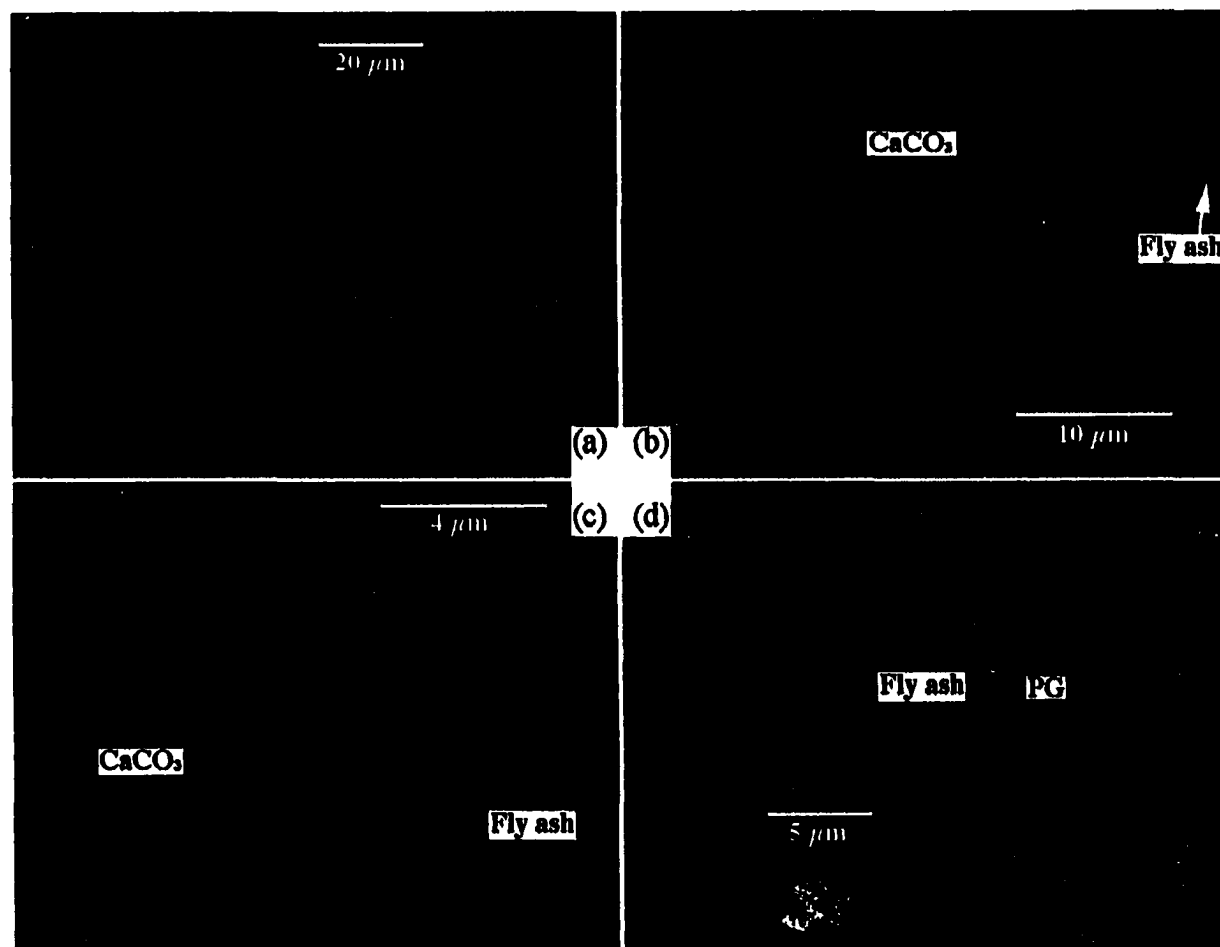
Figure 6.5 SEM images of the 55%:42%:3% PG:fly ash:cement composite after 28 day artificial saltwater dynamic leaching test

(a) $CaCO_3$ embedded with fly ash on the surface

(b) Figure 6.5(a) under high magnification rate

(c) Figure 6.5(a) under higher magnification rate

(d) PG mixed with fly ash in body zone

(a)

(b)
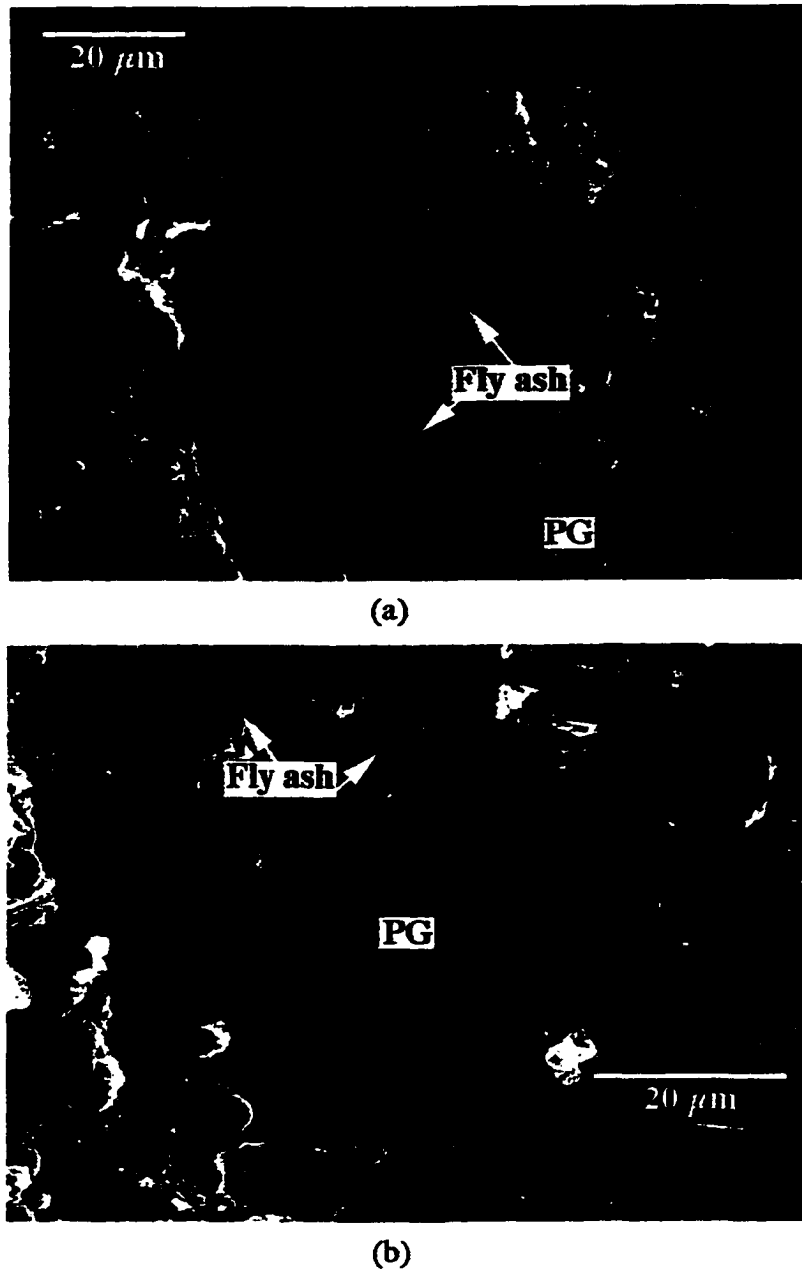
Figure 6.6   SEM images of the 55%:42%:3% PG:fly ash:cement
composite after ten month air curing
(a) PG mixed with fly ash in surface zone
(b) PG mixed with fly ash in body zone
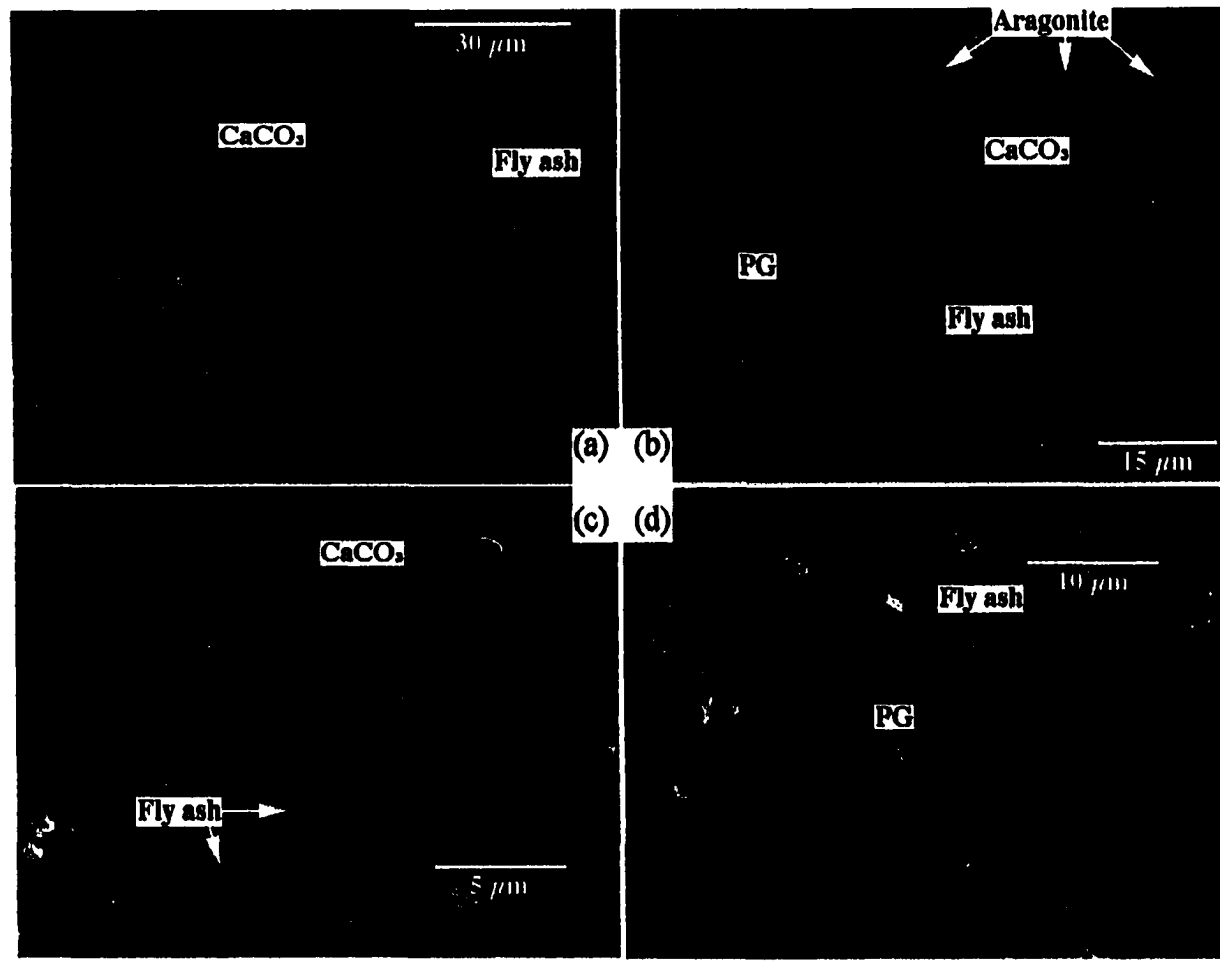
Figure 6.7 SEM images of the 55%:35%:10% PG:fly ash:cement composite after 28 day artificial saltwater dynamic leaching test

(a) CaCO3 embedded with fly ash on the surface (b) Aragonite on a layer of CaCO3 embedded with fly ash
(c) Figure 6.7(a) under high magnification rate (d) PG mixed with fly ash in body zone

(a)
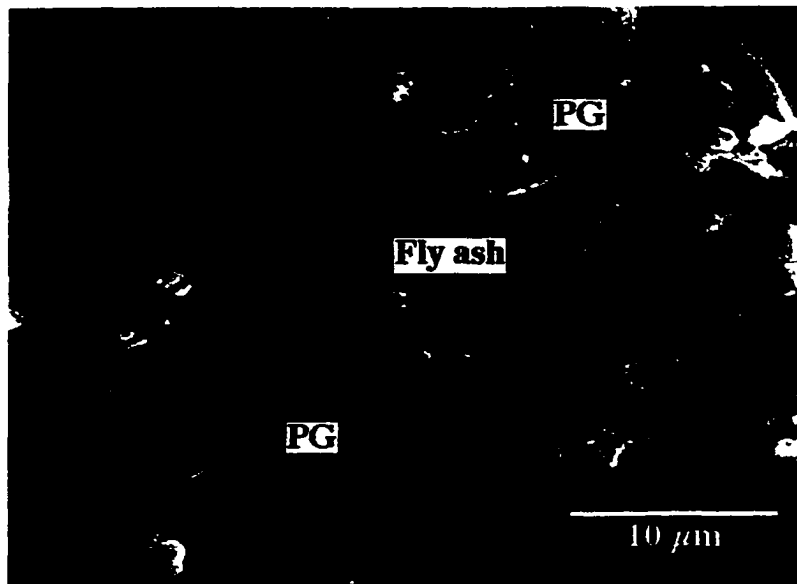
(b)

Figure 6.8 SEM images of the 55%:35%:10% PG:fly ash:cement
composite after ten month air curing
(a) PG and fly ash exposed on the surface
(b) PG mixed with fly ash in body zone

control composite body zone showed that the PG and fly ash were mixed together to form the PG composites which is the same as the body zone of the submergence group.

Microprobe Observations

The back-scatter (BS) electron image and X-ray elemental content images of calcium (Ca), silicon (Si), sulfur (S) and aluminum (Al) for 62%:35%:3% PG:fly ash:cement composite surface zone are presented in Figure 6.9. The BS image shows that some spherical fly ash particles exist in the surface zone. The Ca content image shows that there exists a high Ca content zone along the PG composite surface. But the high calcium content region is not uniform. It randomly includes some low calcium content spots. The Si content image shows that in the low Ca content regions, the Si content is continuous, showing spherical shapes in places. The Al content image shows that in high Ca content regions, the low calcium spots correspond to high Al content area. The Al content image also shows that in low Ca content region, Al content is continuous and showed spherical shapes in places. The Mg content image shows that a higher Mg contents exists between the $CaCO_3$ coating and composite. The S content image indicates that no S exists in the PG composite surface. The 58.5%:38.5%:3% PG:fly ash:cement (Figures 6.10), 55%:42%:3% PG:fly ash:cement (Figures 6.11) and 55%:35%:10% PG:fly ash:cement (Figures 6.12) composites have similar distribution patterns for Ca, Al, Mg, Si, S and BS.
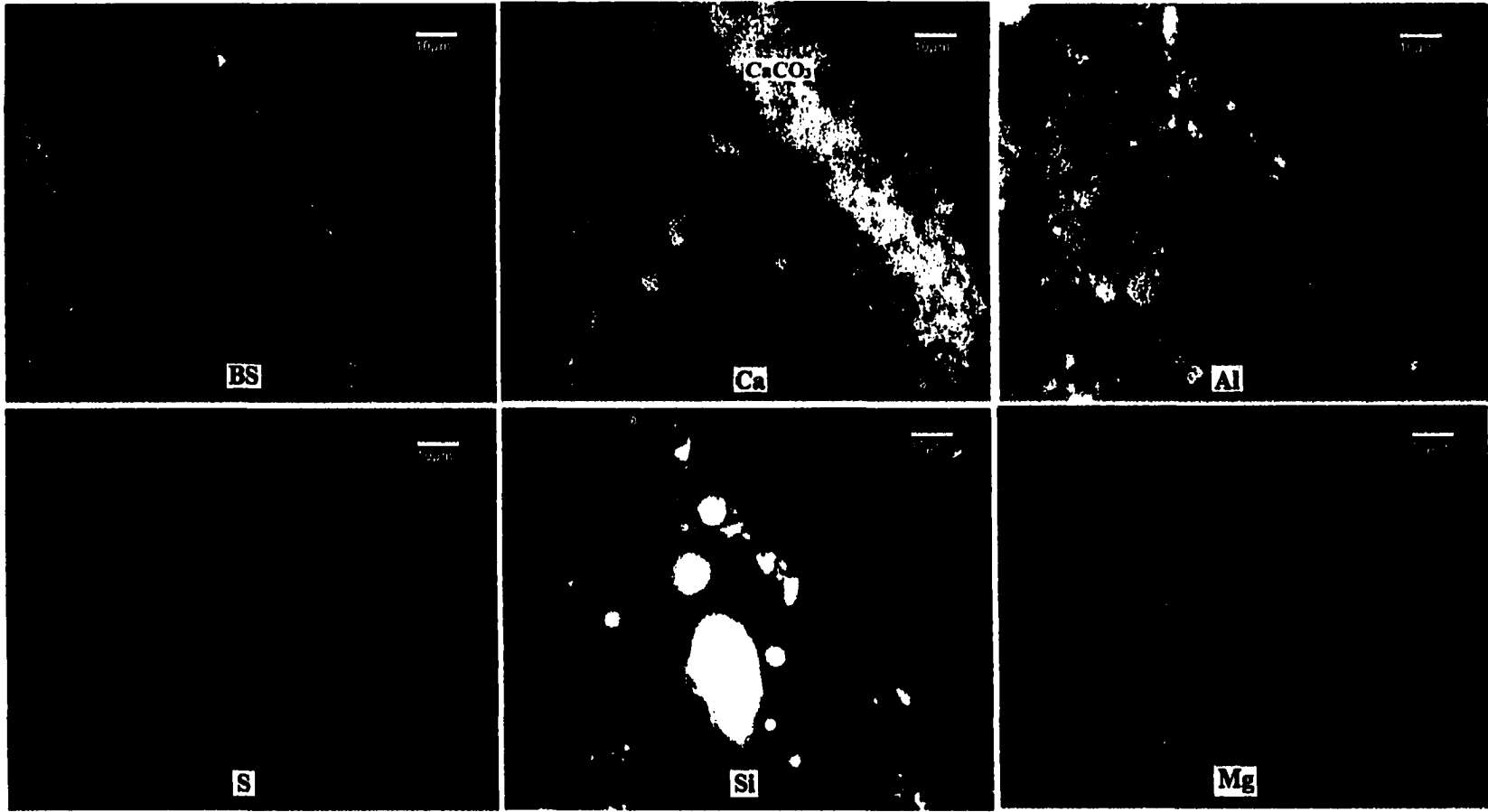
Figure 6.9 Microprobe element content and BS images of the 62%:35%:3% PG:fly ash:cement composite surface zone after 28 day artificial saltwater dynamic leaching test
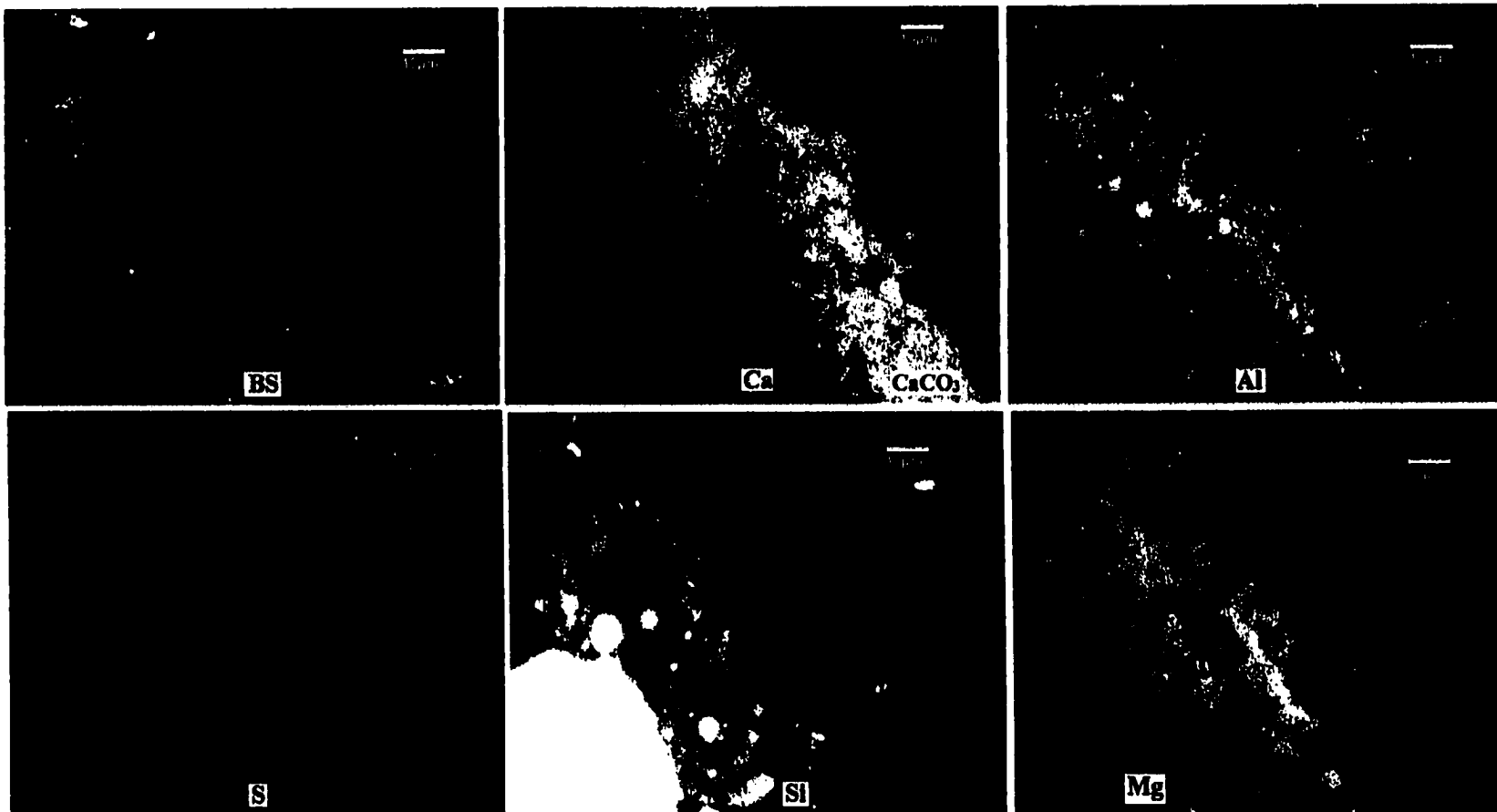
Figure 6.10 Microprobe element content and BS images of the 58.5%:38.5%:3% PG:fly ash:cement composite surface
zone after 28 day artificial saltwater dynamic leaching test
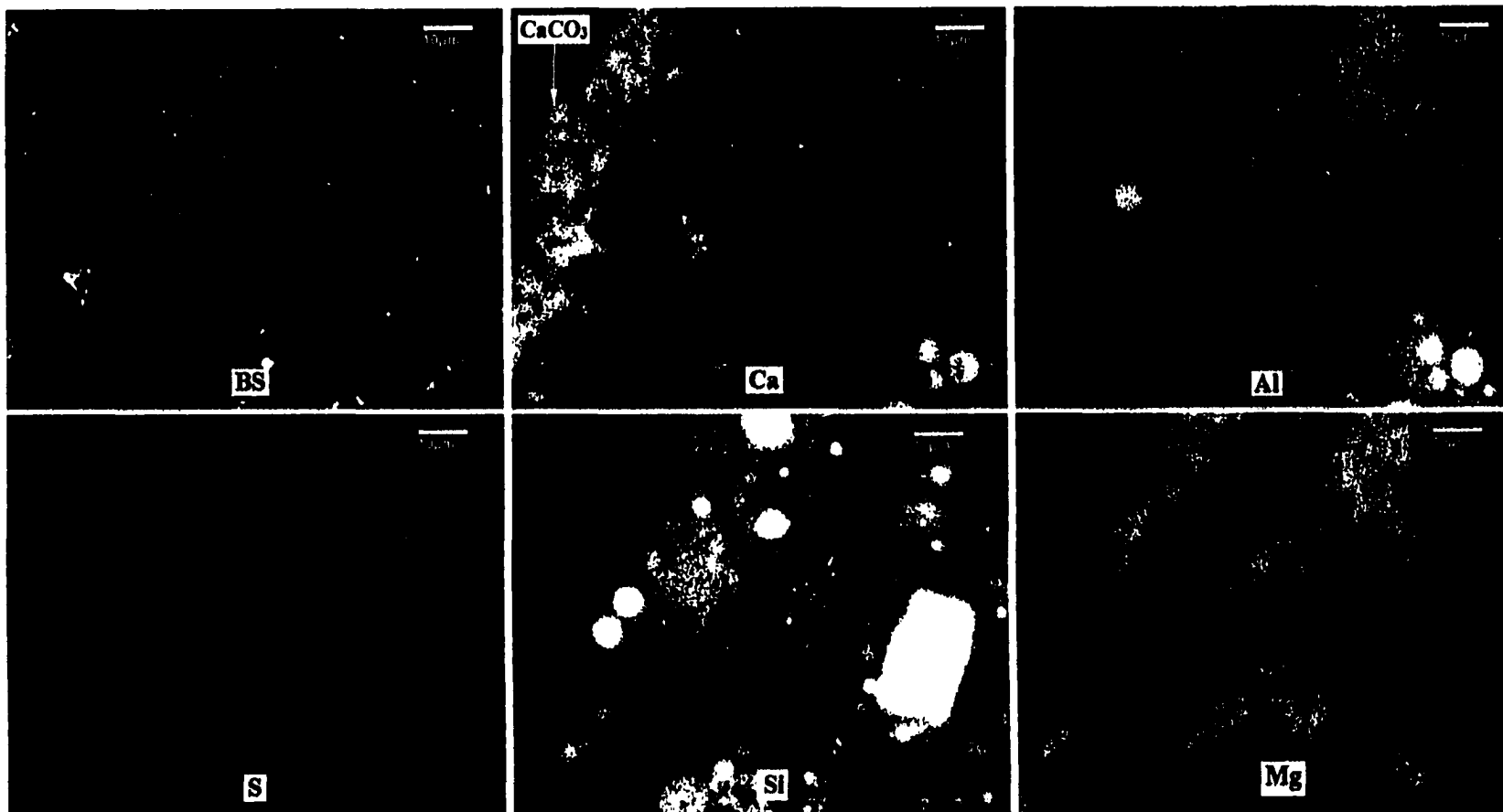
Figure 6.11 Microprobe element content and BS images of the 55%:42%:3% PG:fly ash:cement composite surface
zone after 28 day artificial saltwater dynamic leaching test
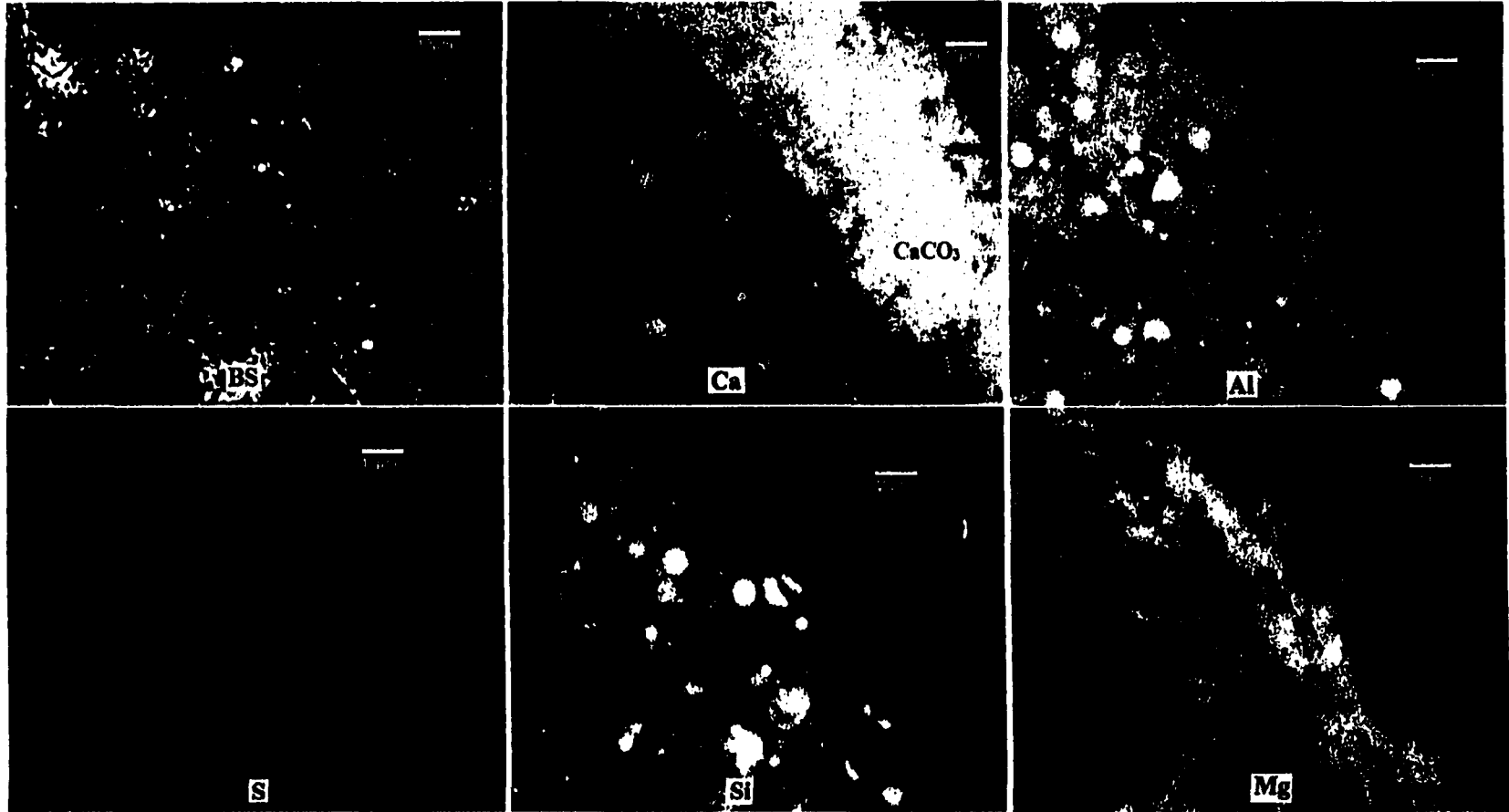
Figure 6.12 Microprobe element content and BS images of the 55%:35%:10% PG:fly ash:cement composite surface
zone after 28 day artificial saltwater dynamic leaching test

Diffusion Coefficient

The diffusion coefficients of the composites were calculated based on one dimension diffusion model (See Chapter 4). The calculated diffusion coefficients are listed in Table 6.2.

Table 6.2 Diffusion coefficients (D) and leachate pH value
of PG:fly ash:cement composites

Cement	Fly ash	PG	D (cm^2·day^{-1})	pH(leachate)
3	35	62	6.49E-5	8.56
3	38.5	58.5	5.39E-5	8.57
3	42	55	4.00E-5	8.58
4.2	36.2	59.6	6.14E-5	8.63
4.2	39.6	56.2	4.60E-5	8.61
5.3	37.3	57.4	5.01E-5	8.69
6.5	35	58.5	5.01E-5	8.71
6.5	38.5	55	3.46E-5	8.71
7.6	36.2	56.2	3.46E-6	8.76
10	35	55	1.91E-6	8.81

Diameter Measurements

Diameters (D) of the ten different combinations are listed in Table 6.3. The percent diametrical expansion α is defined to be $(D_{10\ month} - D_{1\ day})/\ D_{1\ day}$. Table 6.3 shows that as the lime content increases, the diameters of the PG composites increase too. From Table 6.3 it is found that the maximum percent diametrical expansion, α_{max} is 1.8%. This value can be considered the maximum percent diametrical expansion of stabilized PG composites because of their ability to maintain structural integrity.

Table 6.3 Diameter (D) of PG:fly ash:cement composites after 10 month air curing, the original diameter was 38.1 mm

Cement(%)	Fly ash(%)	PG(%)	D(mm)	α (%)
3	35	62	38.5	1.1
3	38.5	58.5	38.5	1.1
3	42	55	38.7	1.6
4.2	36.2	59.6	38.5	1.1
4.2	39.6	56.2	38.7	1.6
5.3	37.3	57.4	38.5	1.1
6.5	35	58.5	38.5	1.1
6.5	38.5	55	38.6	1.3
7.6	36.2	56.2	38.6	1.3
10	35	55	38.8	1.8

Discussion

When the PG:fly ash:cement composite surface came in contact with the saltwater, the phosphogypsum on the surface (Figures 6.4a and 6.8a) or near the surface (Figures 6.2a and 6.6a) dissolved, leaving some empty pores. On the other hand, the high local pH environments near the fly ash particles and cement paste in the composite surface allowed Ca^{2+} and CO_3^{2-} in the saltwater to form a dense layer of $CaCO_3$ (Figures 6.1a-c, Figures 6.3a-c, Figures 6.5a-c and Figures 6.7a-c) on its surface. The 35-42% fly ash could continuously provide a strong matrix for $CaCO_3$ to grow on. Gradually, the $CaCO_3$ layer would occupy the empty pores from PG crystal dissolution. This 30-50 μm calcium carbonate coating embedded with fly ash particles

(Figures 6.9-12) made the calcium carbonate coating stronger and more able to survive saltwater submergence.

The PG:fly ash:cement composites contained at least 35% fly ash. This high content of fly ash can greatly enhance their sulfate resistance ability by reacting with Ca_3Al oxides or its hydration products in cement (Dodson, 1988; Smith, 1988; Neville, 1995). The above reactions would reduce the content of ettringite that is the main reason for PG composite dissolution (See Chapter 4). No ettringite was found in either the leached or control PG:fly ash:cement composites . The included saltwater under the coating could not degrade the composites but the Mg ion in the included saltwater exhibited an ion exchange reaction with insoluble calcium in the solid cement matrix that did lead to a higher Mg content between the $CaCO_3$ coating and the composite. The stronger calcium carbonate coating embedded with fly ash particles and the higher sulfate resistance composites contributed to the pG:fly ash:cement composites survival in the Grand Isle bay for more than one year.

The SEM and microprobe observation did not find significant rupture development in the PG:fly ash:cement composites, but the diffusion coefficients do reveal some information about the overall situation on the PG:fly ash:cement composites. Table 6.2 shows that when cement content is fixed, an increase in fly ash content yields a lower diffusion coefficient, and when fly ash content is fixed, an increase in cement content yields a lower diffusion coefficient. The lowest diffusion coefficient obtained is for PG:fly ash:cement 55%:35%:10% which has highest cement content. This is because both cement and fly ash are less soluble materials, the higher

content of the less soluble materials reduces the dissolution rate and the calcium diffusion coefficients.

CHAPTER 7

DETERMINATION OF OPTIMUM INGREDIENTS FOR STABILIZED PG
COMPOSITES — RESPONSE SURFACE ANALYSIS WITH PROCESS
VARIABLES

Introduction

Solidification is a widely used solid waste treatment technology that immobilizes

harmful substances through the addition of inorganic binders, including lime, cement

and fly ash; to aqueous or solid wastes to produce a solid matrix that decreases the

waste leachability (Conner 1990). The solid matrix is reduced through the reduction

of contact surface area between the leaching medium and the waste, and the

transformation of toxic metals (Malone et al., 1980). The determination of optimum

ingredient composition means finding the lowest content of inorganic binders which

account for the major part of solidified composite cost while meeting performance

criteria. This research is going to apply the design, modeling, and analysis of the

mixture experiment to the optimum ingredient determination used in solidification

technology. An example of determination of optimum ingredients for solidified

phosphogypsum composites is shown.

Phosphogypsum (PG), a solid waste by-product of phosphoric acid production,

has been classified as a "Technologically Enhanced Natural Radioactive Material"

(Federal Register, 1978). Consequently, its disposal is regulated by the US EPA and is

limited to stockpiling. It is estimated that by year 2000, the total inventory of

phosphogypsum in US alone will be 2 billion metric tons. Phosphogypsum, which

100

contains trace amount of toxic metals and radionuclides, such as lead, chromium, cadmium, uranium and radium, has created long term and serious environmental problems (Taha and Seals, 1991). Solidified phosphogypsum composites are a possible method for dealing with this environmental problem.

Mixture Experimental Design

Simplex Coordinate System

Percentages of the mixture ingredients, in the experimental design, must be positive and sum to 100%. The levels of one ingredient are not independent of the others. If x_1, x_2, and x_3 are the proportions of the three components of the mixture, the value of x_i is constrained such that

$0 < x_i < 1$ $i = 1, 2, 3$

and the summation of the three ingredients in the mixture must equal to 1, or

$x_1 + x_2 + x_3 = 1$

Simplex factor space to express three components is an equilateral triangle. Figure 7.1 shows the three component simplex coordinate system. Three components 1, 2 and 3, whose proportions are denoted by x_1, x_2 and x_3. The coordinate system used for the values of the x_i, i=1,2,3...q, is called a simplex coordinate system. In Figure 7.1, we see that the vertices of the triangle represent single component mixtures with one xi = 1 and the other components are all equal to 0. The sides of the triangle represents the design coordinates for two component mixtures with one x_i = 0. Design coordinates in the triangle interior represent all three components present in the

mixture. Any mixture combination must be on the boundaries or inside the triangle of

coordinates.

Component 1
(1, 0, 0)

$x_1 = 1$
(1, 0, 0)

Component 3 (0, 1, 0)
(0, 0, 1) $x_2 = 1$

(0, 0, 1)
$x_3 = 1$
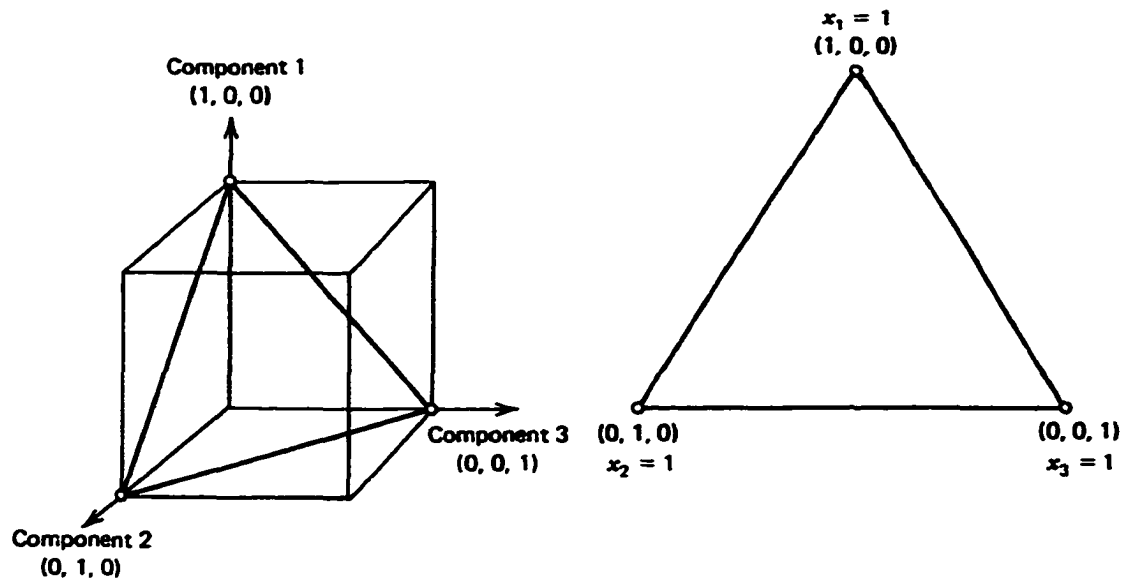
Component 2
(0, 1, 0)

Figure 7.1 Three component simplex coordinate system

Ingredient Content Selection for Mixtures

Simplex-Lattice Design

The array, made up of a uniform distribution of design coordinates on the

simplex coordinate system, is known as a lattice. The simplex-lattice design consists

of a lattice of design coordinates. The designation {k, m} is used for a simplex-lattice

design with k components to estimate a polynomial response surface equation of

degree m (Hinkelmann, et al., 1994 and Kuehl, 1994). The proportions of every

component included in a {k, m} simplex-lattice design are

$x_i = 0, 1/m, 2/m, \cdots\cdots , 1$

This design consists of all possible combinations for these levels of x_i (Figure 7.2).
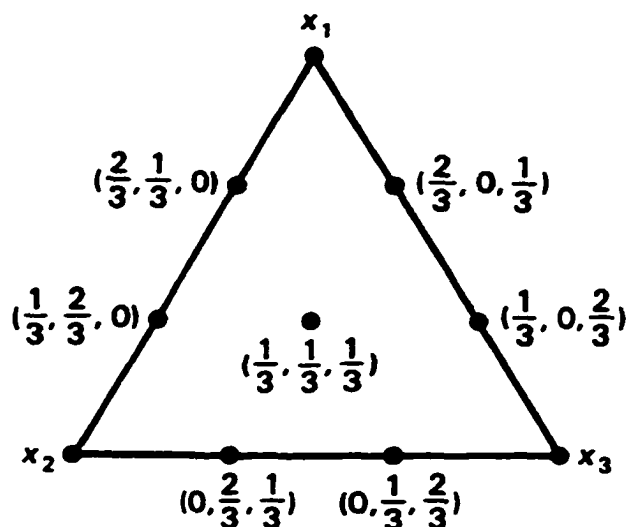
Figure 7.2 Simplex-lattice $\{3, 3\}$ design for three components

Simplex-Centroid Design

The simplex-centroid design is a design on the simplex coordinate system consisting of all components, each in equal proportions. Consequently, there are k single component mixtures, all possible two component mixtures with proportions 1/2 for each component, and so forth up to all possible three component mixtures with proportions 1/3 for each component, finally to one k component with proportions 1/k for each component (Figure 7.3) (Hinkelmann, et al 1994, Kuehl, 1994).

Augmented Simplex-Centroid Design

The combination of mixtures for the simplex-lattice and simplex-centroid designs lie on the edges of the simplex factor space with the exception of one centroid point, which contains all mixture components. A more complete mixture design is augmenting the simplex-centroid design with mixture on the axes of the simplex factor space. The design points are positioned on each axis equidistant from the centroid toward the vertices. A three component design will have three additional

design points with coordinates, and so forth so that a k component design will have k additional design points with coordinates. The addition of these axis points will provide a better distribution of information throughout the experimental region (Figure 7.4) (Hinkelmann et al, 1994, Kuehl, 1994).
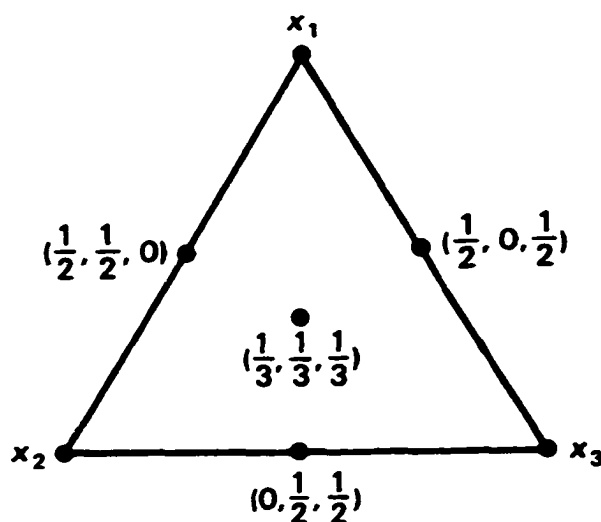
Figure 7.3 Simplex-centroid design for three components
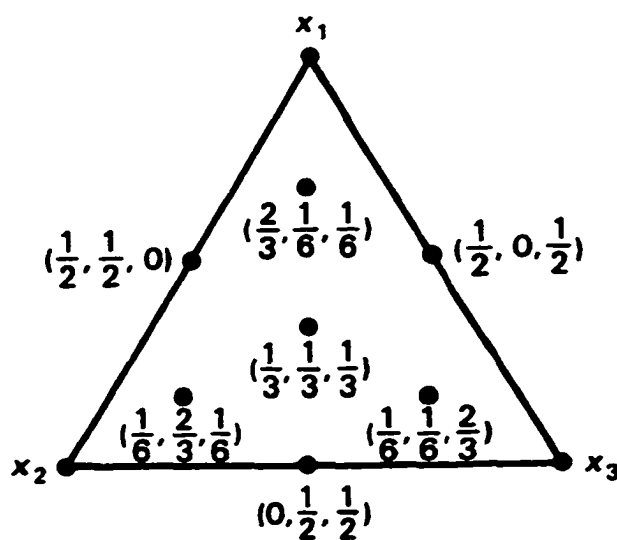
Figure 7.4 Augmented simplex-centroid design for three components

Augmented Simplex-Centroid Design with Pseudocomponents

For some mixture experiments, all three components will be present in some minimum proportions. Lower bounds (L_i) on component proportions are constrained by: $0 < L_i < x_i < 1$ on the component proportions. Suppose the lower bounds for cement (x_1), PG (x_2), and lime (x_3) are :

$$L_1 \leq x_1 \qquad L_2 \leq x_2 \qquad L_3 \leq x_3$$

To simplify the construction of the design coordinates, pseudocomponents are constructed by coding the original component variables to a simplex system for the pseudocomponents variables x_i' with constraint $0 \leq x_i' \leq 1$. If the lower bound for component i is L_i and $L = \Sigma L_i$, then the pseudocomponent x_i' is computed as (Hinkelmann et al 1994, Kuehl, 1994):

$$x_i' = (x_i - L_i)/(1-L)$$

For example, the lower bound for x_1, x_2, and x_3 are 0.35, 0.20 and 0.15 respectively, the projection from pseudocomponents (right triangle) to original components (left triangle) is shown in Figure 7.5 (Cornell, 1990).

Analysis of Mixture Experiment Data

<u>**Response Surface Analysis**</u>

Generally, the dependence of treatment effects on treatments can be represented as a response curve or a response surface. If the levels of one treatment factor represent the treatments, the dependency is the response curve. If the treatments are a combination of levels of two or more treatment factors, the dependency is the response surface. Such curves or surfaces can be used to judge not only the treatment structure

but also the relationship between treatments and responses. The response surface analysis enables the determination of the treatment combinations, that give the optimum (highest or lowest) response. The true relationship is commonly unknown and so polynomial functions usually provide good approximations for relatively small regions of quantitative factor levels. The most common polynomial models for approaching response surfaces are the linear (first order) and quadratic (second order) models (Hinkelmann, et al 1994, Kuehl, 1994). Figure 7.6 represents a surface contour of the estimated response surface for three independent components (Cornell, 1990). The contour lines represent the response, or dependency, values.
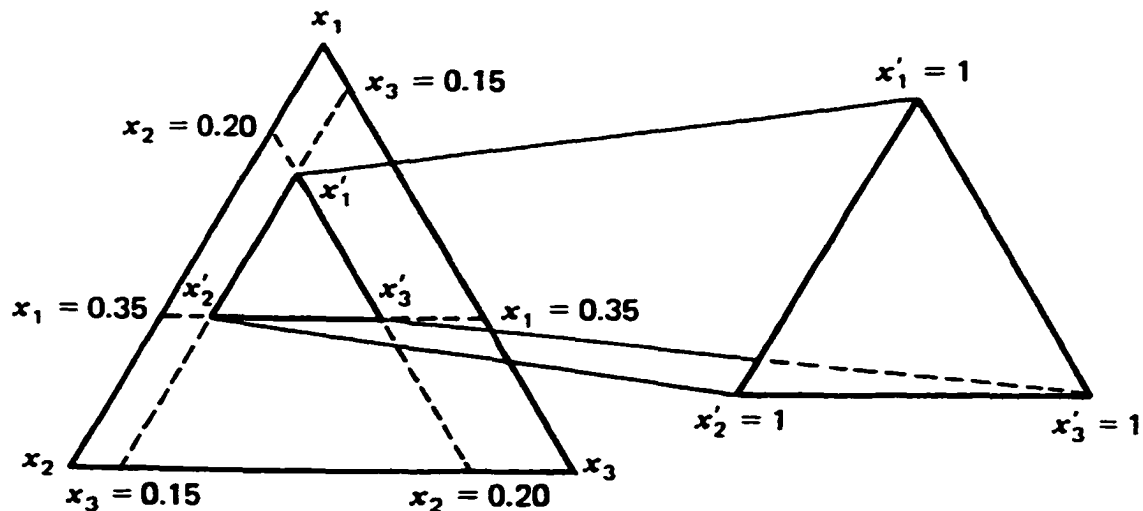
Figure 7.5 A sub-region (interior triangle) of the original simplex redefined as a simplex in the pseudocomponents x_i', i=1, 2 and 3
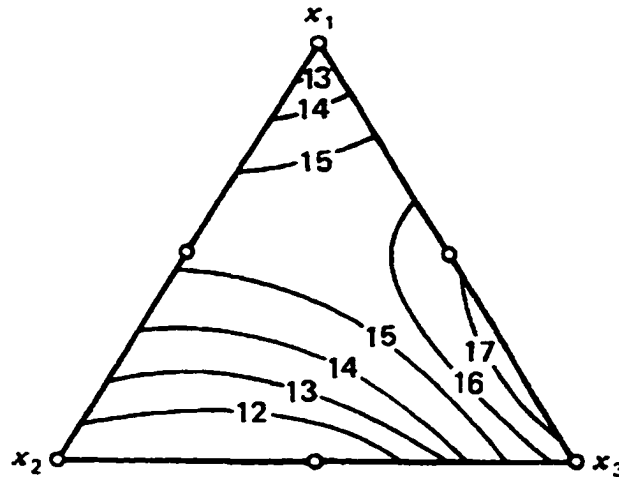
Figure 7.6 Surface contour of response surface for three component mixtures

Quadratic Canonical Polynomial Model

The quadratic polynomial model used to approximate response surfaces was

$$y(x) = \beta_0 + \sum_{i=1}^{k} \beta_i x_i + \sum_{i=1}^{k} \beta_{ii} x_i^2 + \sum_{i<} \sum_{j} \beta_{ij} x_i x_j + e_i \qquad (1)$$

where e_i is the random error (normal distribution with mean zero and variance σ^2). The number of points has to be at least as large as the number of parameters to be estimated in the above equation. The restriction $\sum_{i=1}^{k} x_i = 1$ has to be applied to the above equation, that is,

$$x_i = 1 - \sum_{j \neq i} x_j.$$

Then the quadratic canonical polynomial becomes

$$y(x) = \sum_{i=1}^{k} \beta_i^* x_i + \sum_{i<} \sum_{j} \beta_{ij}^* x_i x_j + e_i \qquad (2)$$

Where $\beta_i^* = \beta_0 + \beta_i + \beta_{ii}$ and $\beta_{ij}^* = \beta_{ij} - \beta_{ii} - \beta_{jj}$

The new parameters of the quadratic canonical polynomial for a three-ingredient mixture, expressed in terms of the original polynomial parameters, are

$$\beta_1^* = \beta_0 + \beta_1 + \beta_{11} \qquad \beta_2^* = \beta_0 + \beta_2 + \beta_{22} \qquad \beta_3^* = \beta_0 + \beta_3 + \beta_{33}$$

$$\beta_{12}^* = \beta_{12} - \beta_{11} - \beta_{22} \qquad \beta_{13}^* = \beta_{13} - \beta_{11} - \beta_{33} \qquad \beta_{23}^* = \beta_{23} - \beta_{22} - \beta_{33}$$

If all β_{ii} and β_{ij} equal zero, then the quadratic canonical model become a linear model.

Inclusion of Process Variables

Process variables are factors in an experiment that do not form any portion of the mixture but whose levels may affect the properties of the mixture. For the PG composite example, composite submergence is a process variable. Under submergence conditions, the level of the process variable takes the value of one, while under control (no submergence) condition, the level of the process variable takes the value of zero.

Let us look at a mixture experiment consisting of three components (x_1, x_2, and x_3) and two process variables whose coded values are denoted by $z_1 = 0$, 1 and $z_2 = 0$, 1. The mixture model without the process variable is a quadratic canonical model. A 2^2 factorial arrangement is considered for fitting the model in the two process variables:

$$\eta_{pv} = \alpha_0 + \alpha_1 z_1 + \alpha_2 z_2 + \alpha_{12} z_1 z_2$$

The combined simplex-centroid by 2^2 factorial design is shown in Figure 7.7 (Cornell, 1990). This design includes a three component seven point simplex-centroid design and two process variables with a 2^2 factorial arrangement.
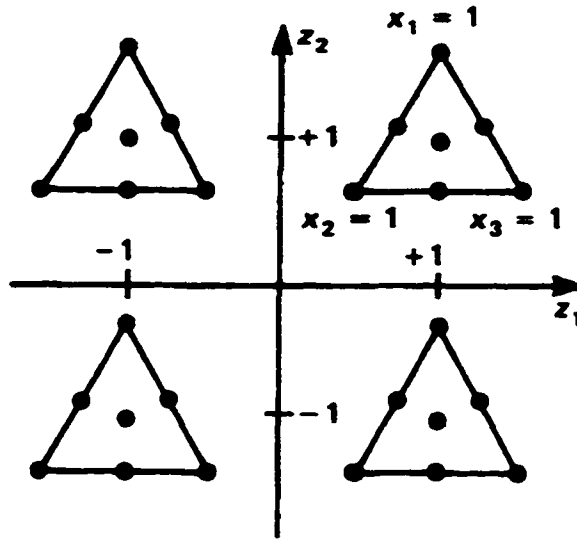
Figure 7.7 A combined simplex-centroid by 2×2 factorial design

The model combines three ingredients and two process variables where $(1 = 1,2)$:

$$y(x, z) = \sum_{i=1}^{3} \gamma_i^0 x_i + \sum_{i<}\sum_{j}^{3} \gamma_{ij}^0 x_i x_j + \alpha_1 z_1 + \alpha_2 z_2 + \alpha_{12} z_1 z_2 + \sum_{l=1}^{2}[\sum_{i=1}^{3} \gamma_i^l x_i +$$

$$\sum_{i<}\sum_{j}^{3} \gamma_{ij}^l x_i x_j + \gamma_{123}^l x_1 x_2 x_3] z_l + [\sum_{i=1}^{3} \gamma_i^{12} x_i + \sum_{i<}\sum_{j}^{3} \gamma_{ij}^{12} x_i x_j + \gamma_{123}^{12} x_1 x_2 x_3] z_1 z_2 + e_I \quad (3)$$

In equation (3), $\sum_{i=1}^{3} \gamma_i^0 x_i$ represents the linear blending portion of the model and γ_i^0 is

the expected response value for the component i average over all combinations of

levels for z_1 and z_2. $\sum_{i<}\sum_{j}^{3} \gamma_{ij}^0 x_i x_j$ represents the nonlinear blending portion of the

model and γ_{ij}^0 is the nonlinear blending portion between component i and j over all

combinations for the levels of z_1 and z_2. $\alpha_1 z_1 + \alpha_2 z_2$ represents the linear portion of the

process variables. $\alpha_{12} z_1 z_2$ represents the interaction between two process variables.

$$\sum_{l=1}^{2} [\sum_{i=1}^{3} \gamma_i^l x_i + \sum_{i<}\sum_{j}^{3} \gamma_{ij}^l x_i x_j + \gamma_{123}^l x_1 x_2 x_3] z_l \text{ represents the effect of process variable}$$

levels z_1 and z_2 on the linear and nonlinear blending properties of the components.

γ_i^l is the change of expected response to component i for a 1-unit change in z_l, while

γ_{ij}^l is the change in the nonlinear blending of component i and j for a 1-unit change in

$$z_l. [\sum_{i=1}^{3} \gamma_i^{12} x_i + \sum_{i<}\sum_{j}^{3} \gamma_{ij}^{12} x_i x_j + \gamma_{123}^{12} x_1 x_2 x_3] z_1 z_2 \text{ represent the interaction effect of the}$$

two process variables z_1 and z_2 on the linear and nonlinear blending properties of the

three components. The typical response surface for equation 3 is presented in Figure

7.8. This response surface includes three component composites and two process

variables which have two levels respectively

For our phosphogypsum composite example, besides two process variables

described in equation (3), there is one process variable with two levels, submerged and

control. Assuming the process variable takes the values of 0 and 1, then the quadratic

canonical polynomial becomes

$$y(x) = \sum_{i=1}^{k} \beta_i^* x_i + \sum_{i<}\sum_{j} \beta_{ij}^* x_i x_j + \alpha_1 z + \sum_{i=1}^{k} \beta_i^{**} x_i z + \sum_{i<}\sum_{j} \beta_{ij}^{**} x_i x_j z + e_1 \qquad (4)$$

β_i^{**} and β_{ij}^{**} are coefficients for the $x_i z$ and $x_i x_j z$ terms.

This is the model applied in the optimum ingredient searching experiment.

When z = 0 the equation (4) becomes equation (2).

When z = 1, the equation (4) becomes equation (5).

$$y(x) = \sum_{i=1}^{k} (\beta_i^* + \beta_i^{**})x_i + \sum_{i<} \sum_j (\beta_{ij}^* + \beta_{ij}^{**})x_i\, x_j + \alpha_1 + e_i \qquad (5)$$

Equation (5) is the same as equation (2) in nature, but the different coefficients represent the different shape of the response surface in treatment conditions. The response surface for equation (4) is shown in Figure 7.9 (Cornell, 1990). It includes three component mixtures under one process variable with two levels
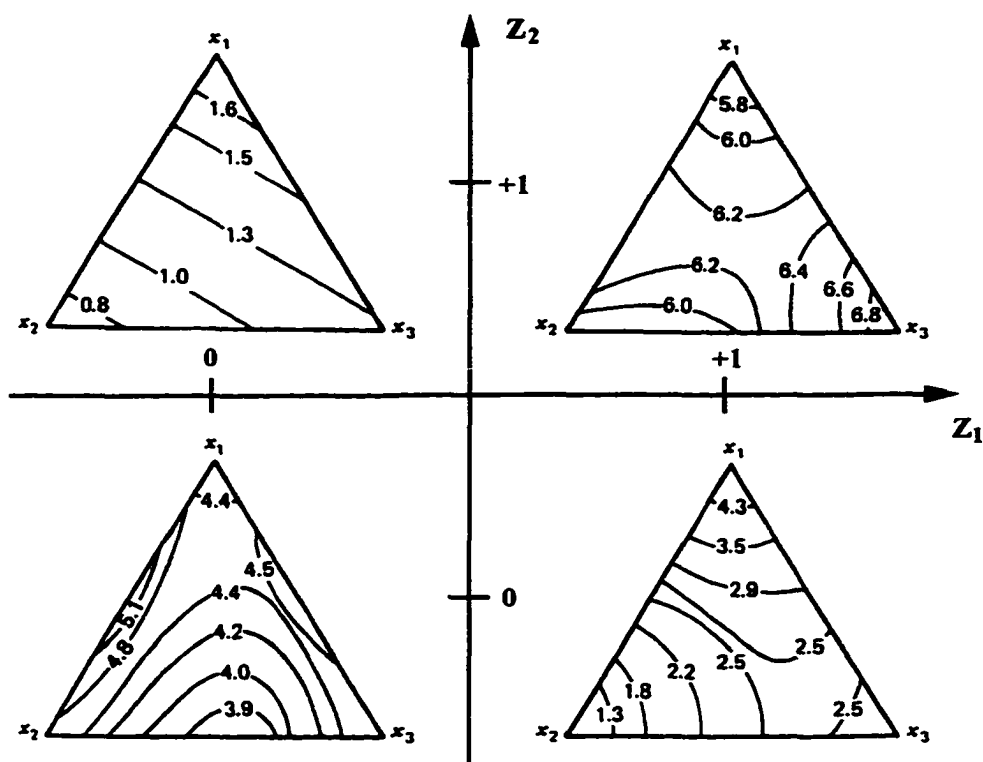
Figure 7.8 A response surface with two process variables
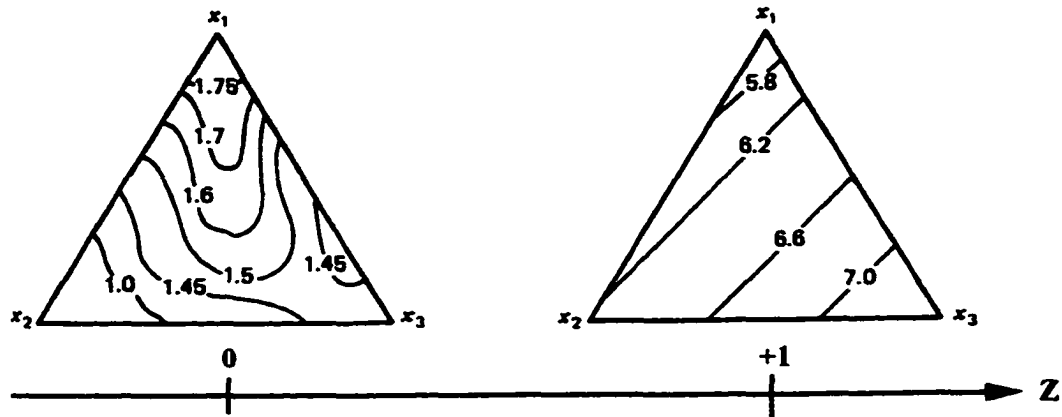
Figure 7.9 A response surface with one process variable

Following similar procedures, the response surface of the three ingredient mixture, including three process variables z_1, z_2 and z_3 each containing two levels, is shown in Figure 7.10. The shaded regions represent blends estimated to have acceptable values within the range of s in 2.0 - 3.5 (Cornell, 1990).

Least-Squares Estimation Formulas for the Polynomial Coefficients and Variances

The general form of the mixture model is $y = X\beta + \epsilon$, where y is an $N*1$ vector of observations, X is an $N*p$ matrix whose elements are the mixture component proportions and functions (such as pairwise products) of the component proportions, β is a $p*1$ vector of parameters and ϵ is an $N*1$ vector of random errors. The normal equations used for estimating the elements of the parameter vector β are

$X'Xb = X'y$

The solution for the coefficients is then (Cornell, 1990)

$b = (X'X)^{-1}X'y$.
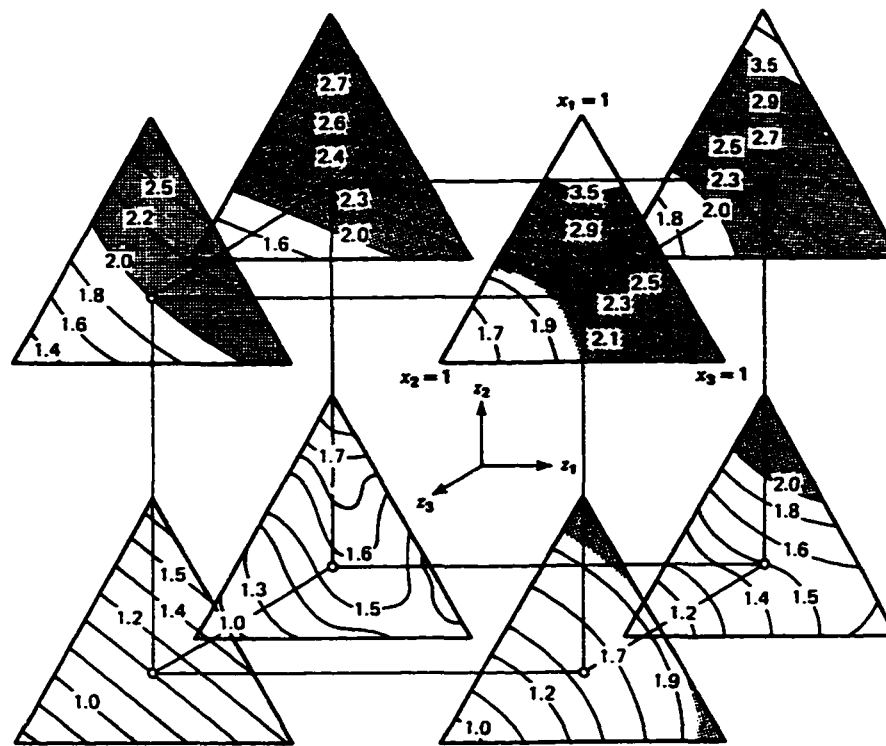
Figure 7.10 A response surface under three process variables

Furthermore, if a measure of the error variance σ^2 is available, then the variance-covariance estimate is (Cornell, 1990)

Var (b) = $(X'X)^{-1}\sigma^2$. The predicted value of the response surface at a point x = $(x_1, x_2...x_p)'$ in the experiment region is expressed as

$\hat{y}(x) = x_p' b$

where: x_p' is a $1*p$ vector whose elements correspond to the elements in a row of the

matrix X. The variance of the $\hat{y}(x)$ is then (Cornell, 1990)

$$var[\hat{y}(x)] = var[x_p'\,b] = x_p'var[b]\,x_p = x_p'(X'X)^{-1}\,x_p\sigma^2$$

Hypothesis Test of the Quadratic Model

For the quadratic model, $y(x) = \sum_{i=1}^{k} \beta_i^* x_i + \sum_{i<}\sum_{j} \beta_{ij}^* x_i x_j + e_i$

The hypothesis for the above model includes:

H_0 : The response does not depend on the mixture components, that is $\beta_i = \beta_{ij} = 0$, and

H_a : The response surface does depend on the mixture components, that is not all β_i

and β_{ij} equal zero.

To perform a hypothesis test, an ANOVA table (Table 7.1) should be presented first,

Table 7.1 ANOVA table of the quadratic model

Source of Variation	Degree of Freedom	Sum of Squares	Mean of Squares	F-value
Model	p-1	SSR	MSR=SSR/(p-1)	MSR/MSE
Error	N-p	SSE=SST-SSR	MSE=SSE/(N-p)	
Total	N-1	SST		

Then the F statistics is used, such that

$F^* = MSR/MSE$

The decision rule to control the Type I error at α is :

If $F^* \leq F(1-\alpha; p-1, n-p)$, conclude H_0

If $F^* \geq F(1-\alpha; p-1, n-p)$, conclude H_a

A failure to reject indicates that the response surface can be adequately modeled as a horizontal plane over the corresponding mixture points.

Rejection of H_0 implies that the response surface is not a horizontal plane. Instead, mixture ingredients determine the response surface.

SAS Data Analysis in Mixture Experiments

The quadratic canonical polynomial model can be fitted using the least-squares method. Appropriate tests of the hypothesis, including lack of fit analysis, can be performed using the usual regression methods. In the SAS software, both GLM and REG procedures can be used for analysis of mixture experiments. The NOINT option should be used to express the constraint that all components sum to unity in the mixture design. The options: 'Forward', 'Backward' and 'Stepwise' under PROC REG in SAS can be used to select appropriate models of predictor variables. The data analysis is composed of two steps (Cornell, 1990).

Step one, to test the hypothesis whether the response depends on the mixture components in equation (3) and (4), a quadratic canonical polynomial model with deleting one of the linear blending terms and including an intercept term is applied. The option NOINT will not be included in the SAS model statement. Consequently, the degrees of freedom, sum of squares, and error sum of squares for the model are correct for the quadratic canonical polynomial model. Therefore the F test and R-square are correct.

Step two, to estimate the coefficients and the variances of the coefficients in the quadratic canonical polynomial model, the original terms in the quadratic canonical polynomial model should be used with the option of NOINT. The coefficients and their variances can be obtained directly from the SAS output.

Lack of Fit Test

After being selected, the model should be tested to see whether it fits the data adequately. This test is called the lack of fit test (LOF), which assumes that the observations Y for the given X are independent, normally distributed, and the distribution of Y has the same variance. The LOF test also requires repeated observations at one or more X levels. The basic idea of the LOF test is to compare the selected model with the ideal (full) model to see whether there is a difference. If there is no significant difference between the selected model and the full model, then the selected model fits the data well. If all independent X's are assumed to be categorical variables, then the model is

$$Y_{ij} = \mu_j + \varepsilon_{ij}$$

This model is the full model and it fits the data ideally. It can be shown that the estimators of $\hat{\mu}_j$ are simply the sample means $\bar{Y}_j$ (Nester et al.,1996). Thus the error sum of squares for the full model is

$$SSE(F) = \sum_j \sum_i (Y_{ij} - \bar{Y}_j)^2$$

The degrees of freedom associated with the full model is the sum of the component degrees of freedom, that is :

$$df_F = n - c$$

where: c is the number of the parameters in the full model.

The F test is performed to test the appropriateness of the selected model, the alternatives are:

H_0 : The selected model fits the data well

H_a : The selected model does not fit the data well

$$F^* = \frac{SSE(R) - SSE(F)}{df_R - df_F} \Bigg/ \frac{SSE(F)}{df_F}$$

If $F^* < (F_{1-\alpha}; df_R - df_F, df_F)$, conclude H_0, else

If $F^* > (F_{1-\alpha}; df_R - df_F, df_F)$, conclude H_a, where

α is the type I error (Nester et al.,1996).

Experimental Design of Stabilized PG Composites

Ingredient Combination Selection

For the stabilized phosphogypsum composite experiment, all three ingredients should be present, therefore the pseudocomponents with augmented simplex-centroid design is used to construct the ingredient combination. The lower bounds are 0.04, 0.03 and 0.83 for the cement, lime and phosphogypsum respectively in PG:cement:lime composites. The lower bounds are 0.03, 0.35 and 0.55 for the cement, fly ash and PG respectively in PG:fly ash:cement composites. The lower bounds are 0.03, 0.35 and 0.55 for the lime, fly ash and PG respectively in PG:fly ash:lime composites. The principle for choosing the lower bounds, from an economic point of

view, are the lowest values of cement (or lime) and highest value of phosphogypsum.

The calculated results of the PG composites are shown in Table 7.2 - 4.

Table 7.2 Ingredients (%) of PG:cement:lime composites

Cement	Lime	PG
14	3	83
9	3	88
4	3	93
9	8	83
4	13	83
4	8	88
10.7	4.7	84.6
5.7	9.7	84.6
5.7	4.7	89.6
7.3	6.3	86.4

Table 7.3 Ingredients (%) of PG:fly ash:cement composites

Cement	Fly ash	PG
3	35	62
3	38.5	58.5
3	42	55
4.2	36.2	59.6
4.2	39.6	56.2
5.3	37.3	57.4
6.5	35	58.5
6.5	38.5	55
7.6	36.2	56.2
10	35	55

Table 7.4 Ingredients (%) of PG:fly ash:lime composites

Lime	Fly ash	PG
3	35	62
3	38.5	58.5
3	42	55
4.2	36.2	59.6
4.2	39.6	56.2
5.3	37.3	57.4
6.5	35	58.5
6.5	38.5	55
7.6	36.2	56.2
10	35	55

Dynamic Leach Test of PG Composites

The PG: fly ash :cement (or lime) composites were divided into two groups. Group one, with two PG composites, was under a dynamic leaching condition in seawater for 28 days (see Chapter 4). Group two, with three PG composites, was the control group where no treatment was applied. For both groups, surface hardness (SH) was measured for each PG composite under wet and dry conditions.

The PG:cement:lime composites were divided into two groups. Group one, with five PG composites, was under a dynamic leaching condition in seawater for 28 days. Group two, with three PG composites, was the control group where no treatment was applied. For group one, surface hardness (SH) and unconfined strength (UCS) were measured for every PG composite under the dry condition, but diffusion coefficients (D) were only measured for the two PG composites. For the control group, surface hardness (SH) and unconfined strength (UCS) were measured under the dry condition.

Analysis of PG Composite Data

PG:Fly Ash:Cement Composites

Quadratic model (3), which combines three ingredients and two process variables, was used to regress the response surfaces of surface hardness (SH).

$$y(x, z) = \sum_{i=1}^{3} \gamma_i^0 x_i + \sum_{i<}\sum_{j}^{3} \gamma_{ij}^0 x_i x_j + \alpha_1 z_1 + \alpha_2 z_2 + \alpha_{12} z_1 z_2 + \sum_{l=1}^{2}[\sum_{i=1}^{3} \gamma_i^l x_i +$$

$$\sum_{i<}\sum_{j} \gamma_{ij}^l x_i x_j + \gamma_{123}^l x_1 x_2 x_3] z_1 + [\sum_{i=1}^{3} \gamma_i^{12} x_i + \sum_{i<}\sum_{j}^{3} \gamma_{ij}^{12} x_i x_j + \gamma_{123}^{12} x_1 x_2 x_3] z_1 z_2 + e_1 \qquad (3)$$

where x_1 is the cement content; x_2 is the fly ash content; x_3 is the phosphogypsum content; z_1 is a process variable, leach, which has two levels, control ($z_1 = 0$) and submergence ($z_1 = 1$); z_2 is a process variable, wet, which has two levels, wet ($z_2 = 0$) and dry ($z_2 = 1$); y is the Log(SH) for the PG composites; and e_i is the random error term assumed to be normally distributed with a mean equal to zero and a common variance (σ^2). SAS, MS Excel, MS Access, and Sigma Plot were used for data analysis and plot drawing.

The Shapiro-Wilk statistics and residual plots were used to test the normality assumption of the error term. The p-value for the Shapiro-Wilk test was 0.9297, which indicated that the error term is normally distributed. The residual plots provided provided support that the error term had homogeneous variance. Model (3) was regressed to find the parameters (Table 7.5) and related p-values for the model and lack of fit as follows:

Table 7.5 SAS output for surface hardness of PG:fly ash:cement composites

Variable	DF	Parameter Estimate	Standard Error	T for H_0: Parameter = 0	Prob > |T|
PG	1	3.013327	0.59820085	5.037	0.0001
CEMENT	1	6.389983	1.22316335	5.224	0.0001
FLYASH	1	3.864410	0.89181168	4.333	0.0001
WET	1	0.055525	0.07324960	0.758	0.4503
LEACH	1	-1.280128	0.08189554	-15.631	0.0001
WET*LEACH	1	-0.425498	0.11581779	-3.674	0.0004

The p-values for the model and lack of fit were 0.0001 and 0.2073 respectively, which indicated that the model was appropriate. Therefore the model is:

Log(SH) = 3.013*PG + 6.390*CEMENT + 3.866*FLYASH + 0.0555*WET - 1.280*LEACH - 0.4255*WET*LEACH

for PG:fly ash:cement composites. This model is a linear surface with respect to all three components with no significant interaction between all the ingredients. The two process variables do not affect the shape of the response surface, but they do affect the values of the response surface. This is plotted as response surface plot in Figure 7.11. From a ten month seawater submergence experiment in Grand Isle, Louisiana, it was found that the minimum wet submergence surface hardness for surviving PG composites was 5.8 mm⁻¹. The shaded area in the right top subfigure for wet and submergence condition shows that surface hardness was greater than 5.8 mm⁻¹, and the cement content was less than 0.1 for economic considerations. While the little triangle is in the experimental region, the joint region of the shaded and triangle areas is the optimum ingredient combination. The disjoint region of the shaded and triangle areas

is the region with predicted value of surface hardness greater than 5.8 mm^{-1}, (Log5.8=1.76) but not verified by the experiment. From Figure 7.11, there exists a joint region of the shaded and triangle areas. Therefore, therefore PG:fly ash:cement ingredient combinations are a possible substrate for artificial reefs. Table 7.6 lists the possible economic ingredients.

Table 7.6 Possible economic ingredients (%) with minimum surface hardness 5.8 mm^{-1}

Cement	Fly ash	PG
2.6	35.8	61.6
2.6	36.6	60.8
2.8	36	61.2
3	35	62
3.2	34	62.8
3.4	32.6	64
3.4	33.4	63.2
3.6	32.8	63.6
3.8	32	64.2
4	31	65
4.2	30.4	65.4

PG:Fly Ash:Lime Composites

The quadratic model (3), combining three ingredients and two process variables, was used to regress the response surfaces of the surface hardness (SH),

$$y(x, z) = \sum_{i=1}^{3} \gamma_i^0 x_i + \sum_{i<}\sum_{j}^{3} \gamma_{ij}^0 x_i x_j + \alpha_1 z_1 + \alpha_2 z_2 + \alpha_{12} z_1 z_2 + \sum_{l=1}^{2}[\sum_{i=1}^{3} \gamma_i^l x_i +$$

$$\sum_{i<}\sum_{j}^{3} \gamma_{ij}^l x_i x_j + \gamma_{123}^l x_1 x_2 x_3]z_1 + [\sum_{i=1}^{3} \gamma_i^{12} x_i + \sum_{i<}\sum_{j}^{3} \gamma_{ij}^{12} x_i x_j + \gamma_{123}^{12} x_1 x_2 x_3]z_1 z_2 + e_1 \qquad (3)$$

where x_1 is the lime content; x_2 is the fly ash content; x_3 is the phosphogypsum content; z_1 is a process variable, leach, which has two levels, control ($z_1 = 0$) and
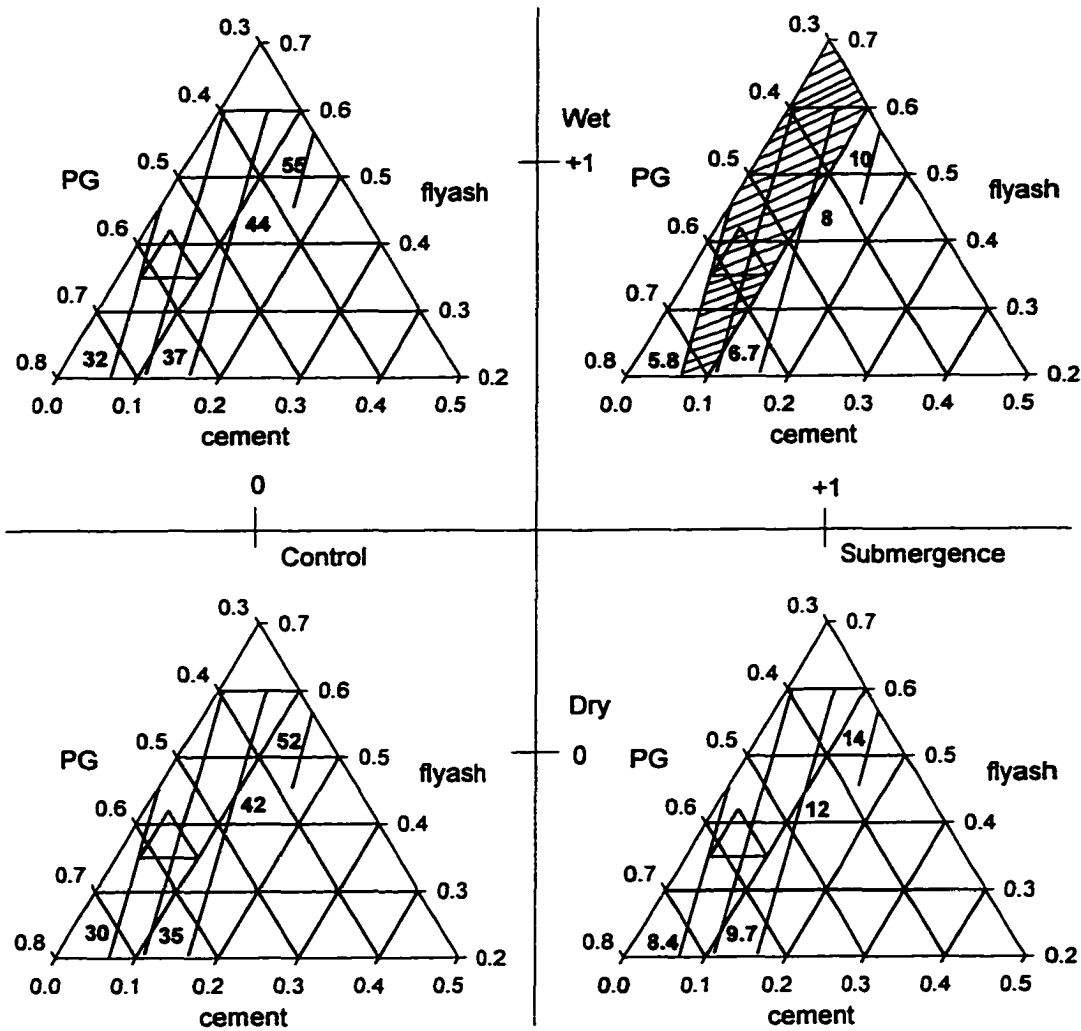
Figure 7.11 Contour plots of the fitted response surfaces of selected model for surface hardness of PG:fly ash:cement composites

submergence ($z_1= 1$); z_2 is a process variable, wet, which has two levels, wet ($z_2 = 1$)

and dry ($z_2 = 0$); y is the Log(SH) of the PG composites; and e_i is the random error

term assumed to be normally distributed with a mean equal to zero and a common

variance (σ^2). SAS, MS Excel, MS Access, and Sigma Plot are used for data analysis

and plot drawing.

Shapiro-Wilk statistics and residual plots were used to test the normality

assumption of the error term. The p-value for the Shapiro-Wilk test was 0.5477, which

indicated that the error term was normally distributed. The residual plots provided

support that the error term had homogeneous variance. Model (3) was regressed to

find the parameters (Table 7.7) and related p-values for the model and lack of fit as

follows:

Table 7.7 SAS output for surface hardness of PG:fly ash:lime composites

Variable	DF	Parameter Estimate	Standard Error	T for H_0: Parameter=0	Prob > |T|
PG	1	0.163462	2.43882951	0.067	0.9467
LIME	1	-193.5272	74.3364444	-2.603	0.0110
FLYASH	1	8.597745	3.20357308	2.684	0.0088
WET	1	-0.213314	0.09487309	-2.248	0.0272
LEACH	1	-1.820823	0.10720812	-16.984	0.0001
PG*LIME	1	330.3183	137.649630	2.400	0.0187

The p-values and lack of fit for the model were 0.0001 and 0.0018 respectively. Lack

of fit exists for this model, but this model is the best model except the full model. The

R^2 for this model is 0.788 while the R^2 for the full model is 0.908. Therefore the model

equation is:

$$Log(SH) = 0.1635 * PG - 193.53 * LIME + 8.598 * FLYASH - 0.2133 * WET - 1.8208 * LEACH + 330.32 * PG * LIME$$

for PG:fly ash:lime composites. This model is a quadratic surface with respect to all three components. Interactions exist between PG and lime. The two process variables do not affect the shape of the response surface, but they do affect the values of the response surface. This is plotted as a response surface plot in Figure 7.12. The shaded area in the subfigure for wet and submergence condition shows that surface hardness is greater than 5.8 mm^{-1}, and lime content is less than 0.1 due to economic considerations. While the little triangle is the experimental region, the joint region of the shaded and triangle areas is the optimum ingredient combination. From Figure 7.12, no joint region of the shaded and triangle areas is found. Therefore, PG:fly ash:lime ingredient combinations are not a suitable substrate for artificial reefs.

PG:Cement:Lime Composites

Diffusion Coefficient

The quadratic model (1), which includes three ingredients, was used to regress the response surfaces for diffusion coefficient of PG:cement:lime composites,

$$y(x) = \beta_0 + \sum_{i=1}^{k} \beta_i x_i + \sum_{i=1}^{k} \beta_{ii} x_i^2 + \sum_{i<} \sum_{j} \beta_{ij} x_i x_j + e_i \tag{1}$$

where x_1 is the cement content ; x_2 is the lime content; x_3 is the phosphogypsum content; y is $Log_{10}D$ of the PG composites; and e_i is the random error term assumed to be normally distributed with a mean equal to zero and a common variance (σ^2). SAS, MS Excel, MS Access, and Sigma Plot were used for data analysis and drawing.
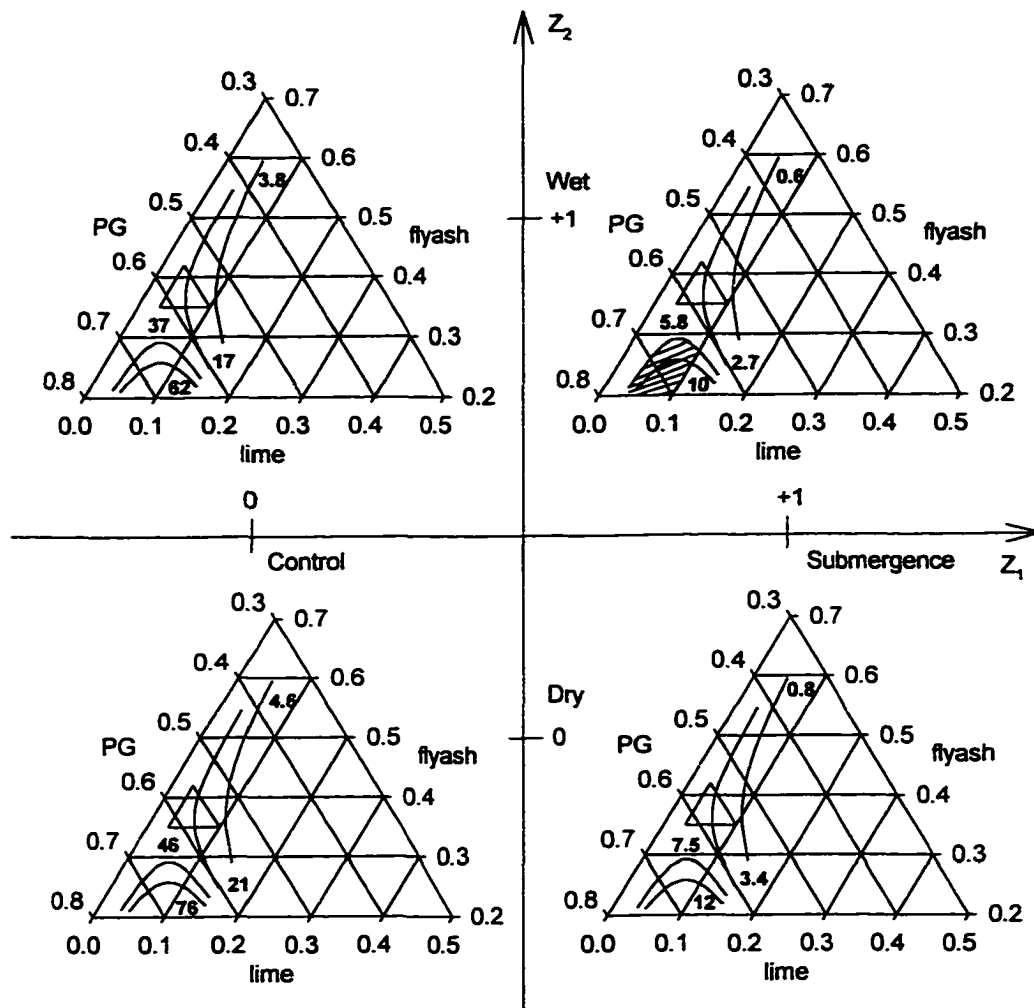
Figure 7.12 Contour plots of the fitted response surfaces of selected model for surface hardness of PG:fly ash:lime composites

Shapiro-Wilk statistics and residual plots were used to test the normality assumption of the error term. The p-value for Shapiro-Wilk test was 0.1848, which indicated that the error term is normally distributed. The residual plots provided support that the error term had a homogeneous variance. Model (3) was regressed to find the parameters (Table 7.8) and related p-values for the model and lack of fit as follows.

Table 7.8 SAS output for diffusion coefficient of PG:cement:lime composites

Variable	DF	Parameter Estimate	Standard Error	T for H_0: Parameter=0	Prob > |T|
PG	1	-2.835329	0.16527931	-17.155	0.0001
LIME	1	-16.273322	1.22578736	-13.276	0.0001
CEMENT	1	-9.701592	1.21823954	-7.964	0.0001

The p-values for the model and lack of fit were 0.0001 and 0.1878 respectively, which indicated that the model was appropriate. Therefore, the model is selected to be:

$Log_{10}D = -2.835*PG - 16.273*Lime -9.702*Cement$

for PG:cement:lime composites. It was plotted as a response surface plot in Figure 7.13. This model is a linear surface with respect to all three components.

Unconfined Strength

The quadratic model (4), which includes three ingredients and one process variable, was used to regress the response surfaces of unconfined strength of PG:cement:lime composites,

$$y(x) = \sum_{i=1}^{k} \beta_i^* x_i + \sum_{i<} \sum_{j} \beta_{ij}^* x_i x_j + \alpha_1 z + \sum_{i=1}^{k} \beta_i^{**} x_i z + \sum_{i<} \sum_{j} \beta_{ij}^{**} x_i x_j z + e_1 \quad (4)$$
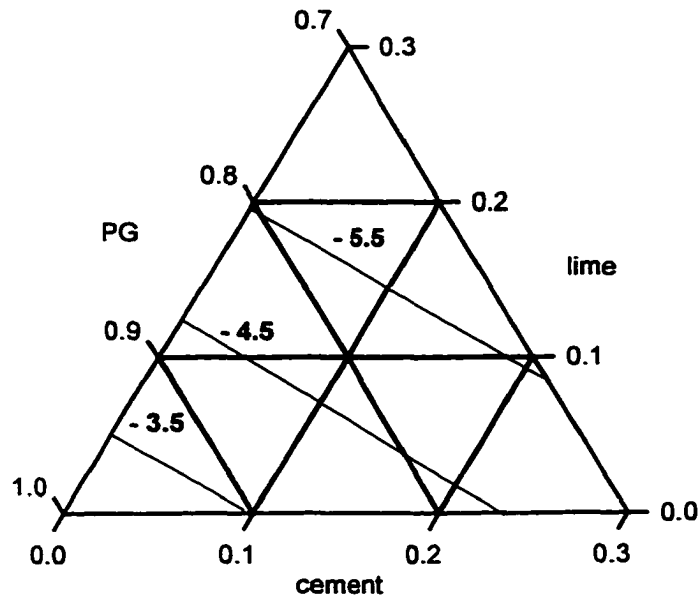
Figure 7.13   Contour plots of the fitted response surface of selected model for $Log_{10}D$ of PG:cement:lime composites

where x_1 is the cement content; x_2 is the lime content; x_3 is the phosphogypsum content; z is a process variable, treat, which has two levels, control ($z = 0$) and submergence ($z = 1$); y is the Log(UCS) of the PG composites; and e_i is the random error term assumed to be normally distributed with a mean equal to zero and a common variance (σ^2). SAS, MS Excel, MS Access, and Sigma Plot are used for data analysis and plot drawing.

Shapiro-Wilk statistics and residual plots were used to test the normality assumption of the error term. The p-value for the Shapiro-Wilk test was 0.6760, which indicated that the error term was normally distributed. The residual plots provided support that the error term had homogeneous variance. Model (3) was regressed to find the parameters (Table 7.9) and related p-values for the model and lack of fit as follows.

Table 7.9 SAS output for unconfined strength of PG:cement:lime composites

Variable	DF	Parameter Estimate	Standard Error	T for H0: Parameter=0	Prob > |T|
PG	1	1.821864	0.30499113	5.973	0.0001
CEMENT	1	-46.731353	24.79109615	-1.885	0.0634
LIME	1	5.792292	2.27675368	2.544	0.0131
TREAT	1	3.099797	1.24330627	2.493	0.0149
TREAT*PG	1	-4.580445	1.43937983	-3.182	0.0021
CEMENT*PG	1	68.969409	30.99085373	2.225	0.0291
CEMENT*LIME	1	52.897456	30.93867192	1.710	0.0916

The p-values for the model and lack of fit were 0.0001 and 0.0823 respectively, which indicated that the model was appropriate. Therefore, the model is:

Log(UCS) = 1.822*PG - 46.73*cement + 5.792*lime + 3.100*treat - 4.580*treat*PG + 68.97*cement*PG + 52.90*cement*lime

for PG:cement:lime composites. This model is a quadratic surface with respect to all three components. Interactions exist between PG and lime, cement and lime, and PG and treat. It was plotted as response surface plots in Figure 7.14. From these plots, it is known that in the low cement region the response surface is nearly linear, while in

the high cement region the response surface is quadratic. The unconfined strength for the submergence is lower than that of the control group.
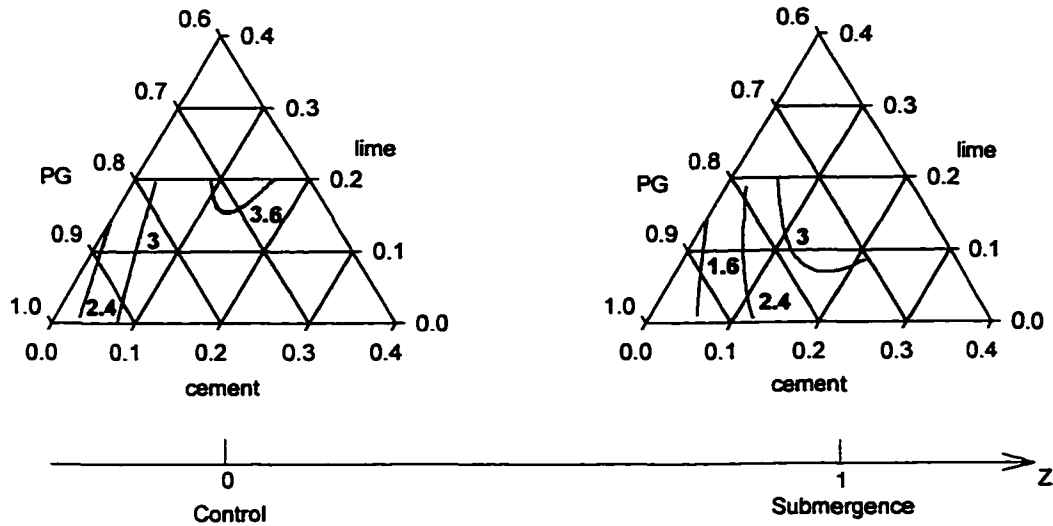
Figure 7.14 Contour plots of the fitted response surface of the selected model for Log(UCS) of PG:cement:lime composites

Surface Hardness

The quadratic model (4), which includes three ingredients and one process variable, was used to regress the response surfaces of unconfined strength for the PG:cement:lime composites.

$$y(x) = \sum_{i=1}^{k} \beta_i^* \, x_i + \sum_{i<} \sum_{j} \beta_{ij}^* \, x_i \, x_j + \alpha_1 z + \sum_{i=1}^{k} \beta_i^{**} \, x_i z + \sum_{i<} \sum_{j} \beta_{ij}^{**} \, x_i \, x_j z + e_1 \qquad (4)$$

where x_1 is the cement content; x_2 is the lime content; x_3 is the phosphogypsum content; z is a process variable which has two levels, control and submergence; y is Log(SH) for the PG composites; and e_i is the random error term assumed to be

normally distributed with a mean equal to zero and a common variance (σ^2). SAS, MS Excel, MS Access, and Sigma Plot were used for data analysis and plot drawing.

Shapiro-Wilk statistics and residual plots were used to test the normality assumption of the error terrm. The p-value for the Shapiro-Wilk test was 0.2711, which indicates that the error term is normally distributed. The residual plots provided support that the error term had a homogeneous variance. Model (3) was regressed to find the parameters (Table 7.10) and related p-values for the model and lack of fit as follows.

Table 7.10 SAS output for surface hardness of PG:cement:lime composites

Variable	DF	Parameter Estimate	Standard Error	T for H_0: Parameter=0	Prob > |T|
PG	1	3.994706	0.34123259	11.707	0.0001
TREAT	1	8.645167	2.65450628	3.257	0.0017
CEMENT	1	4.528093	2.26434497	2.000	0.0492
LIME	1	6.252898	2.27085354	2.754	0.0074
TREAT*PG	1	-11.430158	3.07313080	-3.719	0.0004

The p-values for the model and lack of fit were 0.0001 and 0.4213 respectively, which indicated that the model was appropriate. Therefore the model is:

Log(SH) = 4.000*PG + 8.645*treat + 4.528*cement + 6.253*lime - 11.43*treat*PG

for PG:cement:lime composites. They are all linear response surfaces, but interactions exist between treat and PG. In different treatment conditions the shapes of the linear response surfaces are different. It was plotted as response surface plots in Figure 7.15.

The surface hardness for submergence is lower than that of the control group in the experimental region.
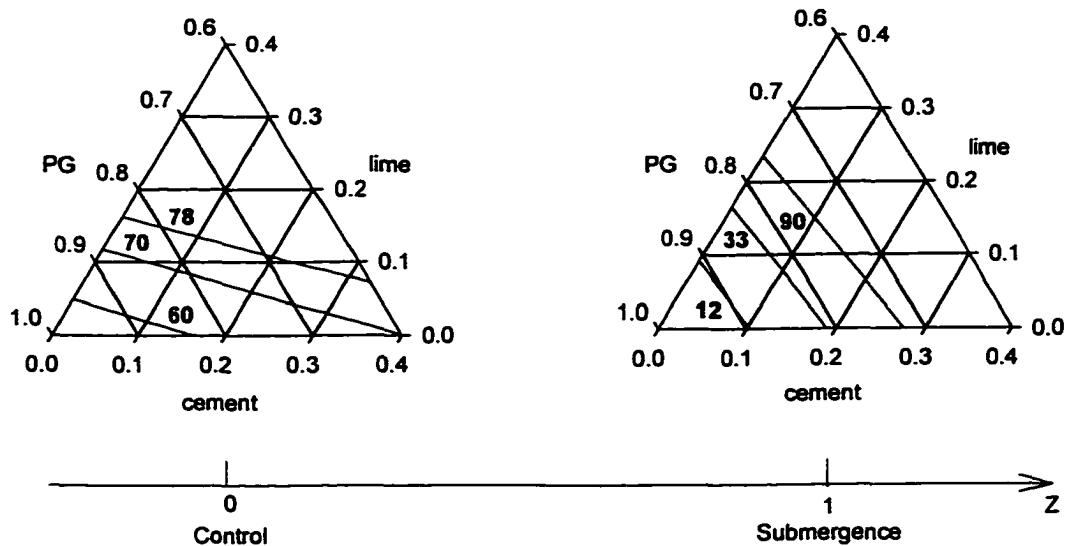
Figure 7.15   Contour plots of the fitted response surface of the selected model for surface hardness of PG:cement:lime composites

From ten month seawater submergence experiment in Grand Isle, Louisiana, it is found that the minimum dry submergence surface hardness for survived PG composites is 8.4 mm^{-1}. From Figure 7.15, the dry submergence surface hardness of most of the PG:cement:lime composites is greater than 8.4 mm^{-1}. It seems that PG:cement:lime composites work for artificial reefs, but in fact, all PG:cement:lime mixture did not survive in seawater in Grand Isle, Louisiana for two months. The reason may be that the minimum dry submergence surface hardness is not a good

criterion for expressing the actual, wet situation. It seems that the minimum wet submergence surface hardness is a good criterion.

Summary

(1) Response surface analysis with process variable model is appropriate for searching the optimum ingredients for phosphogypsum composites.

(2) The PG:flyash:cement ingredient combination is a possible substrate for artificial reef.

(3) Minimum wet submergence surface hardness is a good criterion to judge whether the stabilized PG composites will survive in the seawater environment.

(4) Minimum dry submergence surface hardness is not a good criterion to judge whether the PG composites will survive in the seawater environment.

CHAPTER 8

DISCUSSION

Economic analysis conducted by Dr. Wilson, C. A. shows that cement levels for PG cement composites need to be in the range of 3% - 5% to be economic and practical for aquatic applications such as artificial reefs or oyster substrates. One of our research objectives is to find low cement ingredient compositions that can maintain structural integrity when submerged in saltwater.

Cement stabilized phosphogypsum (PG) can provide the integrity necessary to prevent dissolution in the face of saltwater submergence. However, the necessary cement content of 30% is too high to be economical. The PG:cement composites with cement content of 15% showed severe degradation in field saltwater submergence tests. All PG:cement:lime composites with upper bounds of 83%:14%:3% PG:cement:lime and 83%:3%:14% PG:cement:lime also showed severe degradation in the saltwater environment so the PG:cement and PG:cement:lime composites would not be recommend for possible aquatic applications such as artificial reefs or oyster substrates.

Since the PG:cement and the PG:cement:lime composites do not meet economic requirements, more cost-effective materials are being searched to replace or significantly reduce cement as a binding agent. Type C fly ash with both cementous and pozzolanic properties are able to take the place of cement as the binding agent. The cementous properties make fly ash function like cement and the pozzolanic properties can enhance the sulfate resistance ability of cement paste in the PG

134

composites. The PG:fly ash:cement composites have been found to survive in the field under saltwater submergence for more than one year. The PG:fly ash:cement composites are able to maintain their physical structural integrity while keeping cement content less than 10%. On the other hand, the PG:fly ash:lime composites showed severe degradation because the pozzolanic reaction between lime and fly ash resulted in the formation of ettringite that lead to the development of ruptures. Therefore, PG:fly ash:cement composites would be recommend for possible aquatic applications such as artificial reefs or oyster substrates.

The formation of a calcium carbonate coating on the surface of the composites was found to be effective in protecting the composites from saltwater attack. For the 70%:30% PG:cement composites, the calcium carbonate coating formed on the composite surface aiding in its survival in the saltwater environment. The 85%:15% PG:cement composites formed a calcium carbonate coating also, but the composite surface was too loose to keep the coating. Without the protection of this coating, saltwater was able to intrude and resulted in the formation of ettringite that lead the development of ruptures. The 85%:15% PG:cement ingredient composition was not able to survive in the saltwater environment. All the cement:lime:PG composites with upper bounds 83%:14%:3% PG:cement:lime and 83%:3%:14% PG:cement:lime behaved the same as the 85%:15% PG:cement composite.

For PG:fly ash:cement composites, the calcium carbonate coating was formed on the composite surface and was able to survive under saltwater submergence. In addition to the calcium carbonate coating, the PG on the composite surface region

(<30 μm) dissolved leaving pores from dissolution that were filled by calcium carbonate. This process makes the calcium carbonate coating stronger. For the PG:fly ash:lime composites, the pozzolanic reaction lead the ruptures and the saltwater intrusion lead to the recrystallization of PG on the fly ash sphere surface.

The response surface analysis with process variables, SEM, microprobe, field and laboratory experiments show that of composites with less than 10% cement content, PG:fly ash:cement composites were the only composites to survive in the Gulf coast saltwater environment out of the PG:cement, PG:cement:lime, PG:fly ash:lime and PG:fly ash:cement ingredient composites tested.

CHAPTER 9

CONCLUSIONS AND RECOMMENDATIONS

Conclusions

The conditions for stabilized PG composites to survived in the saltwater environments are: (1) The stabilized PG composites should have a strong sulfate resistant surface. (2) The local pH environments on the stabilized PG composites should be above than 11. This higher local pH environment will result in the formation of calcium carbonates, which protect the PG composites and reduce the diffusion of toxic metals and radium. The main reason for degradation of PG stabilized composites is the formation of ettringite that lead the development of ruptures.

Among the tested ingredient combinations the PG composites with ingredient of PG:fly ash:cement has the best economic characteristics and saltwater resistance. Statistical analysis and experimental observations show that only PG:fly ash:cement composites can survive in Gulf coast saltwater for long time when cement content is less than 10%. Therefore PG:fly ash:cement composites would be recommend for possible aquatic applications such as artificial reefs or oyster substrates.

Calcium diffusion coefficient is a good indicator for PG:cement:lime composite long term dissolution potential, but this relationship does not apply to the PG:fly ash:lime stabilized composites.

Recommendations

Several areas of research are listed below and should be completed before the PG composites are allowed for use as artificial reefs or oyster substrate.

137

(1) Determination of the survival-time curve for the PG composites using statistical reliability analysis.

(2) TCLP leaching test.

(3) Dynamic leaching tests of toxic metal and radium.

(4) Biological food chain model of toxic metal and radium release from the PG composites.

(5) Degradation processes caused by H_2S generating anaerobic bacteria and aerobic sulfur oxidizing bacteria.

REFERENCES

American Public Health Association. (1995) Standard Methods for Examination of Water and Wastewater,American Public Health Association, American Waterworks Association, and Water Environment Federation. ed. A. Eaton, L. Clesceri, and A. Greenburg. 19th ed.

ANSI/ANS, 16.1. (1986) Measurements of the Leachability of Solidified Low-level Radioactive Wastes,ANSI/ANS 16.1, American Nuclear Society. La Grandge Park, Illinois.

Atalay, Asmare and Joakim G. Laguros. (1990) Environmental Assessment of Bottom Ash and Fly Ash used in Road Stabilization. Fly Ash and Coal Conversion By-Products: Characterization, Utilization and Disposal VI, Material Research Society Symposium Proceedings: V178.

Baretka, J. (1990) The Future of Phosphogypsum, Proceedings of the Third International Symposium on Phosphogypsum. The Florida Institute for Phosphate Research, Number 01–060-083, December.

Barth, E.F. (1990) Stabilization and Solidification of Hazardous Wastes. Noyes Data Corporation. Park Ridge, New Jersey, USA.

Berate, C.W. (1990) Potential environmental hazards of phosphogypsum storage in central Florida. pp.1-29. In W.F.Chang (ed.)., Proc. of the 3 rd Int. Symp. on Phosphogypsum, Orlando, FL. Dec.1990. Publ.01-060-083. Florida Inst. Of Phosphate Res., Bartow, FL.

Brown, C. W. (1990) Potential Environmental Hazards of Phosphogypsum Storage in Central Florida. U. S. Environmental Agency, Region IV, December.

Chen, S., Rusch, K.A., Malone, R.F., Seals, R.K., Wilson, C.A., and Fleeger, J.W. (1995) Preliminary evaluation of stabilized phosphogypsum for use within the aquatic environment. In Toxic Substances in Water Environmental: Assessment and Control, Proceedings of the Water Environment Federation, Special Workshop on food chain toxicity, May 14-17, Cincinnati, Ohio.

Conner, J. R. (1990) Chemical Fixation and Solidification of Hazardous Wastes. Van Norstrand Reinhold, New York.

Cornell, J.A. (1990) Experiments with Mixtures: Design, Model and the Analysis of Mixture Data. 2nd ed. New York: Wiley.

Darnay, A. J. (1992) Statistical Record of the Environment. Gale Research Inc. 835 Penobscot Bldg. Detroit, MI 48226-4094.

DRI/MaGraw-Hill and Standard & Poor's and U.S. Department of Commerce/International Trade Administration (1998) U.S. Industry & Trade Outlook's 98, Washington.

Dodson, V. H. (1988) Low Cement/High Fly Ash Concrete: Their Properties and Response to Chemical Admixtures. Fly Ash and Coal Conversion By-Products: Characterization, Utilization and Disposal IV, Material Research Society Symposium Proceedings: V113.

DRI/MaGraw-Hill and Standard & Poor's and U.S. Department of Commerce/International Trade administration (1998) U.S. Industry & Trade Outlook's 98, Washington.

Duedall, I., Kester, D, Park, P.,and Ketchum, B. eds. (1985) Wastes in the Ocean. Vol. 4, Energy Wastes in the Ocean. John Wiley and Sons, New York, Chapter 32.

Federal Register, (1978) December 18, 1978, Volume 43, Number 243, pp58946-59028.

Ferguson, F (1988) Phosphogypsum - An Overview. Proceedings of the Second International Symposium on Phosphogypsum. Vol. 2, January.

Ferrell, R.E. J., Arman, A. and Baykal, G. (1988) Micromophology and Mineralogy Fly Ash and Lime Stabilized Bentonite. Fly Ash and Coal Conversion By-Products: Characterization, Utilization and Disposal IV, Material Research Society Symposium Proceedings: V113.

Gerwick, B. C. (1986) Construction of Offshore Structures. Wiley-Interscience.

Glasser, F.P., Diamond S. and Roy, D. M. (1987) Hydration Reactions in Cement Pastes Incorporating Fly Ash and Other Pozzolanic Materials. Fly Ash and Coal Conversion By-Products: Characterization, Utilization and Disposal III, Material Research Society Symposium Proceedings: V86.

Goldstein, J.I., Newbury, D.E., Echlin, P., Joy, D.C., Romog, A.D. Jr., Lyman, C.E., Fiori, C., and Lifshin, E. (1992) Scanning Electron Microscope and X-Ray Microanalysis. Plenum Press, New York, A division of Plenum Publishing Corporation, 233 Spring Street, New York, N.Y. 10013.

Gregory, C. A. (1983) Enhancement of Phosphogypsum with High Lime Fly Ash. Master of Science Thesis. Texas A&M University.

Guo, Tingzong, Qinhui Xu and Yuduan Wu. (1989) The Interstitial Water Chemistry of Ca^{2+}, Mg^{2+}, SO_4^{2-} and Alkalinity Model. J. Xiamen University (Natural Sci) 28(6), 632-636.

Gutti, C.S., Roy, A., Metcalf, J.B., and Seals, R.K. (1996) The influence of admixtures on the strength and linear expansion of cement-stabilized phosphogypsum. Cement and Concrete Research. 26, 1083-1094.

Higgins, T. E. (1995) Pollution Prevention Handbook. Lewis publishers, CRC Press, Inc., 2000 Corporate Blvd., N.W., Boca Raton, Florida 33431.

Hinkelmann, K. and O.Kempthorne (1994) Design and Analysis of Experiments. Volume 1: Instruction to Experimental Design. Wiley : NY.

Hutchison, C.S. (1974) Laboratory Handbook of Petrographic Techniques. John Wiley & Sons, Inc. New York.

James, A.N. (1992) Soluble Materials in Civil Engineering. Ellis Horwood Limited Market Cross House, Cooper Street, Chickester. West Sussex, PO19 1 EB, England

James, I. D. (1977) Sea Water Cycles of the Major Elements. Bowden, Hutchinson & Ross, Inc. Stroudsburg, Pennsylvania.

Kalvakaalva, R. (1995) Investigation of the Hydration Products of Portland Cement Stabilized Reagent Grade and Phosphogypsum A Thesis, Louisiana State University.

Kuehl, P.O. (1994) Statistical Principles of Research Design and Analysis. Duxbury Press, Belmont.

Lea, F. M. (1971) The Chemistry of Cement and Concrete. 3rd edn, Chemical Publishing Co., New York.

Lopez, A. M. and Seals, R.K. (1991) The Environmental and Geotechnical Aspects of Phosphogypsum Utilization and Disposal. Louisiana State University.

Luther, S.M. and Dudas, M.J. (1993) Pore water chemistry of phosphogypsum-treated soil. Journal of Environmental Quality. 22 :103-108.

Malek, R.I.A., Roy, D. M. (1988) A Method for Measuring the Self-Cementing Characteristics of Fly Ash Pastes. Fly Ash and Coal Conversion By-Products: Characterization, Utilization and Disposal IV, Material Research Society Symposium Proceedings: V113

Malone, P.G., Jone, L.W., and Larson, R.J. (1980) Guide to the Disposal of Chemically stabilized and Solidified Waste. SW-872, Office of Water and Waste Management, U.S. Environmental Protection Agency, Washington, D.C., pp126.

May, A. and J. W. Sweeney (1982) Assessment of Environmental Impacts Associated with Phosphogypsum in Florida. RI 8776.

May, A. and J. W. Sweeney (1983) Evaluation of Radiation and Toxic Element Leaching Characteristics of Florida Phosphogypsum Stockpiles. BuMines RI 8776.

May, A. and Sweeney, J. W. (1984) Assessment of environmental impact associated with phosphogypsum in Florida. p.116-139. In R.A. Kuntze (ed.).The Chemistry and Technology of Gypsum. Spec.Tech. Publ. 861.ASTM, Tuscaloosa, AL.

Mehta, P. K. (1991) Concrete in the Marine Environment. Elsevier Science Publishers LTD, New York.

Mehta, P. K. (1986) Concrete: Structure, Properties, and Materials. Prentice-Hall, Englewood Cliffs, NJ.

Metcalf and Eddy, INC. (1979) Wastewater Engineering, Treatment/Disposal/Reuse. Second Edition. Mcgraw-Hill Book Co., New York.

Minnick, L.J. (1967) Reactions of Hydrated Lime with Pulverized Coal Fly Ash. Proceedings, Fly Ash Utilization Conference. Bureau of Mines Information Circular 8348.

Miyamoto, M. (1980) Phosphogypsum Utilization in Japan. Proceedings of the International Symposium on Phosphogypsum. The Florida Institute of Phosphate Research, Vol.2.

Naff, D. B. (1984) The Classification of Phosphogypsum for the Environmental Purposes. Proceedings of the Fertilizer Institute's Environmental Symposium. The Fertilizer Institute, Kissimmee, Florida.

Neil, R. A. and Malahoff, A. (1977) The Fate of Fossil Fuel CO_2 in the Ocean. Plenum Press 227 West 17th Street, New York, N.Y. 10011.

Neter, J., Kutner, M. H., Natchtsheim, C. J. and Wasserman, W. (1996) Applied Linear Statistical Models. Times Mirror Higher Education Group, Inc., Chicago.

Neville, A. M. (1995) Properties of Concrete. John Wiley & Sons, Inc., 605 Third Avenue, New York, NY 10158.

Neville, A. M. (1995) Properties of Concrete. 4th edition. Longman Group Limited. Longman House, Burnt Mill, Harlow, Essex CM20 2JE, England

Roessler, C. E., Smith, Z. A., Bolch, W. E. and Prince, R. J. (1979) Uranium and radium-226 in Florida phosphate materials. Health Phys. 37: 269-277.

Roy, A., Kavakaalva, R. and Seals, R. K. (1996) Microstructural and Phase Characteristics of Phosphogypsum and Cement mixtures. ASCE Journal of Materials in Civil Engineering. 8, 11-88.

Rusch, K. A., Malone, R. F., Seals, R. K., and Wilson, C.A. (1998) The Use of Phosphogypsum for Oyster Substrate. Final Report submitted to the Florida Institute of Phosphate Research (FIPR) Contract # 95-01-127, 42 pp.

River Cement Co. (1997) St. Louis, Missouri.

Smith, R. L. (1988) Is the Available Alkalitest a Good Durability Predictor for Fly Ash Concrete Incorporating Reactive Aggrerate? Fly Ash and Coal Conversion By-Products: Characterization, Utilization and Disposal IV. Material Research Society Symposium Proceedings: V113.

Steinour, H. H. (1952) The Reactions and Thermochemistry of Cement Hydration at Ordinary Temperature. Proc.3rd Int. Symposium on the Chemistry of Cement. London.

Swayze,M. A. (1946) The Quarternary System CaO-C$_5$A$_3$-C$_2$F-C$_2$S as Modified by Saturation with Magnesia, American Journal of Science., 244 : 65-94.

Taha, R. and Seals, R.K. (1991) Phosphogypsum Literature Review. A report by the Institute for Recyclable Materials to Freeport McMoRan, Inc, Report No.1-90-4.

Thimmegowda, H. (1994) Generation and Evaluation of Raw Cement Stabilized Phosphogypsum Leachates. A Thesis. Louisiana State University.

Thomas, E. Higgins (1995) Pollution Prevention Handbook. Lewis publishers, CRC Press, Inc., 2000 Corporate Blvd., N.W., Boca Raton, Florida 33431.

Wilson, C.A., Nieland, D.L., Fleeger, J.W., Todaro, A. Malone, R.F., and Rusch, K.A.(1998) (In Press) Preliminary evaluation of the use of phosphogypsum for reef substrate. II. A study of the effects of phosphogypsum exposure on diversity and biomass of aquatic organisms, Chemistry and Ecology.

APPENDIX A   RAW DATA FOR DYNAMIC LEACH TEST; TEST ONE

Time (days)	Cement	Lime	PG	FA	pH 0.08	alk 0.08	calcium 0.08	pH 0.29	alk 0.29	calcium 0.29
1	0.14	0.03	0.83	0	8.55	110	69.91	8.72	114	113.08
	0.14	0.03	0.83	0			47.31			47.30
2	0.09	0.03	0.88	0	8.55	110	63.74	8.54	108	111.03
	0.09	0.03	0.88	0			49.36			53.46
3	0.04	0.03	0.93	0	8.47	104	96.64	8.44	102	174.76
	0.04	0.03	0.93	0			80.21			121.31
4	0.09	0.08	0.83	0	9.30	142	69.91	8.82	112	115.14
	0.09	0.08	0.83	0			43.20			43.18
5	0.04	0.13	0.83	0	9.09	124	71.96	8.83	110	121.31
	0.04	0.13	0.83	0			49.36			67.86
6	0.04	0.08	0.88	0	8.86	120	78.13	8.83	112	172.71
	0.04	0.08	0.88	0			67.87			76.08
7	0.107	0.047	0.846	0	9.08	134	76.08	8.86	106	111.03
	0.107	0.047	0.846	0			28.80			49.35
8	0.057	0.097	0.846	0	9.45	144	69.91	9.06	116	141.87
	0.057	0.097	0.846	0			32.92			59.63
9	0.057	0.047	0.896	0	9.10	138	92.52	8.51	102	162.43
	0.057	0.047	0.896	0			76.09			115.15
10	0.073	0.063	0.864	0	8.82	118	78.13	8.86	114	119.25
	0.073	0.063	0.864	0			53.48			45.24
11	0	0.07	0.93	0	8.61	112	111.03	8.51	106	156.26
	0	0.07	0.93	0			57.59			63.74
12	0	0.1	0.9	0	9.46	156	123.36	9.07	108	195.33
	0	0.1	0.9	0			43.20			98.70
13	0	0.13	0.87	0	9.50	122	108.97	9.07	114	199.44
	0	0.13	0.87	0			71.98			127.48
14	0.15	0	0.85	0	8.46	106	69.91	8.61	106	111.03
	0.15	0	0.85	0			55.53			45.24
15	0.3	0	0.7	0	8.75	118	53.45	9.00	116	67.85
	0.3	0	0.7	0			39.08			18.51
SW Blank 20ppt					7.99	102	187.10	8.01	102	187.11
							191.20			213.83

Note: Calcium values presented have the saltwater calcium concentration subtracted out

145

Time (days)	pH 1	alk 1	calcium 1	pH 2	alk 2	calcium 2	pH 3	alk 3	calcium 3
1	8.75	90	191.21	8.66	87	201.50	8.79	87	150.10
	8.80	102	199.34	8.80	90	205.96	8.81	90	137.76
2	8.75	97	209.72	8.48	93	226.17	8.62	87	148.04
	8.90	106	198.43	8.83	94	211.98	8.73	94	121.31
3	8.64	96	277.57	8.45	90	289.91	8.58	89	275.52
	8.61	98	287.65	8.71	88	289.06	8.45	92	257.01
4	8.86	97	158.32	8.93	93	125.42	8.97	94	88.42
	9.10	106	108.56	9.12	88	87.90	9.06	94	47.29
5	8.88	97	133.64	8.96	82	102.80	9.06	96	82.25
	9.09	104	125.36	9.11	94	104.78	9.02	96	92.53
6	8.64	93	259.07	8.63	89	228.22	8.88	90	164.50
	8.76	100	206.41	8.93	88	176.54	8.72	92	158.32
7	8.75	94	168.60	8.75	87	145.98	8.88	92	108.98
	9.01	100	156.92	9.08	88	122.60	8.92	92	84.30
8	8.75	90	207.66	8.73	82	168.60	8.91	90	96.64
	9.22	106	142.71	9.20	88	124.80	9.09	92	78.13
9	8.60	89	273.46	8.43	83	312.52	8.67	81	238.51
	8.85	102	239.50	8.88	96	276.63	8.64	88	187.11
10	8.57	95	211.77	8.63	86	230.28	8.78	87	178.88
	9.05	108	135.82	9.02	86	156.87	8.96	82	88.41
11	8.53	92	324.86	8.50	83	320.75	8.67	84	291.97
	8.58	102	199.65	8.63	94	208.46	8.43	92	168.60
12	8.69	91	308.41	8.51	82	328.97	8.73	78	306.36
	9.25	108	230.87	9.06	84	267.54	8.69	88	220.00
13	8.71	95	271.40	8.58	83	289.91	8.88	83	205.61
	9.17	96	215.37	9.20	92	217.52	8.90	84	158.32
14	8.66	94	189.16	8.57	89	191.21	8.76	93	154.21
	8.84	102	121.32	8.81	100	124.60	8.67	90	111.03
15	8.99	100	59.62	9.14	93	30.84	9.08	97	20.56
	9.20	112	24.35	9.17	102	17.50	9.18	98	16.45
SW Blank	7.80	93	197.39	7.80	93	197.39	7.93	93	193.27
20ppt	8.10	100	210.55	7.97	92	177.01	7.89	92	178.88

Note: Calcium values presented have the saltwater calcium concentration subtracted out

APPENDIX A - (cont.)

Time (days)	pH 4	alk 4	calcuim 4	pH 5	alk 5	calcuim 5	pH 8	alk 8	calcuim 8
1	8.67	85	127.48	8.64	84	111.03	8.37	75	230.28
	8.88	100	118.29	8.86	90	90.47	8.87	86	205.60
2	8.56	88	141.88	8.68	92	129.53	8.40	72	269.35
	8.91	100	89.21	8.85	96	63.74	8.91	88	170.66
3	8.44	93	257.01	8.49	92	269.35	8.28	82	419.45
	8.69	100	244.96	8.62	94	234.39	8.38	92	378.33
4	9.00	92	43.18	8.97	90	49.35	9.02	88	98.69
	9.23	96	77.89	9.14	94	82.22	9.41	82	69.91
5	9.03	93	49.35	9.20	84	24.67	9.05	68	106.92
	9.30	104	52.50	9.14	90	22.61	9.42	90	119.26
6	8.75	90	137.76	8.77	86	119.25	8.62	76	283.74
	8.93	100	142.86	8.87	90	106.92	8.86	86	238.51
7	8.83	92	82.25	8.95	92	67.85	8.73	78	162.43
	9.08	96	77.29	8.99	88	51.40	9.14	88	131.59
8	8.86	83	102.81	8.94	78	69.91	8.75	66	232.34
	9.34	96	56.76	9.18	86	22.61	9.4	76	82.25
9	8.57	84	207.67	8.73	96	193.27	8.61	74	347.48
	8.82	98	156.78	8.84	96	143.92	8.58	88	236.46
10	8.67	88	160.38	8.79	88	137.76	8.48	74	294.02
	9.23	104	62.97	9.14	96	47.29	9.26	88	119.26
11	8.57	84	259.07	8.53	88	257.01	8.31	66	429.73
	8.60	100	169.20	8.62	80	164.49	8.55	96	259.07
12	8.67	85	257.02	8.52	90	234.40	8.36	74	394.77
	8.84	92	202.34	8.60	82	176.82	8.73	82	277.58
13	8.72	87	160.38	8.88	84	137.76	8.58	68	275.52
	9.12	98	117.94	9.02	88	82.24	9.11	88	176.82
14	8.67	92	125.43	8.84	94	108.97	8.50	78	224.12
	8.88	104	97.34	8.77	98	86.35	8.73	96	166.55
15	9.10	91	4.16	9.18	88	2.06	8.98	72	8.22
	9.37	102	6.09	9.13	94	-2.06	9.42	86	6.17
SW Blank	7.93	93	193.27	7.71	94	195.33	7.71	94	195.33
20ppt	8.01	102	190.43	8.10	96	189.16	7.9	96	182.99

Note: Calcium values presented have the saltwater calcium concentration subtracted out
APPENDIX A - (cont.)

Time (days)	pH 11	alk 11	calcium 11	pH 14	alk 14	calcium 14	pH 21	alk 21	calcium 21
1	8.40	71	201.50	8.22	76	176.83	7.73	64	234.40
	8.75	78	175.45	8.77	90	117.19	8.42	64	250.85
2	8.40	72	254.96	8.35	74	217.95	8.00	62	312.53
	8.77	75	156.78	8.80	88	76.07	8.58	68	178.88
3	8.28	80	466.73	8.12	79	374.21	7.94	74	639.45
	8.30	89	402.34	8.56	92	331.03	8.49	74	606.55
4	8.85	65	69.91	8.75	63	57.57	8.27	58	108.97
	9.10	72	56.78	9.00	78	10.28	8.76	64	28.13
5	8.99	70	78.13	8.80	65	61.69	8.48	56	69.91
	9.05	74	78.99	9.00	77	43.18	9.02	56	119.25
6	8.66	74	244.68	8.40	83	213.84	8.15	62	234.40
	8.80	76	203.45	8.82	95	162.43	8.73	64	322.81
7	8.69	78	125.42	8.59	84	108.98	8.16	62	160.38
	9.05	86	108.76	8.92	92	55.51	8.84	76	133.65
8	8.82	68	170.66	8.63	64	145.99	8.35	48	166.55
	9.35	70	56.97	8.90	78	20.56	9.07	58	100.75
9	8.35	70	353.65	8.16	72	306.36	7.95	64	479.07
	8.30	76	252.36	8.45	84	189.16	8.81	76	355.71
10	8.51	70	267.29	8.40	74	261.13	8.14	64	361.88
	8.99	78	89.35	8.67	88	59.62	8.96	66	160.38
11	8.34	69	450.29	8.23	70	427.67	7.92	62	614.78
	8.67	82	299.86	8.50	82	275.51	8.83	78	509.91
12	8.47	61	440.01	8.24	70	357.77	8.28	60	551.04
	8.69	70	304.56	8.55	84	189.16	8.22	78	363.93
13	8.58	64	211.78	8.41	71	185.05	8.13	68	203.56
	8.56	72	154.27	8.80	83	82.24	8.43	68	190.81
14	8.58	86	209.72	8.42	8	187.11	8.12	74	287.86
	8.55	95	145.57	8.83	97	129.53	8.31	88	285.80
15	8.73	64	8.22	8.48	64	0.00	7.98	70	18.51
	9.25	70	5.34	8.87	75	-2.26	8.30	84	26.73
SW Blank	7.50	89	185.05	7.50	89	189.16	7.56	96	199.44
20ppt	7.89	98	180.35	8.01	102	217.95	7.74	98	215.89

Note: Calcium values presented have the saltwater calcium concentration subtracted out
APPENDIX A - (cont.)

149

Time (days)	pH 28	alk 28	calcuim 28
1	8.09	99	281.68
	8.15	94	298.76
2	8.10	72	341.31
	8.16	70	203.46
3	8.16	78	573.65
	8.20	74	586.32
4	8.10	80	129.53
	8.15	82	78.90
5	8.20	59	115.14
	8.22	60	176.98
6	8.14	78	310.47
	8.10	76	400.76
7	8.14	86	180.93
	8.12	82	154.23
8	8.12	64	228.23
	8.10	62	179.04
9	8.11	72	504.69
	8.09	70	403.65
10	8.09	70	415.33
	8.10	69	215.49
11	8.24	68	542.81
	8.30	65	458.04
12	8.28	60	544.87
	8.30	62	373.61
13	8.20	68	291.97
	8.15	69	305.87
14	8.16	90	289.91
	8.17	92	297.56
15	8.10	84	26.73
	8.09	88	29.78
SW Blank	7.81	96	199.44
20ppt	8.00	96	210.65

Note: Calcium values presented have the saltwater calcium concentration subtracted out

APPENDIX A - (cont.)

APPENDIX B RAW DATA FOR DYNAMIC LEACH TEST; TEST TWO

Time (days)	Cement	Lime	PG	FA	pH 0.08	alk 0.08	calcium 0.08	pH 0.29	alk 0.29	calcium 0.29
1	0.03	0	0.62	0.35	8.50	102	-2.28	8.37	101	73.67
	0.03	0	0.62	0.35	8.50	101	-10.10	8.40	99	68.00
2	0.065	0	0.585	0.35	8.58	103	-22.34	8.50	101	59.53
	0.065	0	0.585	0.35	8.55	101	-25.55	8.48	102	61.77
3	0.1	0	0.55	0.35	8.61	101	-29.93	8.51	101	59.25
	0.1	0	0.55	0.35	8.61	103	-37.56	8.53	100	47.67
4	0.03	0	0.585	0.385	8.53	101	-6.28	8.43	101	69.45
	0.03	0	0.585	0.385	8.49	99	-16.48	8.44	100	64.98
5	0.03	0	0.55	0.42	8.49	101	-12.50	8.45	101	54.41
	0.03	0	0.55	0.42	8.50	100	-10.88	8.44	101	58.70
6	0.065	0	0.55	0.385	8.57	102	-12.46	8.52	100	59.89
	0.065	0	0.55	0.385	8.56	102	-15.34	8.52	101	54.01
7	0.042	0	0.596	0.362	8.46	998	17.34	8.47	101	75.31
	0.042	0	0.596	0.362	8.43	100	4.46	8.49	99	71.36
8	0.042	0	0.561	0.397	8.58	102	-6.32	8.48	101	72.33
	0.042	0	0.561	0.397	8.56	101	-15.27	8.52	101	66.37
9	0.077	0	0.561	0.362	8.56	100	-1.83	8.49	98	66.84
	0.077	0	0.561	0.362	8.50	100	-19.27	8.47	97	70.91
10	0.053	0	0.574	0.373	8.45	101	27.87	8.51	101	77.43
	0.053	0	0.574	0.373	8.43	99	86.10	8.50	99	76.96
11	0	0.03	0.62	0.35	8.40	101	73.47	8.46	100	108.40
	0	0.03	0.62	0.35	8.39	101	60.67	8.45	101	101.05
12	0	0.065	0.585	0.35	8.48	97	40.62	8.53	94	80.14
	0	0.065	0.585	0.35	8.53	99	53.89	8.54	94	79.49
13	0	0.1	0.55	0.35	9.02	146	63.67	8.85	103	92.33
	0	0.1	0.55	0.35	9.38	200	49.95	8.99	118	85.45
14	0	0.03	0.585	0.385	8.49	101	52.75	8.47	101	103.40
	0	0.03	0.585	0.385	8.48	98	42.89	8.46	97	103.66
SW Blank 20ppt					8.31	96	199.17	8.14	94	204.75

Note: Calcium values presented have the saltwater calcium concentration subtracted out

Time (days)	pH 1	alk 1	calcuim 1	pH 2	alk 2	calcuim 2	pH 3	alk 3	calcuim 3
1	8.55	102	208.12	8.56	109	144.59	8.49	101	93.92
	8.57	102	226.70	8.55	107	153.39	8.44	100	95.68
2	8.75	104	179.68	8.70	108	140.21	8.40	98	108.03
	8.69	104	158.01	8.71	111	127.07	8.61	105	73.70
3	8.60	102	151.11	8.82	111	106.66	8.67	101	57.95
	8.69	102	136.70	8.79	112	103.72	8.60	101	30.69
4	8.44	100	166.80	8.58	110	131.49	8.49	101	87.34
	8.49	102	177.22	8.56	107	126.57	8.43	102	101.54
5	8.45	98	167.16	8.58	110	126.90	8.35	98	69.10
	8.42	101	169.20	8.58	106	116.83	8.44	99	95.46
6	8.59	101	173.69	8.69	108	92.00	8.58	99	72.25
	8.60	103	156.20	8.73	114	116.09	8.62	101	81.44
7	8.51	102	206.54	8.61	112	142.49	8.55	101	116.88
	8.61	102	185.93	8.64	107	132.49	8.51	101	122.46
8	8.43	101	190.43	8.61	108	124.68	8.55	99	86.15
	8.55	101	167.68	8.61	109	135.68	8.55	101	95.74
9	8.62	98	137.88	8.75	107	140.60	8.64	99	69.07
	8.61	99	154.85	8.76	108	105.85	8.65	99	75.70
10	8.58	103	159.59	8.69	108	138.37	8.61	103	89.57
	8.63	103	158.05	8.68	110	146.77	8.61	101	120.68
11	8.44	98	216.09	8.53	100	154.41	8.55	96	132.41
	8.47	101	178.48	8.53	104	151.82	8.53	97	108.48
12	8.55	91	184.95	8.74	89	137.66	8.58	88	127.74
	8.56	93	167.87	8.80	95	126.18	8.60	89	89.62
13	9.42	97	89.92	9.55	102	54.53	9.32	96	27.95
	9.59	104	146.62	9.61	116	70.66	9.35	94	23.31
14	8.61	100	191.61	8.66	103	176.05	8.56	95	84.43
	8.67	97	183.54	8.67	101	181.03	8.56	93	107.08
SW Blank 20ppt	8.26	98	165.12	8.24	100	151.56	8.07	93	174.16

Note: Calcium values presented have the saltwater calcium concentration subtracted out

APPENDIX B - (cont.)

Time (days)	pH 4	alk 4	calcium 4	pH 5	alk 5	calcium 5	pH 8	alk 8	calcium 8
1	8.47	107	105.38	8.41	112	98.22	8.44	104	230.04
	8.43	104	125.02	8.35	109	106.97	8.41	105	219.10
2	8.54	104	115.23	8.49	111	136.99	8.55	103	211.36
	8.60	107	194.88	8.53	110	83.45	8.46	100	207.00
3	8.67	108	68.50	8.60	110	61.04	8.58	102	160.03
	8.67	108	72.37	8.57	107	77.03	8.58	106	181.37
4	8.45	105	102.97	8.45	113	94.70	8.38	102	200.77
	8.38	101	108.31	8.41	109	107.41	8.52	110	215.36
5	8.44	103	100.99	8.52	113	97.36	8.46	102	190.58
	8.50	101	87.11	8.46	108	81.62	8.43	102	180.38
6	8.47	105	100.54	8.49	110	99.92	8.60	101	231.89
	8.66	109	92.13	8.49	107	138.13	8.58	104	186.08
7	8.56	107	104.71	8.46	111	102.36	8.40	104	188.46
	8.54	102	117.35	8.44	107	117.73	8.46	105	219.63
8	8.55	105	107.12	8.65	110	107.01	8.42	100	216.63
	8.55	104	104.46	8.48	111	107.94	8.43	102	217.10
9	8.67	107	107.11	8.56	111	99.13	8.58	104	212.31
	8.67	105	105.56	8.58	108	93.71	8.58	104	210.95
10	8.61	107	122.14	8.53	111	113.54	8.42	104	219.48
	8.59	104	126.78	8.47	108	119.82	8.40	104	193.69
11	8.50	98	167.06	8.41	107	138.88	8.39	97	251.11
	8.50	100	127.28	8.44	106	135.22	8.32	98	223.65
12	8.59	90	144.77	8.49	94	132.48	8.55	78	282.41
	8.64	92	130.59	8.55	94	121.50	8.47	79	197.36
13	9.30	98	46.09	9.20	97	41.20	9.26	79	225.05
	9.29	99	69.92	9.14	90	138.91	9.32	82	230.17
14	8.53	99	146.83	8.50	109	155.20	8.45	96	293.08
	8.54	98	159.20	8.48	105	152.33	8.46	98	227.22
SW Blank 20ppt	8.04	96	194.26	8.06	100	200.39	8.05	100	185.52

Note: Calcium values presented have the saltwater calcium concentration subtracted out

APPENDIX B - (cont.)

Time (days)	pH 11	alk 11	calcium 11	pH 14	alk 14	calcium 14	pH 21	alk 21	calcium 21
1	8.33	126	224.53	8.33	104	210.60	8.26	109	337.05
	8.34	120	148.44	8.35	104	201.11	8.33	117	353.00
2	8.36	116	149.47	8.41	104	202.19	8.36	105	393.04
	8.44	116	196.05	8.47	110	182.28	8.40	114	353.87
3	8.54	117	208.38	8.46	106	127.68	8.40	106	348.87
	8.45	125	168.20	8.47	106	159.44	8.33	106	277.55
4	8.38	104	135.12	8.41	115	208.37	8.33	111	363.93
	8.22	114	121.08	8.34	104	166.65	8.28	102	334.83
5	8.35	110	127.22	8.36	106	172.02	8.31	105	327.82
	8.36	108	113.52	8.37	102	157.42	8.32	110	319.61
6	8.43	108	142.41	8.40	102	180.42	8.36	99	320.65
	8.43	112	124.17	8.49	115	178.19	8.39	116	309.50
7	8.30	110	124.78	8.37	105	164.49	8.33	103	335.59
	8.30	106	170.11	8.37	102	207.03	8.36	103	359.50
8	8.34	100	140.75	8.42	108	194.70	8.36	103	326.76
	8.36	98	136.42	8.39	104	244.55	8.33	101	345.76
9	8.45	100	246.93	8.53	110	192.90	8.40	100	344.03
	8.42	100	134.07	8.52	108	194.52	8.37	99	344.75
10	8.39	108	155.91	8.44	109	160.79	8.23	104	396.42
	8.41	104	158.11	8.41	104	220.75	8.22	99	381.71
11	8.34	94	180.42	8.30	99	223.42	8.13	92	404.43
	8.37	92	176.02	8.37	98	244.11	8.17	93	411.48
12	8.35	90	225.18	8.40	76	368.36	8.13	51	644.88
	8.38	80	241.54	8.42	74	387.51	8.14	51	679.53
13	8.74	72	368.52	8.83	56	506.60	8.90	64	976.98
	8.89	76	243.71	8.95	52	496.03	8.88	88	1035.54
14	8.42	92	311.38	8.39	98	293.09	7.96	90	503.82
	8.50	96	241.64	8.36	99	280.49	7.89	93	481.42
SW Blank 20ppt	7.78	96	244.32	7.72	96	193.90	7.68	102	201.64

Note: Calcium values presented have the saltwater calcium concentration subtracted out

APPENDIX B - (cont.)

Time (days)	pH 28	alk 28	calcium 28
1	8.34	118	314.97
	8.32	121	307.45
2	8.44	112	362.04
	8.47	121	305.08
3	8.48	116	287.14
	8.44	116	285.01
4	8.46	122	306.59
	8.39	114	339.84
5	8.40	118	290.15
	8.41	116	284.93
6	8.40	112	314.69
	8.41	116	305.60
7	8.43	112	313.88
	8.42	114	347.52
8	8.50	114	303.17
	8.43	114	424.92
9	8.47	112	313.71
	8.45	112	289.73
10	8.48	116	336.25
	8.45	108	343.45
11	8.35	98	339.76
	8.35	102	376.43
12	8.37	56	729.56
	8.40	54	573.71
13	8.30	42	1243.93
	8.35	45	1255.95
14	8.32	100	423.54
	8.31	100	410.33
SW Blank 20ppt	7.77	112	213.69

Note: Calcium values presented have the saltwater calcium concentration subtracted out

APPENDIX B - (cont.)

APPENDIX C RAW DATA FOR DYNAMIC LEACH TEST; TEST THREE AND FOUR

Time (days)	Cement	Lime	PG	FA	pH 0.08	alk 0.08	calcium 0.08	pH 0.29	alk 0.29	calcium 0.29
	0.000	0.030	0.550	0.420	8.44	94	6.29	8.40	97	40.37
	0.000	0.030	0.550	0.420	8.40	99	-7.13	8.37	95	47.55
2	0.000	0.065	0.550	0.385	8.58	117	-7.61	8.56	120	31.30
	0.000	0.065	0.550	0.385	8.55	141	-1.91	8.54	135	20.89
3	0.000	0.042	0.596	0.362	8.25	183	-20.59	8.26	190	92.99
	0.000	0.042	0.596	0.362	8.26	200	-12.39	8.24	220	95.05
4	0.000	0.042	0.561	0.397	8.40	89	-19.10	8.35	95	91.99
	0.000	0.042	0.561	0.397	8.23	95	0.70	8.23	94	103.39
5	0.000	0.077	0.561	0.362	8.52	117	-2.93	8.44	120	10.48
	0.000	0.077	0.561	0.362	8.38	129	-14.82	8.39	131	44.11
6	0.000	0.053	0.574	0.373	8.30	91	-2.46	8.28	96	92.38
	0.000	0.053	0.574	0.373	8.26	93	-24.72	8.30	98	50.58
7	0.000	0.010	0.790	0.200	7.98	168	-1.77	8.05	150	48.71
	0.000	0.010	0.790	0.200	7.89	221	-11.22	8.00	210	129.61
8	0.000	0.010	0.690	0.300	8.15	101	-18.23	8.14	108	34.10
	0.000	0.010	0.690	0.300	8.12	119	-4.68	8.15	125	34.01
9	0.010	0.010	0.680	0.300	8.05	152	7.82	8.11	136	60.00
	0.010	0.010	0.680	0.300	7.85	258	26.94	7.85	240	60.23
SW Blank 1	0.010	0.005	0.785	0.200	8.08	89	247.11	8.03	93	199.23
	0.010	0.005	0.785	0.200	8.03	88	64.67	8.44	118	120.91
2	0.020	0.010	0.770	0.200	8.05	87	65.70	8.51	136	127.80
	0.020	0.010	0.770	0.200	8.08	91	82.22	8.43	142	131.94
3	0.020	0.010	0.670	0.300	8.09	92	74.02	8.42	156	116.82
	0.020	0.010	0.670	0.300	8.08	97	57.13	8.43	178	102.34
4	0.020	0.010	0.775	0.200	8.04	100	71.19	8.4	208	109.70
	0.020	0.010	0.775	0.200	8.09	85	70.40	8.54	106	125.04
5	0.030	0.010	0.760	0.200	8.02	88	53.44	8.46	126	104.73
	0.030	0.010	0.760	0.200	8.08	89	44.71	8.47	112	102.45
6	0.030	0.010	0.660	0.300	8.11	95	77.34	8.45	120	120.17
	0.030	0.010	0.660	0.300	8.08	94	81.05	8.43	132	136.55
7	0.030	0.010	0.765	0.300	8.11	104	92.23	8.48	128	134.13
		0.010		0.200	7.94	85	70.66	8.35	108	121.84
SW Blank 20ppt	0.030	0.005			8.02	76	216.40	8.02	76	216.03

Note: Calcium values presented have the saltwater calcium concentration subtracted out
APPENDIX C - (cont.)

Time (days)	pH 1	alk 1	calcium 1	pH 2	alk 2	calcium 2	pH 3	alk 3	calcium 3
	8.35	104	126.63	8.35	113	201.17	8.34	106	125.88
2	8.36	106	98.62	8.37	115	193.82	8.37	108	95.55
	8.55	110	93.40	8.60	105	151.78	8.57	103	73.95
3	8.59	112	102.92	8.63	110	138.92	8.60	105	57.77
	8.30	110	90.51	8.35	109	232.54	8.33	106	167.78
4	8.25	108	105.86	8.32	110	241.18	8.29	107	174.58
	8.40	103	128.55	8.39	107	228.14	8.36	103	133.02
5	8.30	101	109.88	8.32	106	196.51	8.30	101	144.79
	8.88	115	109.95	8.92	110	97.95	8.90	104	32.35
6	8.89	112	79.10	9.03	116	73.87	9.00	106	12.40
	8.40	111	82.77	8.44	118	188.60	8.38	109	132.68
7	8.36	115	149.81	8.39	120	176.08	8.36	105	135.32
	8.05	143	173.15	8.20	130	204.21	8.19	115	114.36
8	8.10	135	133.32	8.22	128	214.84	8.20	118	131.77
	8.19	116	74.30	8.26	126	139.98	8.30	116	105.41
9	8.18	124	74.70	8.28	128	154.98	8.25	120	157.80
	8.22	135	183.91	8.33	138	161.98	8.38	128	112.85
	7.85	150	214.00	8.35	142	168.76	8.35	133	169.44
SW Blank	8.03	118	188.19	8.00	120	149.38	8.00	100	247.10
1	8.22	112	197.40	8.26	110	233.86	8.27	111	136.65
	8.21	110	182.12	8.29	110	247.35	8.3	110	112.60
2	8.24	110	191.36	8.35	112	241.11	8.36	111	121.46
	8.29	110	183.36	8.36	110	221.82	8.36	112	109.53
3	8.3	110	148.26	8.39	110	179.10	8.42	111	94.51
	8.3	110	176.15	8.38	108	185.42	8.39	110	107.36
4	8.19	110	133.22	8.34	110	239.22	8.41	112	131.46
	8.25	108	188.91	8.5	110	230.17	8.5	113	145.99
5	8.27	108	159.25	8.42	110	226.40	8.39	112	109.89
	8.32	108	187.54	8.43	110	234.46	8.4	110	118.19
6	8.27	110	175.06	8.38	108	237.96	8.4	114	134.99
	8.33	108	246.24	8.39	110	238.67	8.44	115	144.85
7	8.18	108	229.83	8.25	108	247.12	8.39	111	167.10
SW Blank 20ppt	7.93	103	221.70	7.93	103	223.22	7.93	112	261.82

Note: Calcium values presented have the saltwater calcium concentration subtracted out

APPENDIX C - (cont.)

Time (days)	pH 4	alk 4	calcium 4	pH 5	alk 5	calcium 5	pH 8	alk 8	calcium 8
1	8.33	104	139.15	8.14	100	171.40	8.43	92	348.43
	8.36	102	168.03	8.10	98	163.85	8.43	94	356.44
2	8.52	98	120.70	8.40	98	125.89	8.78	90	246.83
	8.58	102	117.87	8.30	92	121.07	8.76	82	256.14
3	8.32	98	192.03	8.13	92	235.15	8.35	80	472.05
	8.30	98	210.98	8.06	90	198.76	8.36	78	443.01
4	8.36	92	217.70	8.22	94	179.36	8.40	82	405.65
	8.32	92	168.05	8.15	90	242.31	8.34	78	399.80
5	8.88	104	48.76	8.70	98	48.08	9.27	82	159.55
	8.92	104	32.69	8.70	98	85.65	9.19	82	147.04
6	8.35	102	146.18	9.19	96	162.40	8.41	82	334.15
	8.31	102	154.09	8.15	94	160.81	8.45	82	302.09
7	8.20	108	211.60	8.03	104	233.80	8.25	104	377.42
	8.18	106	153.56	8.04	106	269.92	87.25	102	376.13
8	8.33	110	157.62	8.10	102	238.19	8.37	104	280.06
	8.26	112	111.10	8.14	104	174.03	8.40	104	267.09
9	8.40	110	154.11	8.13	104	148.46	8.46	102	302.01
	8.38	120	164.15	8.21	108	174.86	8.49	104	277.71
SW Blank	8.01	102	218.35	7.77	96	218.46	7.88	100	201.31
1	8.31	118	171.77	8.31	121	230.87	8.39	122	372.46
	8.33	116	151.42	8.3	123	280.77	8.37	120	369.98
2	8.38	118	156.18	8.36	125	276.03	8.41	125	408.75
	8.39	118	187.76	8.36	126	283.80	8.43	124	325.64
3	8.44	118	124.54	8.39	124	197.93	8.43	123	297.85
	8.48	120	145.51	8.49	123	229.21	8.42	122	290.70
4	8.45	116	161.60	8.46	121	275.00	8.4	130	374.31
	8.5	118	185.81	8.43	124	261.61	8.38	133	417.52
5	8.36	119	174.42	8.45	122	336.24	8.48	126	379.99
	8.4	120	185.28	8.44	124	350.18	8.45	123	478.88
6	8.44	115	158.49	8.46	126	301.15	8.39	123	418.28
	8.45	118	193.15	8.48	124	316.75	8.4	121	391.19
7	8.47	117	181.75	8.47	128	319.36	8.38	123	434.05
SW Blank 20ppt	7.85	114	215.33	8.15	149	239.83	8.15	120	204.75

Note: Calcium values presented have the saltwater calcium concentration subtracted out.
APPENDIX C - (cont.)

Time (days)	pH 11	alk 11	calcium 11	pH 14	alk 14	calcium 14	pH 21	alk 21	calcium 21
1	8.43	98	307.86	8.24	88	223.94	8.30	91	332.87
2	8.39	94	297.82	8.32	94	271.48	8.35	93	330.13
	8.66	80	271.53	8.41	76	306.60	8.55	59	760.37
3	8.59	78	226.71	8.38	76	327.67	8.45	58	635.23
	8.33	80	308.69	8.23	92	269.04	8.25	82	410.67
4	8.26	76	330.87	8.23	76	304.83	8.24	73	438.91
	8.37	86	298.05	8.28	84	269.55	8.31	82	404.62
5	8.29	80	349.13	8.25	82	291.13	8.29	79	411.23
	8.93	70	218.38	8.59	74	296.28			
6	8.87	72	220.65	8.67	76	355.73			
	8.37	82	317.46	8.32	100	304.87	8.36	84	244.22
7	8.33	82	320.61	8.32	102	324.22	8.33	81	423.58
	8.26	104	299.70	8.23	106	290.20	8.25	105	328.22
8	8.30	102	293.99	8.21	104	263.45	8.36	106	295.59
	8.32	102	218.92	8.28	114	205.28	8.34	109	241.71
9	8.34	102	224.28	8.25	114	192.12	8.30	109	226.46
	8.40	104	228.77	8.33	118	220.90	8.40	110	452.05
	8.42	110	247.05	8.38	118	217.81	8.38	112	661.41
SW Blank 1	7.85	96	198.74	7.95	125	239.83	7.95	118	342.91
	8.36	144	272.32	8.32	120	223.66	8.42	118	357.19
2	8.28	142	289.40	8.32	118	275.85	8.42	116	372.05
	8.33	126	211.31	8.35	118	225.10	8.47	118	380.46
3	8.29	124	261.95	8.36	116	302.18	8.45	118	376.93
	8.33	122	214.07	8.39	118	226.69	8.5	118	349.82
4	8.3	122	218.46	8.39	120	203.24	8.5	118	340.71
	8.3	136	292.81	8.39	120	253.97	8.47	112	391.39
5	8.27	134	232.18	8.37	118	236.33	8.47	116	398.88
	8.27	128	231.75	8.36	116	218.72	8.41	114	430.37
6	8.24	122	196.44	8.38	112	261.34	8.47	112	432.78
	8.26	120	212.71	8.37	112	248.48	8.39	109	396.71
7	8.36	118	256.88	8.38	116	232.81	8.35	115	386.20
	8.25	120	256.84	8.33	118	272.31	8.33	121	441.40
SW Blank 20ppt	7.77	120	203.28	8.05	118	199.65	8.02	122	219.77

Note: Calcium values presented have the saltwater calcium concentration subtracted out
APPENDIX C - (cont.)

Time (days)	pH 28	alk 28	calcium 28
	8.41	96	706.02
2	8.40	94	665.98
	8.63	46	1478.22
3	8.59	46	1347.49
	8.28	76	755.52
4	8.28	68	769.48
	8.38	80	704.25
5	8.32	74	757.82
	8.40	72	841.78
6	8.35	74	837.94
	8.28	106	679.78
7	8.31	104	648.39
	8.38	108	562.27
8	8.39	108	540.36
	8.44	102	625.59
9	8.45	106	647.40
SW Blank	7.94	94	208.28
1	8.33	120	309.88
	8.35	116	327.59
2	8.38	120	306.50
	8.38	116	328.80
3	8.4	122	280.98
	8.42	120	261.31
4	8.43	120	334.20
	8.424	118	338.58
5	8.43	114	344.56
	8.426	114	359.12
6	8.41	108	362.67
	8.332	110	339.49
7	8.31	126	363.66
SW Blank 20ppt	8.01	122	269.25

Note: Calcium values presented have the saltwater calcium concentration subtracted out

APPENDIX C - (cont.)

APPENDIX D COMPOSITE CHARACTERISTICS FOR CONTROL

Cement	Lime	PG(Test 1)	Penetrometer (6pt.) .01mm						Length (mm)			Weight (g)	UCS (Mpa)
0.140	0.030	0.830	2.0	2.0	2.0	2.0	2.0	3.0	38	39	37	86.3	25.33
			2.0	2.0	2.0	2.0	1.5	1.5	39	38	39	86.9	26.63
			2.0	2.0	2.0	1.0	2.0	1.5	38	39	38	86.2	33.53
0.090	0.030	0.880	3.0	2.0	1.0	1.0	1.0	1.0	38	39	39	85.9	30.02
			1.5	1.5	1.0	3.0	1.0	1.5	38	39	39	86.0	10.50
			2.0	3.0	2.5	1.0	1.5	1.0	38	38	37	85.9	29.12
0.040	0.030	0.930	2.0	2.5	1.5	2.0	2.5	2.0	39	40	39	86.1	14.11
			1.5	2.0	3.0	3.0	2.5	3.0	36	36	37	82.1	12.28
			2.0	2.0	1.0	3.0	3.0	2.0	38	41	40	87.1	12.59
0.090	0.080	0.830	3.0	3.0	2.0	2.0	2.0	1.0	38	39	39	86.2	24.85
			1.5	1.5	2.0	1.0	2.0	2.0	38	38	39	86.7	22.53
			2.0	1.0	2.0	1.0	1.0	1.5	39	38	38	86.2	22.54
0.040	0.130	0.830	3.0	1.0	1.0	1.5	2.0	1.0	40	39	39	86.9	21.23
			2.0	2.0	1.0	2.0	2.5	2.0	39	39	39	86.1	22.19
			2.0	1.0	1.0	1.0	2.0	2.0	39	39	40	86.2	22.51
0.040	0.080	0.880	2.0	0.5	2.0	1.5	1.0	1.5	40	39	39	86.7	16.65
			1.0	1.0	1.0	1.0	2.0	2.0	39	39	39	85.8	13.95
			2.0	2.0	1.0	2.0	2.0	1.5	39	39	39	86.5	15.45
0.107	0.047	0.846	0.5	1.0	1.0	0.5	1.0	1.0	38	39	38	86.6	27.68
			1.5	1.0	1.0	1.0	1.0	1.0	39	39	40	86.4	28.95
			2.0	2.0	1.0	2.0	1.0	1.5	38	38	37	86.3	30.67
0.057	0.097	0.846	2.5	0.5	2.0	1.0	2.0	0.5	40	39	39	87.6	19.02
			2.0	2.0	1.0	2.0	2.0	1.5	39	39	40	87.4	21.03
			1.5	2.0	2.0	1.0	1.0	2.0	40	39	39	86.2	19.46
0.057	0.047	0.896	1.5	1.5	1.5	0.5	1.0	1.0	39	39	40	86.3	15.75
			2.5	1.5	2.0	1.0	1.0	2.0	39	39	38	85.6	17.66
			2.5	2.5	2.0	3.0	2.5	2.0	39	39	39	85.9	18.78
0.073	0.063	0.864	1.5	2.5	2.0	1.0	2.0	2.0	39	39	39	86.6	25.29
			2.0	2.0	1.0	2.0	1.0	1.0	38	39	38	86.8	23.75
			1.5	1.0	2.0	2.0	2.0	1.0	40	40	40	86.8	23.46
0.000	0.070	0.930	2.0	2.5	3.0	3.0	2.0	2.0	40	38	41	84.4	9.43
			0.5	3.0	1.0	2.0	2.0	3.0	38	38	38	83.6	9.47
			2.0	2.5	1.5	2.0	1.5	2.0	39	39	38	84.2	9.80
0.000	0.100	0.900	2.0	1.5	1.5	2.0	1.5	1.5	38	37	38	81.7	8.67
			1.0	2.0	3.0	1.0	1.0	1.5	39	39	39	84.9	7.97
			1.0	2.0	3.0	2.0	3.0	1.0	39	40	39	85.2	10.10
0.000	0.130	0.870	3.0	1.0	2.0	1.0	0.5	0.5	38	38	38	85.3	9.08
			2.5	5.0	3.0	2.0	1.0	2.0	38	38	39	85.4	12.34
			2.0	2.0	3.0	5.0	5.0	1.5	38	39	39	85.7	9.28
0.150	0.000	0.850	2.5	2.5	1.0	1.0	2.0	1.0	38	39	38	86.3	33.30
			3.0	2.0	2.0	1.5	2.0	2.0	39	39	40	86.3	29.96
			1.0	2.0	1.0	3.0	2.0	2.0	39	39	40	86.5	25.62
0.300	0.000	0.700	1.0	1.0	1.0	1.0	1.0	1.5	36	37	37	83.2	31.55
			1.5	1.0	1.0	0.5	1.0	1.0	36	37	37	84.3	19.24
			1.5	1.0	0.5	1.0	1.0	0.5	36	37	37	83.9	29.50

APPENDIX E COMPOSITE CHARACTERISTICS FOR FLOW THROUGH

Cement	Lime	PG(Test 1)	Penetrometer (6pt.) .01mm						Length (mm)			Weight (g)	UCS (Mpa)
0.140	0.030	0.830	3.0	3.0	8.0	5.5	3.0	2.0	40.0	41.0	39.0	91.2	12.94
			3.5	3.0	2.0	2.5	2.0	8.0	39.0	39.0	41.0	90.9	14.61
			6.0	11.0	3.0	5.0	4.0	4.1	39.0	39.0	40.0	90.8	14.52
													14.78
0.090	0.030	0.880	8.0	2.0	2.0	7.5	3.0	3.0	39.0	39.0	40.0	91.6	8.01
			5.0	4.5	4.5	5.0	4.0	11.0	39.0	39.0	39.0	91.2	8.40
			4.0	3.5	4.0	3.0	4.5	3.0	40.0	40.0	39.0	91.8	6.68
													8.78
0.040	0.030	0.930	1.0	11.0	53.0	77.0	20.0	10.0	40.0	40.0	39.0	87.2	4.11
			4.0	9.0	85.0	90.0	94.0	74.0	39.0	39.0	40.0	84.7	4.24
			16.0	66.0	13.0	39.0	4.0	52.0	39.0	40.0	40.0	87.1	3.81
													3.13
0.090	0.080	0.830	6.0	2.0	5.5	4.5	3.0	8.0	39.0	40.0	40.0	93.2	15.29
			7.0	3.0	4.0	2.0	4.0	4.0	40.0	39.0	39.0	92.6	15.29
			2.0	4.0	3.0	6.0	4.0	3.0	40.0	39.0	40.0	92.8	16.35
													14.35
0.040	0.130	0.830	12.0	3.0	7.0	3.0	10.0	4.0	41.0	40.0	40.0	92.3	8.65
			7.0	1.0	2.0	7.0	5.0	10.0	39.0	40.0	39.0	92.5	11.74
			4.0	3.0	4.0	6.0	5.0	1.0	39.0	40.0	39.0	92.2	9.60
													10.84
0.040	0.080	0.880	3.0	16.0	5.0	3.0	3.0	3.4	40.0	41.0	40.0	92.8	4.80
			3.0	3.0	3.0	4.0	5.0	4.0	40.0	40.0	41.0	92.4	8.61
			2.0	5.0	7.0	5.0	3.0	3.0	40.0	40.0	41.0	92.3	8.91
													9.60
0.107	0.047	0.846	8.5	1.0	5.0	3.0	9.5	4.0	39.0	40.0	39.0	91.8	11.40
			4.0	4.0	3.0	5.0	2.0	5.0	39.0	39.0	40.0	91.9	14.91
			8.0	5.0	6.0	3.5	4.0	11.0	41.0	40.0	40.0	92.0	15.68
													17.69
0.057	0.097	0.846	4.0	5.5	3.0	5.0	4.0	3.0	39.0	40.0	39.0	91.2	10.37
			5.0	4.0	3.0	5.0	6.0	5.0	41.0	40.0	40.0	91.8	9.30
			3.0	13.0	5.0	3.0	12.0	15.0	39.0	40.0	39.0	91.3	11.82
0.057	0.047	0.896	10.0	7.0	4.0	16.0	5.0	12.0	40.0	40.0	41.0	90.8	6.55
			16.0	11.0	12.0	7.0	4.0	9.0	40.0	40.0	40.0	90.2	8.23
			4.0	7.0	9.0	7.0	6.0	8.0	40.0	40.0	39.0	89.0	6.13
													5.27
0.073	0.063	0.864	4.0	2.0	3.0	4.5	8.5	3.5	40.0	41.0	41.0	92.7	10.11
			4.5	6.0	3.5	3.5	3.0	3.0	41.0	41.0	40.0	92.3	10.88
			2.0	7.0	3.0	4.0	3.0	3.0	40.0	40.0	40.0	93.0	11.70
0.000	0.070	0.930	8.0	34.0	8.0	5.0	22.0	8.0	41.0	40.0	41.0	87.2	3.08
			3.0	10.0	4.0	10.2	8.0	9.0	39.0	39.0	39.0	85.9	2.61
			12.0	6.0	11.0	8.0	8.0	7.0	40.0	41.0	40.0	86.4	3.08
													3.04
0.000	0.100	0.900	3.0	6.0	11.0	6.0	3.0	12.0	41.0	40.0	41.0	88.9	4.24
			8.0	9.0	11.0	3.0	10.0	8.0	41.0	41.0	41.0	90.6	4.28
			7.0	16.0	16.0	7.0	5.00	5.0	40.0	40.0	40.0	89.1	3.60
													2.57
0.000	0.130	0.870	4.0	13.0	4.0	8.0	12.0	7.0	41.0	41.0	40.0	90.0	3.64
			7.0	11.0	3.0	17.0	2.0	7.0	41.0	41.0	41.0	89.9	3.77
			4.0	9.0	6.0	5.0	11.0	18.0	40.0	39.0	40.0	90.7	3.81
													3.77

APPENDIX F COMPOSITE CHARACTERISTICS FOR DYNAMIC LEACH

Cement	Lime	PG(Test 1)	Penetrometer (6pt.) .01mm						Length (mm)			Weight (g)	UCS (Mpa)
0.140	0.030	0.830	5.0	2.0	60.0	5.0	2.0	8.0	38.0	38.0	38.5	86.2	13.55
			16.0	5.0	15.0	24.0	9.0	36.0	38.5	39.0	39.5	86.6	16.01
0.090	0.030	0.880	4.5	2.0	2.5	3.0	7.0	48.0	38.0	39.0	38.0	88.1	11.05
			7.0	8.0	24.0	77.0	78.0	80.0	38.5	39.0	39.0	86.6	10.10
0.040	0.030	0.930	11.0	34.0	100.0	8.0	76.0	79.0	38.0	39.0	38.0	81.6	5.44
			40.0	8.0	10.0	95.0	69.0	54.0	39.0	39.0	39.0	76.6	7.20
0.090	0.080	0.830	17.0	2.0	3.5	2.0	2.0	3.0	39.0	39.0	39.0	86.7	15.09
			1.5	16.0	25.0	21.0	11.0	2.5	39.0	39.0	39.0	87.9	17.06
0.040	0.130	0.830	6.0	3.0	2.0	5.0	3.0	2.0	39.0	39.0	38.5	89.6	10.15
			5.0	6.0	10.0	1.0	2.0	3.0	39.0	39.0	39.0	90.1	12.08
0.040	0.080	0.880	50.0	22.0	44.0	11.0	6.0	4.0	40.0	40.0	40.0	87.8	6.57
			5.0	6.0	2.5	10.0	76.0	61.0	40.0	40.0	40.0	90.1	6.85
0.107	0.047	0.846	16.0	3.0	2.0	49.0	70.0	3.0	39.0	39.0	38.5	89.1	10.62
			15.0	31.0	16.0	6.0	2.0	8.0	39.0	39.0	38.5	87.7	12.34
0.057	0.097	0.846	30.0	3.0	4.0	40.0	21.0	2.0	39.0	40.0	39.0	89.4	6.93
			30.0	2.0	2.0	2.0	4.0	2.0	39.0	39.0	39.0	86.7	8.50
0.057	0.047	0.896	15.0	94.0	105.0	30.0	25.0	50.0	39.0	39.0	39.0	86.5	5.27
			32.0	38.0	34.0	24.0	5.0	42.0	39.0	40.0	39.0	86.5	6.47
0.073	0.063	0.864	19.0	90.0	3.0	10.0	3.0	8.0	39.0	39.0	39.0	86.3	9.98
			2.0	20.0	2.0	3.0	4.0	92.0	39.0	40.0	40.0	87.9	8.48
0.000	0.070	0.930	19.0	14.0	52.0	78.0	31.0	49.0	39.0	39.0	39.0	84.3	4.80
			100.0	93.0	81.0	85.0	98.0	74.0	39.0	40.0	39.0	75.3	3.04
0.000	0.100	0.900	28.0	38.0	105.0	95.0	2.0	25.0	41.0	40.0	40.0	85.9	3.98
			100.0	87.0	65.0	24.0	23.0	25.0	39.0	38.0	39.0	76.4	6.34
0.000	0.130	0.870	1.0	12.0	31.0	14.0	3.0	20.0	38.0	39.0	39.0	85.5	4.20
			2.0	20.0	24.0	16.0	13.0	8.0	39.0	39.0	40.0	88.8	5.27
0.150	0.000	0.850	27.0	39.0	10.0	32.0	63.0	58.0	39.0	39.0	39.0	85.1	13.41
			58.0	66.0	29.0	11.0	44.0	25.0	39.0	39.0	39.0	85.5	11.87
0.300	0.000	0.700	1.0	1.0	0.5	2.0	1.0	1.0	36.0	36.0	36.0	85.3	22.92
			1.0	0.5	1.0	1.0	1.5	1.0	36.0	36.0	36.0	85.3	29.26

APPENDIX G COMPOSITE CHARACTERISTICS FOR CONTROL TEST

	Cement	Lime	PG	Fly Ash	Penetrometer (6pts) .01mm						Length (mm) (3pts)			Weight(g)	Diameter (mm) 2pts.	
II.	0.030	0.000	0.620	0.350	5.0	3.0	1.0	2.0	3.0	8.0	38.00	37.20	37.90	88.77	38.5	38.4
					3.0	2.0	2.0	4.0	3.0	10.0	38.00	37.80	37.90	88.26	38.5	38.5
					2.0	3.0	2.0	2.0	2.0	3.0	37.10	37.20	37.10	88.11	38.5	38.7
	0.065	0.000	0.585	0.350	6.0	5.0	2.0	3.0	2.0	4.0	37.00	37.80	37.30	90.45	38.7	38.6
					7.0	3.0	1.5	2.0	3.0	3.0	37.10	36.90	37.00	90.04	38.4	38.4
					4.0	3.0	2.0	2.0	2.0	9.0	37.20	37.00	36.80	90.59	38.4	38.5
	0.100	0.000	0.550	0.350	2.0	2.0	1.5	2.0	2.0	0.5	37.00	36.80	37.00	95.00	38.8	38.5
					9.0	2.0	2.0	2.0	5.0	3.0	36.90	36.80	37.30	89.78	38.8	38.7
					3.0	4.0	2.0	3.0	2.0	3.0	38.00	38.10	37.60	91.88	38.8	38.9
	0.030	0.000	0.585	0.385	9.0	2.0	2.0	1.5	2.0	8.0	36.80	36.40	36.80	89.27	38.7	38.3
					9.0	4.0	4.0	2.0	3.0	7.0	37.10	37.40	37.60	89.42	38.4	38.5
					6.0	3.0	6.5	2.5	3.5	4.0	37.00	37.20	37.20	89.52	38.3	38.5
	0.030	0.000	0.550	0.420	3.0	2.0	3.0	3.0	4.0	10.0	37.10	37.00	37.10	89.25	38.6	38.5
					1.5	2.5	2.5	2.5	3.5	4.0	37.10	37.30	37.30	88.85	38.8	38.9
					3.0	2.5	3.0	2.5	2.0	2.5	37.00	36.90	36.70	88.85	38.6	38.6
	0.065	0.000	0.550	0.385	1.5	2.0	1.5	2.0	3.5	3.0	36.80	37.40	37.10	90.57	38.6	38.5
					2.0	3.0	1.0	1.0	3.0	5.0	36.80	37.00	36.80	89.28	38.6	38.7
					2.0	2.0	3.0	3.0	1.0	1.5	36.90	37.40	37.00	89.50	38.5	38.6
	0.042	0.000	0.596	0.362	4.0	2.0	2.0	2.0	2.0	5.0	37.40	37.70	37.40	90.04	38.5	38.5
					4.0	2.0	3.0	3.0	2.5	4.0	37.30	37.10	37.80	90.46	38.5	38.3
					7.0	2.0	2.0	2.0	3.5	6.0	36.50	37.00	37.30	89.37	38.8	38.4
	0.042	0.000	0.561	0.397	2.5	3.5	3.5	3.0	2.5	6.0	36.20	36.30	37.00	89.30	38.5	38.5
					4.0	2.0	2.0	2.0	2.0	3.5	36.50	37.40	37.70	90.23	38.6	38.8
					3.5	1.5	1.0	3.0	3.0	3.0	37.30	37.70	37.30	91.45	38.8	39.0
	0.077	0.000	0.561	0.362	3.0	2.0	4.0	5.0	2.0	4.0	37.40	37.20	36.90	90.50	38.2	38.7
					3.0	3.0	2.5	3.5	2.0	3.0	37.40	37.70	37.60	90.90	38.7	38.7
					2.0	2.0	3.0	2.0	3.0	4.0	37.30	37.70	37.80	91.53	38.5	38.6
	0.053	0.000	0.574	0.373	2.0	2.0	4.0	2.0	4.0	1.5	36.90	36.90	36.70	89.95	38.7	38.5
					2.0	2.5	2.0	1.0	2.0	3.0	36.90	36.50	36.30	89.80	38.6	38.5
					2.0	2.0	2.0	3.0	1.5	3.0	36.70	36.80	36.80	89.20	38.6	38.3

163

Cement	Lime	PG	Fly Ash	Penetrometer (6pts) .01mm						Length (mm) (3pts)			Weight(g)	Diameter (mm) 2pts.	
0.000	0.030	0.620	0.350	3.5	2.0	2.0	2.0	2.5	3.0	38.60	38.30	38.00	89.14	39.1	39.2
				8.0	2.0	2.0	2.0	2.0	2.5	37.10	37.00	37.10	88.12	38.9	38.9
				11.0	3.0	2.0	2.0	5.0	9.0	37.70	37.70	37.90	89.33	39.1	38.6
0.000	0.065	0.585	0.350	6.0	4.0	12.0	9.0	7.0	6.0	42.50	41.90	41.90	93.21	40.8	41.4
				3.0	18.0	7.0	5.0	7.0	7.0	44.20	44.20	44.10	98.37	42.5	43.0
				3.0	3.0	2.0	2.0	2.5	4.0	38.90	38.60	37.80	89.25	44.0	43.0
0.000	0.100	0.550	0.350	13.0	6.0	18.0	5.0	31.0	20.0	42.10	42.30	42.20	90.42	44.2	45.1
				31.0	7.0	12.0	5.0	4.0	2.0	42.20	43.20	43.40	90.49	45.3	44.0
				8.0	23.0	9.0	7.0	8.0	50.0	42.80	42.70	4.20	90.18	45.3	43.8
0.000	0.030	0.585	0.385	4.0	4.0	3.0	2.0	3.0	3.5	38.30	38.50	38.30	92.00	39.2	39.3
				2.5	5.0	4.0	4.0	4.0	3.0	38.00	38.10	37.60	91.39	39.4	39.3
				3.0	4.0	3.5	2.5	3.0	5.0	37.90	37.80	38.10	91.90	39.4	39.1
III 0.000	0.030	0.550	0.420	4.0	2.0	2.0	2.0	3.5	8.0	38.10	37.90	37.70	89.08	39.1	39.7
				30.0	5.0	3.0	3.0	1.5	3.0	38.00	38.20	38.20	89.29	39.1	39.2
				1.0	1.5	2.5	2.0	2.0	4.0	37.50	37.40	37.80	88.87	39.2	39.2
0.000	0.065	0.550	0.385	59.0	7.0	6.0	30.0	6.0	4.0	41.80	41.40	41.40	90.73	42.7	43.1
				4.0	4.0	9.0	6.0	12.0	5.0	41.20	41.50	41.70	90.68	43.2	43.2
				19.0	9.0	6.0	4.0	3.0	6.0	40.60	40.90	41.20	90.58	43.3	43.0
0.000	0.042	0.596	0.362	15.0	2.0	2.0	6.0	11.0	5.0	40.60	41.00	40.20	91.03	41.3	41.2
				2.0	2.0	3.0	3.0	4.0	15.0	38.60	39.40	38.80	89.87	42.4	41.4
				15.0	8.0	2.0	2.0	4.0	7.0	38.90	38.60	38.80	90.08	40.9	41.0
0.000	0.042	0.561	0.397	3.0	3.0	3.0	2.0	2.0	2.0	38.00	38.50	39.10	88.59	40.5	40.1
				6.0	5.0	3.0	4.0	3.0	10.0	39.90	39.60	40.00	90.83	41.2	40.9
				5.0	2.0	1.5	3.0	4.0	16.0	4.03	40.10	40.00	90.89	40.6	40.9
0.000	0.077	0.561	0.362	3.0	2.0	3.0	3.0	1.0	6.0	39.60	39.30	39.60	88.62	41.5	41.6
				16.0	5.0	3.5	3.5	2.0	2.0	39.40	39.40	39.50	88.68	41.3	41.9
				5.0	2.5	2.0	2.0	3.0	12.0	39.40	39.00	38.90	88.01	41.1	41.6
0.000	0.053	0.574	0.373	11.0	3.0	2.5	4.0	2.0	2.0	38.80	38.90	38.80	88.21	40.1	40.0
				6.0	3.0	1.0	2.0	3.0	1.5	38.20	38.20	38.40	87.31	40.8	40.4
				6.0	2.0	2.0	3.0	6.0	4.0	39.20	38.70	39.00	87.92	40.5	40.3

APPENDIX G - (cont.)

	Cement	Lime	PG	Fly Ash	Penetrometer (6pts) .01mm						Length (mm) (3pts)			Weight(g)
	0.000	0.010	0.790	0.200	13.0	5.0	1.0	2.0	1.0	2.0	36.50	37.10	37.00	83.29
					2.0	2.0	12.0	3.0	6.0	9.0	36.20	36.30	36.10	82.45
					3.0	2.0	1.0	2.0	3.0	3.5	37.00	35.90	36.10	82.21
	0.000	0.010	0.690	0.300	3.0	2.5	3.0	2.5	5.0	4.0	35.60	36.20	37.70	84.18
					6.0	1.0	3.5	3.0	3.0	7.0	36.60	36.50	36.70	84.37
					1.5	1.5	2.5	2.0	2.0	6.0	37.30	37.30	37.30	84.26
	0.010	0.010	0.680	0.300	7	2	2	2	3.5	4	37.50	37.60	37.00	84.72
					5	3	3	2	2	10	36.10	36.20	36.40	84.22
					2	2	3.5	4	4	14	36.50	36.50	37.20	83.58
IV	0.010	0.005	0.785	0.200	4.0	1.5	2.0	2.0	2.0	1.0	36.50	36.70	37.80	86.82
					5.0	2.5	3.0	2.5	2.0	2.0	37.40	37.80	38.00	86.18
					1.0	2.0	2.0	2.0	2.0	7.0	37.90	37.80	37.80	85.79
	0.020	0.010	0.770	0.200	2.0	1.0	2.0	2.0	1.0	2.0	38.10	37.40	38.40	86.65
					3.0	1.0	1.5	2.0	2.0	2.0	37.70	37.70	38.40	87.08
					2.0	2.0	2.0	2.0	2.5	1.5	36.20	36.50	36.10	86.02
	0.020	0.010	0.670	0.300	4.0	2.0	2.0	1.0	2.0	2.0	37.20	37.70	37.30	87.23
					2.0	2.0	2.5	2.0	2.0	3.0	37.40	38.20	38.60	87.30
					2.0	1.0	1.5	4.5	3.5	5.0	37.80	38.10	38.20	87.28
	0.020	0.005	0.775	0.200	1.5	1.0	1.5	2.5	2.0	2.0	37.40	38.40	37.60	86.68
					2.0	1.0	2.5	2.0	3.5	2.0	37.50	38.40	38.10	86.54
					2.0	1.5	2.5	2.0	2.0	2.0	38.00	37.50	37.70	86.36
	0.030	0.010	0.760	0.200	3.0	1.5	1.0	2.0	2.0	2.0	37.90	38.80	38.00	86.10
					2.0	2.0	1.0	2.0	1.0	3.0	37.70	38.10	37.90	87.07
					4.0	4.0	2.0	2.5	2.0	2.0	38.30	37.80	38.20	86.74
	0.030	0.010	0.660	0.300	1.0	2.0	2.0	2.0	2.0	11.0	37.90	37.90	37.60	87.70
					2.0	1.0	2.0	2.0	2.5	1.0	38.50	38.30	38.50	88.19
					3.0	2.0	1.5	3.0	2.5	1.5	37.90	37.90	37.90	87.30
	0.030	0.005	0.765	0.200	5.0	2.5	1.0	3.0	3.0	2.5	37.80	37.70	37.50	83.71
					2.5	1.5	1.5	2.5	3.0	2.5	37.10	37.90	37.40	84.23
					1.5	1.0	2.0	2.0	1.5	1.0	37.20	37.80	37.60	83.80

APPENDIX G - (cont.)

165

APPENDIX H COMPOSITE CHARACTERISTICS FOR CONTROL-WET

Cemen	Lime	PG	Fly Ash	SH (6pts)						Length (mm) (3pts)			Weight(g)
II. 0.030	0.000	0.620	0.350	4.0	2.0	2.0	2.0	3.0	4.0	38.00	37.20	37.90	91.30
				6.0	3.0	2.0	2.0	3.0	3.0	38.00	37.80	37.90	90.80
				8.0	2.0	1.0	3.0	2.0	2.0	37.10	37.20	37.10	91.80
0.065	0.000	0.585	0.350	4.0	8.0	3.0	2.0	2.0	3.00	37.00	37.80	37.30	92.00
				2.0	2.0	2.0	2.0	3.0	7.00	37.10	36.90	37.00	92.00
				3.0	1.0	2.0	3.0	2.0	3.0	37.20	37.00	36.80	91.70
0.100	0.000	0.550	0.350	2.0	1.0	2.0	3.0	2.0	5.0	37.00	36.80	37.00	93.30
				2.0	2.0	4.0	2.0	2.0	3.0	36.90	36.80	37.30	91.70
				2.0	2.0	3.0	2.0	2.0	3.0	38.00	38.10	37.60	91.50
0.030	0.000	0.585	0.385	3.0	2.0	1.0	2.0	3.0	5.0	36.80	36.40	36.80	92.40
				4.0	2.0	1.0	1.0	2.0	3.0	37.10	37.40	37.60	91.30
				27.0	2.0	1.0	3.0	2.0	3.0	37.00	37.20	37.20	90.90
0.030	0.000	0.550	0.420	2.0	2.0	2.0	1.5	2.0	7.0	37.10	37.00	37.10	90.90
				2.0	2.0	2.0	2.0	3.0	4.0	37.10	37.30	37.30	91.80
				6.0	3.0	2.0	2.0	3.0	8.0	37.00	36.90	36.70	91.30
0.065	0.000	0.550	0.385	2.0	7.0	2.0	2.0	2.0	6.0	36.80	37.40	37.10	92.20
				2.0	2.0	1.0	1.0	2.0	7.0	36.80	37.00	36.80	91.60
				2.0	1.0	3.0	1.0	2.0	9.0	36.90	37.40	37.00	91.10
0.042	0.000	0.596	0.362	3.0	1.0	1.0	2.0	2.0	8.0	37.40	37.70	37.40	92.20
				8.0	1.0	2.0	1.0	1.0	2.0	37.30	37.10	37.80	91.00
				15.0	1.0	2.0	1.0	2.0	3.0	36.50	37.00	37.30	91.60
0.042	0.000	0.561	0.397	2.0	2.0	3.0	5.0	3.0	4.0	36.20	36.30	37.00	91.30
				2.0	2.0	4.0	1.0	2.0	2.0	36.50	37.40	37.70	91.90
				6.0	3.0	3.0	2.0	2.0	3.0	37.30	37.70	37.30	92.60
0.077	0.000	0.561	0.362	2.0	2.0	3.0	1.0	2.0	4.0	37.40	37.20	36.90	92.20
				2.0	2.0	2.0	1.0	3.0	6.0	37.40	37.70	37.60	93.00
				8.0	1.0	1.0	2.0	1.0	2.0	37.30	37.70	37.80	92.40
0.053	0.000	0.574	0.373	3.0	2.0	1.0	1.0	1.0	2.0	36.90	36.90	36.70	91.60
				10.0	2.0	3.0	1.0	1.0	2.0	36.90	36.50	36.30	91.90
				8	2	1	2	1	1	36.70	36.80	36.80	91.30
0.000	0.030	0.620	0.350	3.0	2.0	2.0	1.0	2.0	3.0	38.60	38.30	38.00	93.60
				2.0	1.0	3.0	1.0	2.0	7.0	37.10	37.00	37.10	93.30
				2.0	1.0	1.0	2.0	2.0	10.0	37.70	37.70	37.90	91.40
0.000	0.065	0.585	0.350	3.0	5.0	10.0	3.0	6.0	8.0	42.50	41.90	41.90	108.40
				20.0	30.0	5.0	6.0	3.0	5.0	44.20	44.20	44.10	110.90
				12.0	8.0	2.0	2.0	2.0	3.0	38.90	38.60	37.80	98.30
0.000	0.100	0.550	0.350	71.0	30.0	12.0	11.0	10.0	11.0	42.10	42.30	42.20	112.20
				12.0	27.0	42.0	32.0	40.0	26.0	42.20	43.20	43.40	111.50
				11.0	43.0	28.0	25.0	65.0	49.0	42.80	42.70	4.20	111.00
0.000	0.030	0.585	0.385	4.0	2.0	1.0	1.0	3.0	8.0	38.30	38.50	38.30	93.50
				3.0	2.0	1.0	2.0	1.0	1.0	38.00	38.10	37.60	94.40
				25.0	2.0	1.0	1.0	2.0	2.0	37.90	37.80	38.10	93.70
III. 0.000	0.030	0.550	0.420	3.0	3.0	1.0	1.0	2.0	15.0	38.10	37.90	37.70	95.10
				21.0	1.0	2.0	1.0	1.0	2.0	38.00	38.20	38.20	94.10
				5.0	3.0	2.0	2.0	1.0	3.0	37.50	37.40	37.80	93.70
0.000	0.065	0.550	0.385	3.0	6.0	11.0	10.0	17.0	28.0	41.80	41.40	41.40	100.10
				9.0	6.0	12.0	5.0	10.0	6.0	41.20	41.50	41.70	101.50
				7.0	4.0	2.0	6.0	10.0	19.0	40.60	40.90	41.20	101.60

Cemen	Lime	PG	Fly Ash	Surhard (6pts)						Length (mm) (3pts)			Weight(g)
0.000	0.042	0.596	0.362	17.0	2.0	3.0	2.0	2.0	2.0	40.60	41.00	40.20	101.90
				24.0	3.0	2.0	3.0	6.0	20.0	38.60	39.40	38.80	99.00
				8.0	23.0	6.0	2.0	2.0	1.0	38.90	38.60	38.80	98.20
0.000	0.042	0.561	0.397	1.0	4.0	3.0	3.0	6.0	9.0	38.00	38.50	39.10	96.90
				7.0	3.0	3.0	3.0	2.0	3.0	39.90	39.60	40.00	101.00
				4.0	25.0	24.0	2.0	3.0	4.0	4.03	40.10	40.00	98.00
0.000	0.077	0.561	0.362	25.0	4.0	11.0	6.0	3.0	2.0	39.60	39.30	39.60	99.10
				8.0	4.0	3.0	6.0	4.0	9.0	39.40	39.40	39.50	99.60
				4.0	2.0	6.0	5.0	19.0	4.0	39.40	39.00	38.90	99.70
0.000	0.053	0.574	0.373	6.0	2.0	2.0	2.0	4.0	4.0	38.80	38.90	38.80	98.70
				9.0	5.0	4.0	3.0	2.0	2.0	38.20	38.20	38.40	98.60
				7.0	2.0	4.0	2.0	2.0	14.0	39.20	38.70	39.00	97.70
0.000	0.010	0.790	0.200	3.0	1.0	3.0	10.0	25.0	64.0	36.50	37.10	37.00	89.40
				5.0	2.0	3.0	4.0	2.0	1.0	36.20	36.30	36.10	87.10
				10.0	4.0	2.0	2.0	3.0	4.0	37.00	35.90	36.10	88.10
0.000	0.010	0.690	0.300	3.0	4.0	3.0	4.0	3.0	6.0	35.60	36.20	37.70	93.40
				7.0	4.0	2.0	1.0	2.0	2.0	36.60	36.50	36.70	88.80
				4.0	2.0	3.0	2.0	1.0	2.0	37.30	37.30	37.30	89.00
0.010	0.010	0.680	0.300	4.0	2.0	2.0	1.0	2.0	5.0	37.50	37.60	37.00	90.90
				4.0	3.0	1.0	1.0	2.0	2.0	36.10	36.20	36.40	90.60
				8.0	3.0	2.0	2.0	1.0	2.0	36.50	36.50	37.20	90.10
IV 0.010	0.005	0.785	0.200	13.0	2.0	2.0	2.0	1.0	2.0	36.50	36.70	37.80	88.30
				6.0	2.0	1.0	2.0	1.0	2.0	37.40	37.80	38.00	88.80
				6.0	2.0	1.0	2.0	3.0	2.0	37.90	37.80	37.80	88.50
0.020	0.010	0.770	0.200	2.0	2.0	1.0	3.0	2.0	3.0	38.10	37.40	38.40	90.90
				2.0	1.0	2.0	2.0	3.0	3.0	37.70	37.70	38.40	91.90
				2.0	1.0	2.0	1.0	1.0	3.0	36.20	36.50	36.10	89.40
0.020	0.010	0.670	0.300	5.0	3.0	1.0	2.0	1.0	1.0	37.20	37.70	37.30	90.80
				7.0	3.0	3.0	2.0	1.0	2.0	37.40	38.20	38.60	91.10
				10.0	3.0	2.0	3.0	2.0	2.0	37.80	38.10	38.20	91.00
0.020	0.005	0.775	0.200	17.0	2.0	2.0	3.0	1.0	2.0	37.40	38.40	37.60	90.60
				3.0	2.0	2.0	1.0	1.0	2.0	37.50	38.40	38.10	90.80
				8.0	3.0	2.0	2.0	1.0	2.0	38.00	37.50	37.70	90.70
0.030	0.010	0.760	0.200	3.0	2.0	2.0	1.0	2.0	2.0	37.90	38.80	38.00	91.40
				8.0	3.0	2.0	1.0	2.0	1.0	37.70	38.10	37.90	91.30
				5.0	4.0	2.0	1.0	2.0	2.0	38.30	37.80	38.20	91.00
0.030	0.010	0.660	0.300	3.0	3.0	2.0	2.0	2.0	1.0	37.90	37.90	37.60	91.20
				3.0	2.0	1.0	1.0	2.0	2.0	38.50	38.30	38.50	90.90
				4.0	2.0	2.0	1.0	1.0	1.0	37.90	37.90	37.90	90.80
0.030	0.005	0.765	0.200	6.0	4.0	2.0	2.0	3.0	1.0	37.80	37.70	37.50	89.90
				6.0	4.0	3.0	1.0	1.0	2.0	37.10	37.90	37.40	90.10
				10.0	3.0	2.0	3.0	2.0	2.0	37.20	37.80	37.60	89.90

APPENDIX H - (cont.)

APPENDIX I COMPOSITE CHARACTERISTICS FOR LEACH TEST

	Cement	Lime	PG	Fly Ash	Penetrometer (6pts) .01mm						Length (mm) (3pts)			Weight(g)
II	0.030	0.000	0.620	0.350	9.0	8.0	7.0	9.0	10.0	5.0	36.80	36.50	36.20	82.45
					16.0	40.0	6.0	6.0	16.0	4.0	37.00	36.50	37.00	82.96
	0.065	0.000	0.585	0.350	5.0	8.0	6.0	6.0	19.0	4.0	36.90	37.30	37.10	85.29
					3.0	17.0	16.0	6.0	12.0	10.0	37.20	37.20	37.70	85.41
	0.100	0.000	0.550	0.350	6.0	6.0	4.0	2.0	4.0	40.0	36.70	37.30	36.70	85.31
					21.0	40.0	4.0	7.0	5.0	4.0	36.70	36.50	36.20	84.62
	0.030	0.000	0.585	0.385	6.0	6.0	6.0	9.0	9.0	31.0	37.50	36.80	36.80	83.26
					19.0	43.0	4.0	9.0	8.0	26.0	37.60	36.90	36.80	83.06
	0.030	0.000	0.550	0.420	11.0	5.0	3.0	8.0	5.0	11.0	36.90	36.30	37.50	83.78
					5.0	6.0	40.0	17.0	8.0	6.0	36.90	37.10	36.90	84.15
	0.065	0.000	0.550	0.385	4.0	5.0	43.0	6.0	27.0	5.0	37.80	37.00	37.60	85.05
					5.0	6.0	4.0	3.0	5.0	6.0	37.40	37.30	36.70	84.96
	0.042	0.000	0.596	0.362	4.0	10.0	7.0	14.0	12.0	13.0	37.30	36.90	37.40	84.06
					6.0	5.0	9.0	7.0	4.0	7.0	36.70	36.80	37.00	83.45
	0.042	0.000	0.561	0.397	8.0	21.0	40.0	30.0	9.0	7.0	37.30	36.30	36.10	83.16
					12.0	15.0	9.0	23.0	12.0	14.0	37.20	36.50	36.50	83.77
	0.077	0.000	0.561	0.362	10.0	8.0	40.0	7.0	10.0	4.0	37.30	38.10	37.60	85.85
					5.0	15.0	5.0	10.0	5.0	6.0	36.80	36.50	36.60	85.25
	0.053	0.000	0.574	0.373	11.0	13.0	15.0	6.0	11.0	11.0	36.70	36.50	36.60	84.05
					12.0	4.0	8.0	12.0	16.0	12.0	37.40	37.00	37.40	85.20
	0.000	0.030	0.620	0.350	7.0	10.0	7.0	12.0	32.0	40.0	38.10	38.00	38.00	82.39
					30.0	14.0	23.0	27.0	30.0	23.0	37.60	37.70	37.40	81.82
	0.000	0.065	0.585	0.350	69.0	7.0	75.0	8.0	7.0	57.0	44.50	44.90	43.90	85.87
					94.0	8.0	15.0	18.0	7.0	17.0	44.00	42.50	42.40	84.77
	0.000	0.030	0.585	0.385	12.0	20.0	14.0	2.0	8.0	15.0	37.90	38.10	38.60	81.69
					8.0	6.0	2.0	5.0	8.0	13.0	38.00	37.70	38.10	81.75
III	0.000	0.030	0.550	0.420	99.0	13.0	30.0	12.0	3.0	51.0	37.90	37.80	37.70	82.26
					22.0	18.0	93.0	3.0	17.0	6.0	38.00	38.20	37.70	83.02
	0.000	0.042	0.596	0.362	8.0	10.0	22.0	18.0	31.0	28.0	37.90	38.40	38.70	81.47
					18.0	23.0	68.0	9.0	16.0	42.0	39.50	39.00	39.00	82.09
	0.000	0.042	0.561	0.397	47.0	36.0	8.0	26.0	23.0	11.0	38.90	38.90	39.00	83.56
					22.0	10.0	23.0	17.0	22.0	70.0	39.80	40.00	40.20	84.50
	0.000	0.053	0.574	0.373	33.0	10.0	24.0	5.0	2.0	5.0	40.20	40.70	40.10	83.91
					28.0	63.0	6.0	4.0	81.0	44.0	40.20	40.10	39.90	83.57
	0.000	0.010	0.790	0.200	14.0	63.0	71.0	68.0	29.0	49.0	36.10	36.40	36.70	72.74
					76.0	85.0	68.0	4.0	28.0	71.0	36.40	36.30	36.90	74.08
	0.000	0.010	0.690	0.300	5.0	65.0	12.0	2.0	55.0	45.0	36.60	37.10	36.90	77.29
					35.0	41.0	10.0	16.0	53.0	10.0	36.40	36.80	36.80	77.69
	0.010	0.010	0.680	0.300	46.0	43.0	10.0	30.0	17.0	16.0	37.40	37.10	37.10	78.69
					13.0	46.0	25.0	26.0	35.0	75.0	36.70	37.80	37.50	77.98
IV	0.010	0.005	0.785	0.200	40.0	36.0	33.0	48.0	22.0	26.0	37.60	37.50	37.90	79.35
					40.0	73.0	51.0	22.0	60.0	63.0	37.60	38.00	37.60	78.32
	0.020	0.010	0.770	0.200	16.0	50.0	23.0	25.0	35.0	32.0	37.30	36.70	36.90	79.90
					14.0	23.0	54.0	18.0	33.0	35.0	36.40	36.50	36.80	77.55
	0.020	0.010	0.670	0.300	5.0	8.0	3.0	9.0	19.0	30.0	37.20	37.40	37.80	82.47
					4.0	5.0	3.0	21.0	18.0	31.0	37.80	37.40	38.00	82.71
	0.020	0.005	0.775	0.200	21.0	38.0	10.0	31.0	9.0	42.0	37.90	37.50	37.30	79.02
					40.0	15.0	90.0	29.0	54.0	8.0	37.20	37.40	37.90	79.65
	0.030	0.010	0.760	0.200	44.0	37.0	31.0	42.0	26.0	23.0	37.60	38.30	38.00	80.17
					60.0	42.0	37.0	17.0	62.0	12.0	37.90	37.70	37.50	80.61
	0.030	0.010	0.660	0.300	35.0	50.0	11.0	25.0	24.0	13.0	38.30	37.90	37.80	81.04
					32.0	36.0	33.0	61.0	22.0	20.0	37.60	37.90	38.40	81.73
	0.030	0.005	0.765	0.200	38.0	60.0	65.0	67.0	46.0	40.0	36.40	36.60	36.20	75.93
					26.0	21.0	48.0	68.0	58.0	21.0	36.40	37.10	36.90	75.87

APPENDIX J COMPOSITE CHARACTERISTICS FOR LEACH TEST-WET

	Cement	Lime	PG	Fly Ash	Penetrometer (6pts) .01mm						Weight(g)
II.	0.030	0.000	0.620	0.350	6.0	21.0	29.5	6.0	13.0	90.0	87.08
					11.0	9.0	11.0	25.0	11.0	17.0	87.59
	0.065	0.000	0.585	0.350	8.0	17.0	7.5	12.0	9.0	8.0	89.60
					13.0	22.0	15.0	4.0	7.0	21.0	89.90
	0.100	0.000	0.550	0.350	18.0	4.0	8.0	6.0	12.0	9.0	89.15
					29.0	5.0	17.0	9.0	23.0	7.0	88.04
	0.030	0.000	0.585	0.385	8.0	6.0	16.5	21.0	12.0	10.0	88.50
					3.0	8.0	50.0	12.0	10.0	15.0	87.67
	0.030	0.000	0.550	0.420	33.0	6.0	9.0	70.0	9.0	11.0	88.15
					13.0	5.0	4.0	9.0	19.0	35.0	88.77
	0.065	0.000	0.550	0.385	10.0	18.0	13.0	6.0	15.0	9.0	88.85
					12.0	7.0	15.0	13.0	19.0	10.0	89.00
	0.042	0.000	0.596	0.362	5.0	10.0	4.0	60.0	10.0	21.0	88.82
					14.0	11.0	8.0	20.0	10.0	9.0	88.15
	0.042	0.000	0.561	0.397	10.0	4.0	23.0	18.0	11.0	13.0	87.81
					24.0	5.0	12.0	14.0	8.0	11.0	88.08
	0.077	0.000	0.561	0.362	31.0	18.0	27.0	19.0	6.0	21.0	89.39
					54.0	16.0	41.0	4.0	12.0	56.0	88.80
	0.053	0.000	0.574	0.373	24.0	15.0	26.0	17.0	32.0	20.0	88.52
					12.5	29.0	8.0	20.0	27.0	13.0	89.77
	0.000	0.030	0.620	0.350	39.0	36.0	11.0	24.0	8.0	10.0	90.41
					28.5	14.0	50.0	47.5	8.0	30.0	89.71
	0.000	0.065	0.585	0.350	7.0	15.0	28.0	35.0	26.0	33.0	109.74
					50.0	45.0	35.0	34.0	11.0	36.0	105.96
	0.000	0.030	0.585	0.385	12.0	26.0	95.0	32.0	8.0	63.0	90.16
					7.0	48.0	7.0	41.0	31.0	101.0	90.65
III.	0.000	0.030	0.550	0.420	60.0	9.0	31.0	9.0	72.0	86.0	90.10
					41.0	38.0	21.0	15.0	9.0	62.0	90.52
	0.000	4.200	0.596	0.362	42.0	24.0	11.0	70.0	20.0	70.0	92.41
					42.0	81.0	34.0	36.0	41.0	32.0	95.32
	0.000	4.200	0.561	0.397	50.0	28.0	50.0	11.0	16.0	30.0	94.08
					24.0	68.0	50.0	14.0	48.0	32.0	97.78
	0.000	5.300	0.574	0.373	18.0	24.0	45.0	17.0	14.0	2.0	97.00
					10.0	42.0	3.0	21.0	7.0	12.0	96.51
	0.000	1.000	0.790	0.200	98.0	84.0	55.0	84.0	71.0	11.0	79.76
					77.0	47.0	90.0	85.0	44.0	14.0	82.19
	0.000	1.000	0.690	0.300	60.0	71.0	86.0	35.0	16.0	65.0	83.01
					15.0	54.0	32.0	21.0	73.0	45.0	83.63
	0.010	1.000	0.680	0.300	88.0	41.0	31.0	82.0	81.0	74.0	85.18
					87.0	61.0	74.0	15.0	98.0	61.0	84.40
IV.	0.010	0.005	0.785	0.200	99.0	45.0	70.0	50.0	51.0	92.0	86.47
					45.0	51.0	65.0	42.0	36.0	42.0	85.51
	0.020	0.010	0.770	0.200	75.0	12.0	41.0	89.0	29.0	35.0	85.93
					61.0	88.0	45.0	94.0	72.0	27.0	84.01
	0.020	0.010	0.670	0.300	8.0	43.0	29.0	54.0	70.0	12.0	87.74
					6.0	17.0	51.0	6.0	37.0	23.0	86.29
	0.020	0.005	0.775	0.200	20.0	41.0	27.0	32.0	42.0	88.0	85.68
					18.0	37.0	30.0	15.0	55.0	54.0	84.17
	0.030	0.010	0.760	0.200	34.0	67.0	74.0	27.0	32.0	56.0	86.29
					40.0	80.0	46.0	58.0	41.0	35.0	86.46
	0.030	0.010	0.660	0.300	45.0	29.0	32.0	9.0	69.0	46.0	87.34
					58.0	37.0	60.0	61.0	59.0	40.0	87.92
	0.030	0.005	0.765	0.200	62.0	10.0	56.0	68.0	75.0	86.0	82.71
					67.0	40.0	41.0	49.0	48.0	89.0	78.80

APPENDIX K MEASUREMENTS OF SURFACE HARDNESS AND UNCONFINED STRENGTH

1. Surface Hardness

A corn penetrometer (Model No. WF 21510, Humboldt Mfg., Inc.) was used to measured the penetration depth of the PG composites following the British Standard methods of Testing Soils for Engineering Purposes (BS 1377:1977). The inverse of the penetration depth was used as a measurement of the surface hardness. The hardness at six equidistance points along the length of each composite was measured.

2. Unconfined Compressive Strength

Unconfined compressive strength of the PG composites was determined using the Matta universal testing machine following the Test for Cylindrical Cement Specimens (ASTM D1633-84). The machine automatically records the axial load and computes for required pressure at the points of composite failure.

VITA

Tingzong Guo received his bachelor of engineering degree for Chemical Engineering from Fuzhou University in 1982. He received his master of science degree for Marine Environmental Chemistry from Xiamen University in 1986. He received his master of science degree in Oceanography from Louisiana State University in 1995. He also received his Professional Engineer License in Louisiana State in 1998. Since 1995 he has been enrolled in a doctoral program in Civil Engineering at Louisiana State University. He is also a candidate for the degree of Master of Science in Applied Statistics at Louisiana State University and will receive both the degrees of Doctor of Philosophy and Master of Science at the December Commencement.

171

DOCTORAL EXAMINATION AND DISSERTATION REPORT
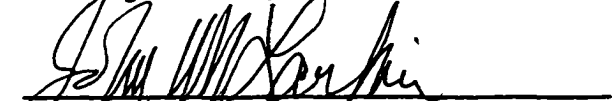
Candidate: Tingzong Guo

Major Field: Civil Engineering

Title of Dissertation: Determination of Optimal Composition of Stabilized Phosphogypsum Composites for Saltwater Application

Approved:

_____
Major Professor and Chairman

_____
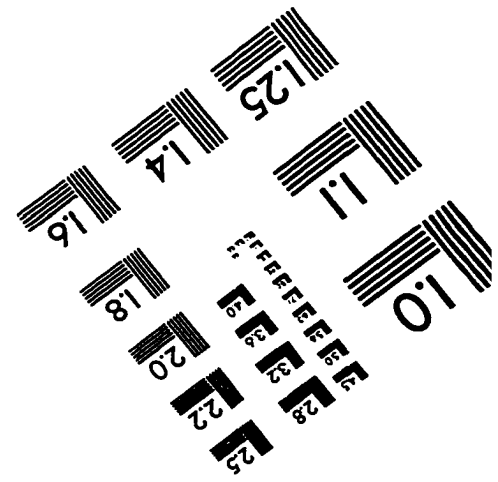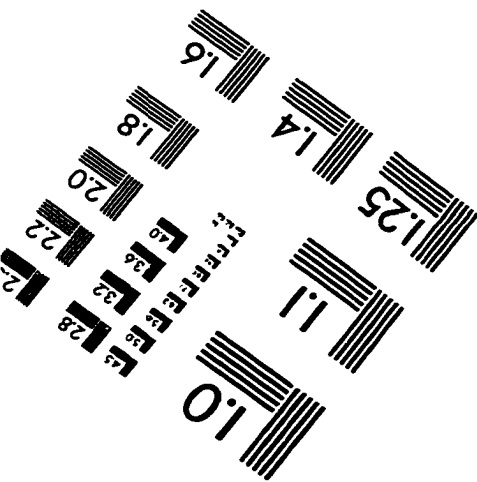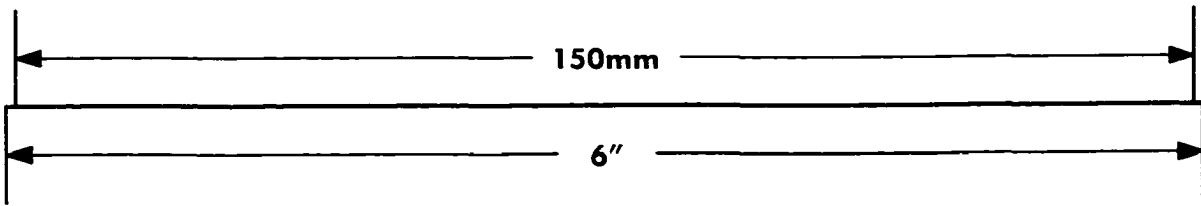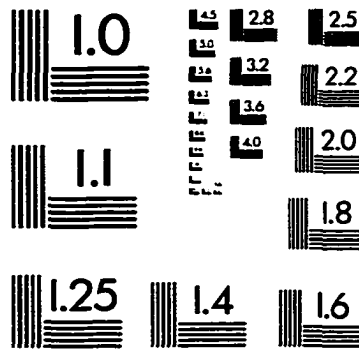Dean of the Graduate School

EXAMINING COMMITTEE:

_____

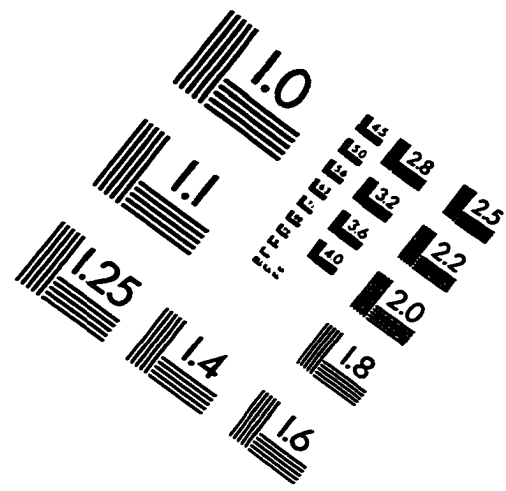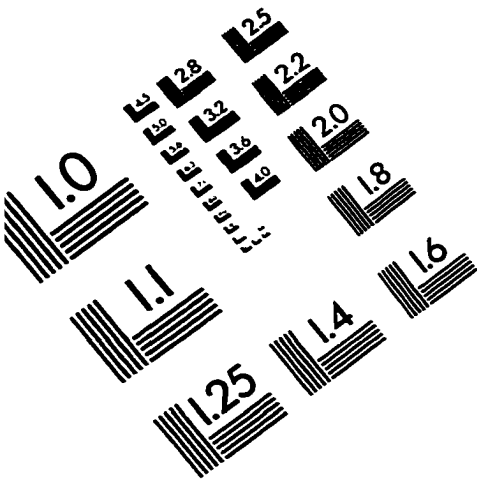_____

_____

_____

_____

Date of Examination:

_____October 20, 1998_____   _____

IMAGE EVALUATION
TEST TARGET (QA-3)

APPLIED IMAGE, Inc
1653 East Main Street
Rochester, NY 14609 USA
Phone: 716/482-0300
Fax: 716/288-5989

© 1993, Applied Image, Inc., All Rights Reserved